University of São Paulo
"Luiz de Queiroz" College of Agriculture

The primary roots of *Sorghum bicolor* as a model to study the mechanisms related to mixed-linkage glucan hydrolysis during the aerenchyma development

Bruno Rubens Flausino Teixeira

Thesis presented to obtain the degree of Doctor in Science. Program: International Plant Cell and Molecular Biology

Piracicaba
2021

Bruno Rubens Flausino Teixeira
Master in Biological Sciences (Major in Genetics)
Licentiate in Biological Sciences

The primary roots of *Sorghum bicolor* as a model to study the mechanisms related to mixed-linkage glucan hydrolysis during the aerenchyma development

Advisor:
Prof. Dr. **MARCOS SILVEIRA BUCKERIDGE**

Thesis presented to obtain the degree of Doctor in Science. Program: International Plant Cell and Molecular Biology

Piracicaba
2021

Dados Internacionais de Catalogação na Publicação
DIVISÃO DE BIBLIOTECA – DIBD/ESALQ/USP

Teixeira, Bruno Rubens Flausino

The primary roots of *Sorghum bicolor* as a model to study the mechanisms related to mixed-linkage glucan hydrolysis during the aerenchyma development / Bruno Rubens Flausino Teixeira - - Piracicaba, 2021.

115 p.

Tese (Doutorado) - - USP / Escola Superior de Agricultura "Luiz de Queiroz".

1. Sorgo 2. Arroz 3. Raízes primárias 4. Aerênquima 5. Liquenano 6. β-glucano 7. Glucano de ligação mista 8. β-glucano de ligação mista 9. β-D-(1,3;1,4)-glucano de ligação 10. (1,3),(1,4)-β-D-glucano de ligação mista 11. Liquenase 12. Glucanases de ligação mista 13. β-D-(1,3;1,4)-endo-glucanases 14. Glicosil hidrolases 16 e 17 15. Celulose sintases-like F, H e J. I. Título

To my mother for being unconditionally supportive

ACKNOWLEDGMENTS

My special thanks to Dr. Buckeridge and Dr. Di.

Dr. Buckeridge gave me the main tool to learn to stand on my own feet: freedom. Above all, he lapidated my ideas into such a jaw-dropping beauty. A pinch of freedom "sculptured" by his talented ideas meant POWER. At a certain point, I clearly could write compelling things!

Dr. Di, on the other hand, was essential to catch "beautiful ideas" and guide me to develop them into scientific data. Thus, she was vital for this work. Also, her patience and constant presence inspired me, especially when I was exhausted. Among several mini preparations we used to do on Sundays' afternoon, I was surprised by the sparkling joy reflected from her almond-eyed view upon successful electrophoresis. Dr. Di, I left Rutgers with magical fingers you "gave" me. Thank you so much for your kindness😊)))))))

To Dr. Carrer, I'll always be grateful for inviting me to join this international Ph.D. The first time I heard "Dr. Carrer" in the Department of Genetics halls in Rio de Janeiro, I could never think of working with you. Intriguingly, you were always in my mind because in Valencian and Catalan, "Carrer" means Street. So, on each Street, I read "Carrer." Jokes aside, thanks for your patience and kindness, which led me to inquire intensively about social behavior.

To Denia Cai Shi, mi amiga costarriqueña, tus esfuerzos te llevarán adonde quieras. Tu adornada simplicidad trasciende lo imaginable afecto que tengo por ti. You and the brave YC Ethan edited my heart cells so they inevitably beat best moments you guys gave by

CRISPR_ING_G ▼*XmaI*

TACCCATACTTCATCTACTCATACAACCCGGGNGGCGGC_TAG????ATG…

▲

To Megan Francis and Nalini Kaul, well, the perfect employees anyone would like to have.

A los compañeros de piso: Keyla, Ernest, Calderón y Luis y Dr. Nirmala.

I thank the USA and, above all, Rutgers for the tuition-free opportunity.

I'm deeply grateful and thank Alexandra Asanovna Elbakyan from Sci-Hub, who contributed to Sciences.

I thank the University of São Paulo and those who contributed to my Ph.D.

I thank MSc. Lopes Ferreira, for being a supportive and loyal friend. MSc. Grayce, you made a big difference in my life because it got lighter than before. I thank Lauana as well for her northeastern Brazilian enthusiastic happiness!

Ao MSc. Pedro Henrique Santos Oliveira, amigo, no lockdown, sem a possibilidade de pegar os cromatogramas digitais, você os transformou em cromatogramas de papel. Obrigado pelos seus conhecimentos químicos da Unicamp lapidados pela USP.

Dr. Rusiska and MSc. Carvalho: how about some coffee?

MSc. Pagliuso, you gave vital information down to the wire. You eventually don't know that. But with little information, you help me so much.

I cannot "requiem" here……. to Eglee Igarashi, who contributed with her suggestions regarding organizing the bench. Dr. Viviane Lopes, we both have green thumbs. Ultimately, you contributed with your finger by touching my little daughters: the primary roots!

I thank all you guys, who contributed for my research: Dr. Soldi, Dr. Scaglia, Dr. Cesarino, Dr. Floh, Dr. Ferrándiz, Dr. Palacios, Dr. Locossell, Msc. Victório Cerruti, Dr. Rodrigues da Silva, Dr. Hernandes, Dr. van Sluys, Dr. Silvestre Lira, the technician Tatiana, Dr. Elbl, Dr. Rossi, Dr. Prut, and Dr. Tamires Rodrigues.

Above all, my other friends who supported me somehow: Felipe Naim, Arilse Chrisostomo, Lane Benau.

Meinem großen Freund Otto, der zu meiner linguistischen, philosophischen und vor allem musikalischen Bildung entscheidend beigetragen hat.

Agradeço aos meus familiares: meu marido Sadyd, irmã, mi sobrinos espanhoizinhos, meu cunhado, ao Don deCea. Ao meu amado pai, quem me deu a vida. E às mulheres da minha vida: minha mãe e minhas avós.

To the Brazilian Federal Agency for Support and Evaluation of Graduate Education (CAPES) for funding all my research in Brazil (88882.378373/2018-01) and in the Rutgers University (88881.187676/2018-01).

"An expert is one who knows more and more about less and less until he knows absolutely everything about nothing. "

Nicholas Murray Butler

TABLE OF CONTENTS

RESUMO....10
ABSTRACT....12
LIST OF FIGURES....14
LIST OF TABLES....17
1. PREFACE....19
REFERENCES....20
2. MIXED-LINKAGE GLUCAN HYDROLYSIS AND THE AERENCHYMA DEVELOPMENT IN PRIMARY ROOTS OF SORGHUM....23
ABSTRACT....23
2.1. INTRODUCTION....24
2.1.1. Sorghum....24
2.1.2. Developmental stages of sorghum....25
2.1.3. Germination....25
2.1.4. Primary root development....26
2.1.5. Plant cell wall and mixed-linkage glucan....26
2.1.6. MLG occurrence....27
2.1.7. MLG fine structure....28
2.1.8. MLG biosynthesis....31
2.1.9. MLG rearrangement....31
2.1.10. GH17 and GH16 MLGases....32
2.1.11. MLG roles....33
2.1.12. The transient and permanent structure....33
2.1.13. Storage....36
2.1.14. Other roles....37
2.1.15. MLG biotechnology....37
2.1.16. Increasing MLG content: application in bioenergy and human nutrition....37
2.1.17. Decreasing MLG content: application in the brewing industry and animal feed....38
2.1.18. Aerenchyma development....40
2.2. GOAL....44
2.3. MATERIAL AND METHODS....44
2.3.1. Plant material....44
2.3.2. Anatomical characterization....45
2.3.2.1. High-resolution microtomography....45
2.3.2.2. Histological cross-sections....45
2.3.3. Phylogenetic reconstructions....46
2.3.4. Quantitative real-time PCR....47
2.3.5. Enzymatic activity assays....47
2.3.6. Cell wall preparation....48
2.3.6.1. MLG quantification....49
2.3.6.2. Monosaccharide composition....49
2.3.7. Chromatographic procedures....49
2.3.7.1. Oligosaccharide profile by HPAEC-PAD....49
2.3.7.2. Oligosaccharide profile by thin-layer chromatography....49
2.3.7.3. Chromatogram data analysis....50

2.3.8. Statistical analysis 50
2.4. RESULTS 50
2.4.1. Anatomical characterization of aerenchyma 50
2.4.2. Cladograms and phylogenetic inferences 52
2.4.3. MLG biosynthesis 54
2.4.4. MLG hydrolysis 55
2.4.5. Expression profile of *Sblic1*, *Sblic2*, and *SbCslF6* 56
2.4.6. Enzymatic activity 57
2.4.6.1. Detection of enzyme activity by thin-layer chromatography (TLC) 57
2.4.6.2. Detection of enzyme activity using HPAEC-PAD 58
2.4.7. Cell wall fractionation 60
2.4.7.1. MLG quantification 60
2.4.7.2. Profile of structural carbohydrates 60
2.5. DISCUSSION 61
2.5.1. Anatomical characterization 61
2.5.2. Cladogram and phylogenetic inferences 62
2.5.3. MLG hydrolysis in sorghum primary roots 63
2.6. CONCLUSION 64

REFERENCES 65

3. CRISPR-EDITING RICE *ENDO-(1,3;1,4)-B-D-GLUCANASES* TO STUDY ITS INVOLVEMENT IN AERENCHYMA DEVELOPMENT 79

ABSTRACT 79

3.1. INTRODUCTION 80
3.1.1. Rice 80
3.1.2. Beginning of CRISPR 80
3.1.3. CRISPR/Cas9 technology 82
3.1.4. CRISPR/Cas9 and knockout 82
3.1.5. Gene knock-in and replacement 83
3.1.6. Rice *endo-(1,3;1,4)-β-D-glucanases* and mixed-linkage-glucan 85
3.1.7. MLG and aerenchyma development 86
3.2. GOAL 86
3.3. MATERIAL AND METHODS 87
3.3.1. Plant material 87
3.3.2. Design of *OsEgl1* and *OsEgl2* sgRNA targets 87
3.3.3. Cloning fragments of *OsEgl1* and *OsEgl2* 88
3.3.4. Biolistic and rice tissue culture 88
3.3.5. Genotyping 89
3.3.6. Heterologous expression of SBLIC1 89
3.3.6.1. Cloning Sblic1 into the bacterial expression vector pET30 89
3.3.6.2. SBLIC1 expression and purification 90
3.4. RESULTS 90
3.4.1. Expression profile of *OsEgl1* and *OsEgl2* 90
3.4.2. Genotyping 91
3.4.2.1. Cas9 confirmation 91
3.4.2.2. *OsEgl1* and *OsEgl2* amplifications using edited gDNA 92
3.4.2.3. *OsEgl1* and *OsEgl2* RFLP analysis 93
3.4.2.4. T7E1 assay 94
3.4.2.5. Sanger sequencing 95
3.4.3. Acquisition of *OsEgl2* T-DNA line 95
3.5. DISCUSSION 95
3.6. CONCLUSION 96

REFERENCES.....96
4. FINAL CONSIDERATIONS 101
APPENDIXES 103

RESUMO

Raízes primárias de *Sorghum bicolor* como modelo para os estudos dos mecanismos relacionados à hidrólise do glucano de ligação mista durante o desenvolvimento do aerênquima

Sorghum bicolor é uma das culturas cerealíferas mais importantes do mundo devido à sua alta eficiência de fixação de carbono, aquisição de nitrogênio, grande adaptabilidade ao cultivo em ambientes distintos e, acima de tudo, utilização como alimento básico na África e na Ásia. A coleção de germoplasma de sorgo, a qualidade do genoma sequenciado e os avanços recentes na transformação genética também colocaram esta espécie como um modelo promissor entre as gramíneas C_4. O sorgo, como todas as gramíneas, é constituído de parede celular do tipo II, cuja principal característica são as quantidades significativas dos polissacarídeos arabinoxilanos e β-D-(1,3;1,4)-glucanos de ligação mista (GLM). O GLM é um polímero hemicelulósico de D-glicose cuja cadeia linear contém principalmente ligações glicosídicas β-(1,4) intercaladas com poucas ligações glicosídicas β-(1,3) que torcem a cadeia, transformando-a em um polímero mais hidrossolúvel. Como resultado, as propriedades químicas do GLM são atrativas para a biotecnologia e, então, a compreensão da síntese e hidrólise de GLM são importantes tópicos. As "liquenases", tecnicamente conhecidas como endo-β-D-(1,3;1,4)-glucanases, hidrolisam especificamente as ligações β(1,3) que são imediatamente seguidas pelas β(1,4). Elas são enzimas codificadas pelos genes das *endo-(1,3;1,4)-β-D-glucanases* da família das glicosil hidrolases 17 (GH17). Estudos recentes com raízes de cana-de-açúcar têm mostrado uma forte correlação entre um aumento gradual no nível de genes e proteínas de endo-β-D-(1,3;1,4)-glucanases à medida que o aerênquima se desenvolve em espaços gasosos. Assim como na cana-de-açúcar e no arroz, o sorgo tem aerênquima lisígeno constitutivo, embora possua genoma diploide sequenciado, diferindo do complexo genoma da cana-de-açúcar que dificulta inferências filogenéticas robustas. Assim, para uma compreensão molecular mais aprofundada em relação à hidrólise de GLM e formação de aerênquima, utilizamos raízes primárias de sorgo. A raiz primária de sorgo com sete dias não está ramificada e, por conseguinte, permite uma caracterização anatômica detalhada e rápida pela técnica de microtomografia de raios-X. Dividimos a raiz em três segmentos (S1, S2 e S3), em que S1 não tem aerênquima, S2 é a iniciação do aerênquima e S3 é um estágio mais avançado no desenvolvimento do aerênquima. Inferências indicaram as GH17 endo-(1,3;1,4)-β-D-glucanases totalmente exclusivas de Poaceae, família em que o sorgo possui três "liquenases" (*Sblic1*, *Sblic2* e *Sblic3*) e arroz duas (*OsEgl1* e *OsEgl2*). Todavia, a PCR em tempo real revelou expressão diferencial somente para *Sblic1*, o qual aumentou dez vezes de S1 para S3. Ensaios enzimáticos com extratos brutos detectaram um aumento na atividade das endo-(1,3;1,4)-β-D-glucanases (S1<S2). Concomitantemente, o fracionamento da parede celular mostrou um declínio na quantidade relativa para GLM (S1> S2). Para verificar se um nocaute nas *endo-(1,3;1,4)-β-D-glucanases* comprometeria o desenvolvimento dos espaços gasosos, decidimos usar a ferramenta de edição CRISPR nos genes do arroz (*OsEgl1* e *OsEgl2*). Nossa decisão levou em consideração a alta estabilidade para a transformação genética do arroz, o tempo de financiamento e, especialmente, o domínio da cultura de tecido de arroz em Rutgers, The State University of New Jersey. *OsEgl1* e *OsEgl2* mostraram ser expressas nas raízes. Ambos os genes candidatos foram alvos de gRNAs, os quais foram clonados no módulo de CRISPR

para arroz psgR-Cas9-Os. Subsequentemente, os cassetes foram subclonados no vetor de transformação de plantas pCAMBIA1300 que foi usado na biobalística. Transformamos calos de arroz e submetemos os transformantes ao meio de seleção com higromicina. A genotipagem de plantas mostrou a presença de Cas9, embora nenhuma mutação específica tenha sido detectada por análises de RFLP, ensaios de T7E1 e sequenciamento Sanger. Notadamente, adquirimos uma linhagem de T-DNA para *OsEgl2*, a qual pode ser um valioso material transgênico para os estudos de hidrólise de GLM em uma eventual mutação de perda de função em *OsEgl2*. Portanto, ela agregaria informações significativas às nossas descobertas, levando-nos a afirmar se a hidrólise de GLM está diretamente envolvida na formação dos espaços gasosos. Em suma, a maior expressão de *Sblic1*, o aumento da atividade enzimática de endo-(1,3;1,4)-β-D-glucanases e a diminuição da quantidade relativa de GLM estão intercorrelacionados e, por conseguinte, concluímos que o GLM é degradado nas raízes e possivelmente associado à formação de aerênquima. Por último, enfatizamos que as raízes primárias do sorgo é um modelo promissor para estudos de GLM e o desenvolvimento de aerênquima.

Palavras-chave: Sorgo, Arroz, Raízes primárias, Aerênquima, Liquenano, β-glucano, Glucano de ligação mista, β-glucano de ligação mista, β-D-(1,3;1,4)-glucano de ligação, (1,3),(1,4)-β-D-glucano de ligação mista, Liquenase, Glucanases de ligação mista, β-D-(1,3;1,4)-endo-glucanases, Glicosil hidrolases 16 e 17 15, Celulose sintases-like F, H e J

ABSTRACT

The primary roots of *Sorghum bicolor* as a model to study the mechanisms related to mixed-linkage glucan hydrolysis during the aerenchyma development

Sorghum bicolor is one of the most important worldwide cereal crops due to its high carbon fixation efficiency, nitrogen acquisition, great adaptability to grow in distinct environments, and, above all, used as a staple food in Africa and Asia. Sorghum germplasm collection, quality of sequenced genome, and recent advances on genetic transformation have set this species as an up-and-coming model among C_4 grasses. Sorghum, like all grasses, is made up of type II cell wall, whose main feature is the significant amounts of arabinoxylan and mixed-linkage (1,3;1,4)-β-D-glucan (MLG) polysaccharides. MLG is a D-glucose hemicellulosic polymer whose linear chain holds mainly β-(1,4) glycosidic linkages intercalated with little β-(1,3) glycosidic linkages that kink the chain turning it into a more water-soluble polymer. As a result, MLG chemical properties are attractive for biotechnology then understanding MLG synthesis and hydrolysis are essential topics. "Lichenases," technically known as endo-β-D-(1,3;1,4)-glucanases, specifically hydrolyze β(1,3)-linkages that are immediately followed by β(1,4) ones. They are enzymes encoded by *endo-(1,3;1,4)-β-D-glucanases* genes of the glycosyl hydrolases family 17 (GH17). By contrast, MLG synthases are associated with the *cellulose synthase-like F, H,* and *J*. Recent studies with sugarcane roots have shown a strong correlation between a gradual increase in the level of endo-β-D-(1,3;1,4)-glucanases genes and proteins as aerenchyma develops into gas spaces. As in sugarcane and rice, sorghum has constitutive lysigenous aerenchyma and owns a diploid sequenced genome, differing from the complex sugarcane genome that hinders robust phylogenetic inferences. Thus, we used sorghum's primary roots for characterizing more in-depth molecular mechanisms involving MLG hydrolysis and aerenchyma formation. A non-branching seven-day-old primary root of sorghum allows a detailed anatomical characterization using the X-Ray microtomography technique. We divided the root into three segments (S1, S2, and S3), in which S1 has no aerenchyma, S2 is the aerenchyma initiation, and S3 a more advanced stage of aerenchyma development. Inferences indicated GH17 endo-(1,3;1,4)-β-D-glucanases utterly Poaceae-specific, family in which sorghum has three "lichenases" (*Sblic1*, *Sblic2*, and *Sblic3*) and rice two (*OsEgl1* and *OsEgl2*). However, real-time PCR revealed differential expression solely for *Sblic1*, which increased tenfold from S1 to S3. Enzymatic assays with crude extracts detected an increase in endo-(1,3;1,4)-β-D-glucanases activities (S1<S2). Concomitantly, cell wall fractioning showed a decline in the relative quantity of MLG (S1>S2). To verify if a knockout at endo-(1,3; 1,4)-β-D-glucanases would compromise gas spaces development, we decided to use the CRISPR-editing tool on rice genes (*OsEgl1* and *OsEgl2*). Our decision took into consideration the high stability for rice genetic transformation, funding time, and, above all, the mastery of rice tissue culture at Rutgers, The State University of New Jersey. *OsEgl1* and *OsEgl2* have shown to be expressed in roots. Both candidate genes were targeted by gRNAs, which were cloned into the rice CRISPR psgR-Cas9-Os module. Subsequently, the cassettes were subcloned into plant transformation pCAMBIA1300 vector that was used in biolistic. We transformed rice calli and submitted transformants to hygromycin selection medium. Genotyping of plants showed the presence of Cas9, although no on-target mutation has been detected by RFLP analysis, T7E1 assays, and Sanger sequencing. Notably, we acquired a T-DNA line for *OsEgl2*, which might

be valuable transgenic material for MLG hydrolysis' studies for an eventual loss-of-function mutation in *OsEgl2*. Therefore, it would aggregate significant information to our findings, leading us to assert whether MLG hydrolysis is directly involved in gas space formation. Ultimately, the higher expression of Sblic1, increase in endo-(1,3; 1,4)-β-D-glucanases activity, and decrease of relative MLG quantity are intercorrelated and, thus, we conclude that MLG is degraded in roots and possibly associated with aerenchyma formation. Lastly, we emphasize that sorghum's primary roots are a promising model for MLG studies and aerenchyma development.

Keywords: Sorghum, Rice, Primary roots, Aerenchyma, Lichenan, β-glucan, Mixed-linkage glucan, Mixed-linkage β-glucan, Mixed-linkage (1,3;1,4)-β-D-glucan, Mixed-linkage (1,3),(1,4)-β-D-glucan, Lichenase, Mixed-linkage glucanases, Endo-(1,3;1,4)-β-D-glucanases, Glycosyl hydrolysis 16 and 17 15, Cellulose synthases-like F, H, and J

LIST OF FIGURES

Figure 1. Primary root of sorghum seedling. (a) 3 days, (b) 4 days, and (c) 7 days after germination. C, coleoptile; FL, first leaf; PR, primary root; SL, second leaf. (Singh et al., 2010). 26

Figure 2. Primary structure of mixed-linkage (1,3;1,4)-β-D-glucan in Poaceae. MLG is a linear homopolymer composed mainly of (1,4)-linkages and less (1,3)-linkages. A single (1,3)-linkage insertion breaks up the chain's regularity, turning it into a more soluble-water polysaccharide. Adapted from Buckeridge and de Souza (2014) 29

Figure 3. Mixed-linkage glucan and aerenchyma development in sugarcane roots. The cross-sections (A, B, and C) correspond with the same developmental phases of the immunolabeled ones (D, E, and F). There is no aerenchyma at the root apex (A and D), and the MLG signals are noticeable in cell walls. Towards the root base, the aerenchyma formation begins (B, E), and MLG signals fade (E) slightly in the cortex (co). In the final phase (C, F) the aerenchyma is utterly developed, comprising many gas spaces. MLG's disappearance is prominent in the cortex (F), although the polymer remains in the vascular cylinder (vc) and peripheral tissues (pe): epidermis, exodermis, and sclerenchymatous cylinder. Controls (A-C) were stained with toluidine blue and immunolabeled (D-E) deployed MLG-directed antibody. (en) means endoderm. Scale bar represents 100 mm. (Leite et al., 2017). 35

Figure 4. Freehand cross-section from roots of mature sorghum. The aerenchyma is comprised of gas spaces, and some of them are indicated by white arrows. The dye used was Safrablau. Magnification of 20X. 51

Figure 5. Microtomography of roots of sorghum seedlings. The top image is a root scheme divided into three segments: no aerenchyma, aerenchyma initiation, and aerenchyma under development. Each segment has nearly 1.5 cm. This same arrangement (apex towards the root base) was adopted for the histological (A, B, and C) and X-Ray (E, F, and G) tomographic images. Figure D is an X-Ray image of the root used in the microtomography, whose total length is 74.1 mm. Figure A shows the root apex without aerenchyma. Figure B is the beginning of aerenchyma formation (asterisk in red showing an enlarged cell). Figure C is the aerenchyma at a further developmental stage, containing several enlarged cells. In D, the letters along the root's length (E, F, G) are the exact locations where cross-sections E, F, and G were taken from, respectively. The yellow arrow is an artifact and constitutes the foam material on which the roots were placed for analysis. The white arrows indicate the position of the gas spaces during the formation of the aerenchyma. Images were subjected to color density range using software CT-Analyzer. E is the root apex with no aerenchyma near the root tip (see the position in D). F is the beginning of aerenchyma formation, while G the aerenchyma is under development. Figures A and E are apical regions without aerenchyma. In contrast, Figures C and G are aerenchymas under development at the root base. Figures B and F, the root's intermediate region, are the gas spaces still at the beginning of its formation. Each section from micrography represents 9 μm. 52

Figure 6. MLG occurrence in living organisms. MLG is found in a bacterium, many fungi, some algae groups, and throughout plants, exempting the eudicots indicated by the dashed lines. The cladogram was generated in PhyloT (Letunic and Bork, 2007) with NCBI taxonomic data. There are groups with polytomy, which are still unranked. This figure was adapted from PhyloT. The names of some clades were placed according to the data of PhyloT and NCBI taxonomic databank. 53

Figure 7. Phylogeny of *CslFs*, *CslHs*, and *CslJs*. The *CslFs* clade are Poaceae-specific genes (red color), and *CslJs* are in green color. The *CslHs* family encompasses monocots (blue) and the magnoliid clade (lilac color). The red arrow indicates *SbCslF6*. The tree is rooted at the midpoint. 54

Figure 8. Phylogeny of GH17 *endo-(1,3;1,4)-β-D-glucanases*. The GH17 encompass the Poaceae-specific *endo-(1,3;1,4)-β-D-glucanases* and the *endo-(1,3)-β-glucanases,* which were used for rooting (Høj and Fincher, 1995) and merged into red triangles. IDs starting by "lichenase" indicate characterized endo-(1,3;1,4)-β-D-glucanases. Black arrows indicate sorghum genes, and blue arrows rice genes. *Sblic1* belongs to α clade and *Sblic2*/*Sblic* to the β one. The two rice genes (*OsEgl1* and *OsEgl2*) are shown in blue. 56

Figure 9. Expression profile of *Sblic1*, *Sblic2*, and *SbCslF6* during aerenchyma development. MLG hydrolases (A and B) and synthase (C). *Sblic1*(A) increases significantly from S1 to S3, while *Sblic2* (B) barely changes its expression. *SbClsF6* expression (C) slightly decreases from S1 to S2. S1 to S3 corresponds to segments from apex to base (1.5 cm each). Values are given as calibrated normalized relative quantities (CNRQ Values are means (n=3) ± standard errors, and letters represent the statistical difference among segments according to Tukey's test ($p < 0.05$). 57

Figure 10. Detection of DP3 and DP4 by thin-layer chromatography. Products of positive control (C+) are DP3 and DP4, indicated by arrows. Negative controls (C-) are pre-boiled crude extracts with barley MLG. The first segment has no bands, whereas the second and third segments display DP3 and DP4 bands, indicating MLGase activity. 58

Figure 11. Enzymatic assays' chromatogram with crude extracts. The positive control (blue) is on the secondary axis (y) on the right side. The first segment is in green color, the second in red, and the third in lilac color. Arrows indicate DP3 and DP4 metabolites upon MLG hydrolysis using commercial MLGase. At 8.0 min elution time, an unknown oligosaccharide could be cellobiose (DP2), a disaccharide produced by further hydrolysis of DP3 and DP4 by exo-β-glucanases (Kuge et al., 2015). 59

Figure 12. Dr. Mojica at Santa Pola's salt flat, Spain. The microbiologist has been invested as Dr. honoris causa from the Complutense University of Madrid due to his contribution to CRISPR technology (Fernández, 2021). One can see a buildup of salt on the lake's edge, located in the Province of Alicante, Valencian Community. Photo by Raúl Belinchón and taken from (Ansede, 2017). 81

Figure 13. *OsEgl1* and *OsEgl2* expression level in roots. In (A), the black arrow indicates a high expression for *OsEgl1* in roots. In (B), the black arrow indicates medium expression for *OsEgl2* in roots. The figures were adapted and obtained using the Genevestigator tool (Hruz et al., 2008), whose analyses are based on public microarray data (Rice Genome Affymetrix). 91

Figure 14. Cas9 confirmation. (A) and (B) show amplification of Cas9 (300 bp) in all samples. C+ are positive controls; Wt means wild type. RD365s are edited plants for *OsEgl1*, and RD366s are *OsEgl2*. 92

Figure 15. *OsEgl1* and *OsEgl2* amplifications using genome-edited plants as templates. 92

Figure 16. *OsEgl1* RFLP analysis. (A) The scheme above photos indicates the bands would be generated from wild-type (Wt) amplicon upon *SacII* digestion. Both, digested and undigested Wt are controls. RD365-1 and RD365-2 (A and B) upon *SacII* digestion generated bands like the digested Wt, indicating no on-target mutation. 93

Figure 17. *OsEgl2* RFLP analysis. (A) and (B) have OsEgl2 amplicons (465 bp). Bands around 291/174 bp indicates eventual digestion by XmaI. Digested RD366s amplicons may contain undigested bands and incomplete digestion (465 bp). 94

Figure 18. T7E1 assays. RD365s are *OsEgl1*amplicons (478 bp) and RD366s are *OsEgl2* (465 bp). The arrow indicates 500 bp. Single bands suggested no DNA heteroduplexes. 94

Figure 19. Micrograph of the first segment. The first segment starts at the root apex and has no aerenchyma. The diagram above comprises the whole primary root of this microtomography, divided into 5 segments, and the first one is in blue. All images are equidistantly displayed from each other (from root apex towards the base). In (1), the ellipse shows the beginning of the apex. The up arrow constitutes the foam material on which the roots were placed for analysis and the down arrow the plastic that involves the root. The root's diameter is slightly larger in (2) and (4) due to the plastic's compression. Images were subjected to color density range using software CT-Analyser. 104

Figure 20. Micrograph of the second segment. The second segment is the initiation of aerenchyma development. The diagram above comprises the whole primary root of this microtomography, divided into 5 segments, and the second one is in blue. All images are equidistantly displayed from each other (from root apex towards the base). In (1), the circle shows the root. The up arrow constitutes the foam material on which the root was placed for analysis and the down arrow the plastic that involves the root. The first gas spaces start to develop and are noticeable in (27) and (28), indicated by arrows. Images were subjected to color density range using software CT-Analyser. 104

Figure 21. Micrograph of the third segment. The third segment is the aerenchyma under development. This pattern has been found in the fourth and fifth segments as well. The diagram above comprises the whole primary root of this microtomography, divided into 5 segments, and the third one is in blue. All images are equidistantly displayed from each other (from root apex towards the base). White arrows indicate some gas spaces in (1), (3), (4), (13), (14), (15), and (19). The ellipses represent a set of merged gas spaces in (21) and (26). Images were subjected to color density range using software CT-Analyser. 104

Figure 22. Micrograph of the fourth segment. The fourth segment is the aerenchyma under development. This pattern has been found in the third and fifth segments. The diagram above comprises the whole primary root of this microtomography, divided into 5 segments, and the fourth one is in blue. All images are equidistantly displayed from each other (from root apex towards the base). The ellipses represent a set of merged gas spaces in (2), (3), (4), (18), (20), (23), (24), (27), (28). Images were subjected to color density range using software CT-Analyser. 104

Figure 23. Micrograph of the fifth segment. The fifth segment is the aerenchyma under development. This pattern has been found in the third and fourth segments as well. The diagram above comprises the whole primary root of this microtomography, divided into 5 segments, and the fifth one is in blue. All images are equidistantly displayed from each other (from root apex towards the base). The ellipses represent a set of merged gas spaces in (1), (2), (3), (4), (6), (8), (9), (13), and (17). White arrows indicate some gas spaces in (18). Images were subjected to color density range using software CT-Analyser. 104

Figure 24. Species tree of tracheophytes. The cladogram shows the clustering pattern of some species used in our work. The cladograms were generated in PhyloT (Letunic and Bork, 2007) with NCBI taxonomic data. There are groups with polytomy that are unranked..... 104

Figure 25. Evolutionary tree of GH17 *endo-(1,3;1,4)-β-glucanases* in Poaceae. Each node's values are related to each branch's length and may represent the extent of divergence. The arrows indicate the sorghum genes. The estimated change average of *Sblic1* is higher than *Sblic2* and *Sblic3*. The two merged red triangles are *endo-(1,3)-β-glucanases* related to callose used as root point. 104

Figure 26. *Sblic2* expression profile. *Sblic2* stands out for its elevated expression in young leaves (0 and -1). Stem, leaves, and mature roots were obtained from sixty-day-old sorghum, while segments were acquired from seven-day-old seedlings. Values are means (n=3) ± standard errors, and letters represent the statistical significance among samples according to Tukey's test ($p < 0.05$). 104

Figure 27. Heterologous expression of SBLIC1 and its solubilization from inclusion bodies. In (A), (1) Molecular eight; (2) pET30b (empty vector); (3) Purified soluble fraction; (4) 1 μg of BSA; (5) 5 μg of BSA; (6) 10 μg of BSA; (9) Cell debris (inclusion bodies). SBLIC1 was found in inclusion bodies (ninth column indicated by blue arrow) but not in the soluble fraction (third column) after protein extraction. In (B), (1) molecular weight; (2) inclusion bodies submitted to affinity purification; (3) 2 μg of BSA; (4) 5 μg of BSA; (5) inclusion bodies not submitted to purification. Eventually, SBLIC1 did not bind to collum upon purification. Bovine serum albumin (BSA), black arrows are 37 kDa, and blue arrows indicate SBLIC1 (37.12 kDa). 104

Figure 28. Sequence of *OsEgl2* T-DNA line aligned with wild type. The alignment of wild type with-DNA line revealed the T-DNA insertion within *OsEgl2* CDS and in the 3'UTR. The mutant ID is M00089780 and was acquired from Taiwan. 104

LIST OF TABLES

Table 1. Identifying characteristics and approximate time intervals among stages of sorghum growth. 25

Table 2. Enzymatic activity as aerenchyma develops. 59

Table 3. MLG relative quantity and DP3:DP4 ratios. 60

Table 4. Percentage of neutral monosaccharides extracted from the alcohol-insoluble residue. 61

Table 5. List of primers. 103

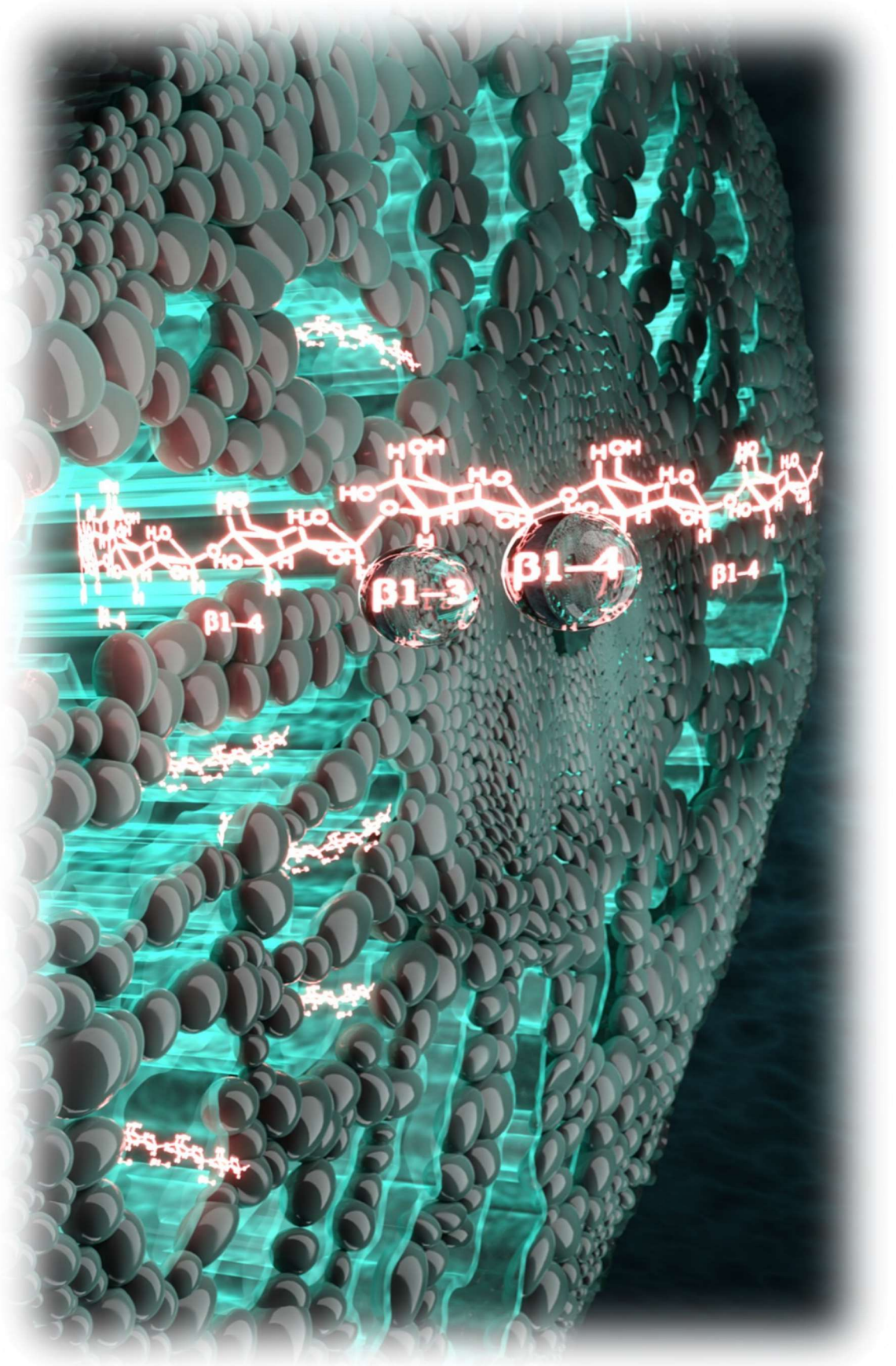
β1–3
β1–4
β1–4
β1–4

1. PREFACE

This work comprises two chapters. In the first chapter, we narrate all experiments related to biochemical and molecular data using sorghum roots, and in the second chapter, we describe the data obtained from CRISPR-editing on rice genes.

The systematic studies of β-glucans started in the early 20th century by German researchers (Karrer et al., 1924). Back then, biochemists did not make a clear distinction between cellulose and β-glucans, considered their structural similarity.

β-glucans are D-glucose polymers linked by glycosidic β-bonds, typically comprising a (1,3)-linkages within the chain (Stone, 2009). Among several categories, mixed-linkage β-D-(1,3;1,4)-glucans (MLG) stand out as a β-glucan polysaccharide, constituting a significant amount of Poaceae cell walls (Buckeridge et al., 2004). Despite known as a "unique" feature of grass cell walls, MLG has been found in divergent organisms, like bacteria, fungi, algae, and plants (Little et al., 2018), which, ultimately, have attempted researchers to postulate that MLG has multiple evolutionary origins (Müller et al., 1998; Planas, 2000). Our systematic review suggests that MLG's primary function seemed to be a structural one. Later, in Poaceae, the polymer appeared as storage and structural polysaccharide (Buckeridge, 2010, 2018).

Given the high importance of MLG in bioenergy (Burton and Fincher, 2009; Pauly and Hake, 2011; de Souza et al., 2013; Loqué et al., 2015; Vega-Sánchez et al., 2015), the brewing industry (Morgan and Gothard, 1977), and nutrition (Kahlon et al., 1993; Bourdon et al., 1999; Behall et al., 2004; De Paula et al., 2005), scientists have intensively studied its synthesis and hydrolyses.

In monocots, MLG is synthesized by enzymes encoded by *cellulose-synthase like H*, *F,* and *J* (*CslF*, *CslH,* and *CslJ*). In Poaceae (Little et al., 2018), MLG hydrolysis occurs by *endo-β-(1,3;1,4)-glucanases* (Akiyama et al., 2009), which have shown to be Poaceae-specific in this work. Also, our GH17 phylogeny indicates three sorghum *endo-β-(1,3;1,4)-glucanases* (*Sblic1*, *Sblic2,* and *Sblic3*) and two in rice (*OsEgl1* and *OsEgl2*).

Interestingly, our group has obtained compelling data correlating MLG hydrolysis with aerenchyma development in sugarcane roots (Leite et al., 2017; Grandis et al., 2019). Aerenchyma in roots are longitudinally interconnected gas spaces that promote gas diffusion between plant radicular and aerial systems (Arber, 1920; Drew et al., 2000). Their development takes place from the root apex towards the base (Leite et al., 2017). In rice (Justin and Armstrong, 1991), sorghum (Promkhambut et al., 2011), and sugarcane (Begum et al., 2013), aerenchyma is constitutively developed, and two distinct phases are remarkable: programmed cell wall death and cell wall

modification (Leite et al., 2017). Researchers have demonstrated that MLG is degraded as aerenchyma develops at this second stage, possibly associated with the higher level of MLG proteins and genes vis-à-vis the polymer hydrolysis (Leite et al., 2017; Grandis et al., 2019).

Even though sugarcane aerenchyma studies on the cell wall disassembling have been established as a model, its genome complexity and ploidy hinder detailed molecular analysis (Thirugnanasambandam et al., 2018). Accordingly, sorghum, known for the quality of its sequenced genome and, above all, importance in bioenergy, was used by our group to investigate molecular details regarding MLG hydrolysis associated with aerenchyma development. Indeed, primary sorghum primary roots have excelled as an up-and-coming model for our purpose. Notably, our results have concurred with sugarcane studies and, significantly, gave more details about the genes related to MLG hydrolysis and synthesis. Ultimately, reinforcing our hypothesis that MLG is associated with aerenchyma development.

Although scientific literature displays several protocols for sorghum genetic manipulation (Do et al., 2016, 2018; Liu et al., 2019a, 2020), few researchers have mastered sorghum tissue culture. Interestingly, some American universities offer CRISPR-editing on sorghum and its transformation for a high price. Presumably, sorghum genetic engineering will be mastered worldwide in a few years.

At the renowned Rutgers University, an institution we collaborate with, rice genetic engineering is mastered. Therefore, we decided to use the CRISPR-editing technique on *OsEgl1* and *OsEgl2*. At the American institution, we obtained potential transgenic lines, which eventually will contribute to the understanding of the MLG hydrolysis regarding aerenchyma formation.

In a nutshell, this doctoral dissertation comprises studies involving biochemical and molecular analysis of MLG hydrolysis associated with aerenchyma development in sorghum and rice. All sorghum data were obtained at the University of São Paulo and are in the first chapter. Rice gene editing was carried out at Rutgers University and is described in the second chapter.

REFERENCES

Akiyama, T., Jin, S., Yoshida, M., Hoshino, T., Opassiri, R., and Ketudat Cairns, J. R. (2009). Expression of an endo-(1,3;1,4)-β-glucanase in response to wounding, methyl jasmonate, abscisic acid and ethephon in rice seedlings. *J. Plant Physiol.* 166, 1814–1825. doi:10.1016/j.jplph.2009.06.002.

Arber, A. (1920). *Water plants, a study of aquatic angiosperms*. Cambridge, UK: Cambridge University Press.

Begum, M. K., Alam, M. R., and Islam, M. S. (2013). Adaptive mechanisms of sugarcane genotypes under flood stress condition. *World J. Agric. Sci.*

Behall, K. M., Scholfield, D. J., and Hallfrisch, J. (2004). Diets containing barley significantly reduce lipids in mildly hypercholesterolemic men and women. *Am. J. Clin. Nutr.* 80, 1185–1193. doi:10.1016/S0084-3741(08)70311-1.

Bourdon, I., Yokoyama, W., Davis, P., Hudson, C., Backus, R., Richter, D., et al. (1999). Postprandial lipid, glucose, insulin, and cholecystokinin responses in men fed barley pasta enriched with β-glucan. *Am. J. Clin. Nutr.* 69, 55–63.

Buckeridge, M. S. (2010). Seed cell wall storage polysaccharides: Models to understand cell wall biosynthesis and degradation. *Plant Physiol.* 154, 1017–1023. doi:10.1104/pp.110.158642.

Buckeridge, M. S. (2018). The evolution of the Glycomic Codes of extracellular matrices. *BioSystems*. doi:10.1016/j.biosystems.2017.10.003.

Buckeridge, M. S., Rayon, C., Urbanowicz, B., Tiné, M. A. S., and Carpita, N. C. (2004). Mixed Linkage (1→3),(1→4)-β- d -Glucans of Grasses. *Cereal Chem.* 81, 115–127. doi:10.1094/CCHEM.2004.81.1.115.

Burton, R. A., and Fincher, G. B. (2009). (1,3;1,4)-β-D-glucans in cell walls of the poaceae, lower plants, and fungi: A tale of two linkages. *Mol. Plant.* doi:10.1093/mp/ssp063.

De Paula, A. C. C. F. F., Sousa, R. V., Figueiredo-Riberio, R. C. L., and Buckeridge, M. S. (2005). Hypoglycemic activity of polysaccharide fractions containing β-glucans from extracts of *Rhynchelytrum repens* (Willd.) C.E. Hubb., Poaceae. *Brazilian J. Med. Biol. Res.* 38, 885–893. doi:10.1590/S0100-879X2005000600010.

de Souza, A. P., Leite, D. C. C., Pattathil, S., Hahn, M. G., and Buckeridge, M. S. (2013). Composition and Structure of Sugarcane Cell Wall Polysaccharides: Implications for Second-Generation Bioethanol Production. *Bioenergy Res.* 6, 564–579. doi:10.1007/s12155-012-9268-1.

Do, P. T., Lee, H., Mookkan, M., Folk, W. R., and Zhang, Z. J. (2016). Rapid and efficient Agrobacterium-mediated transformation of sorghum (Sorghum bicolor) employing standard binary vectors and bar gene as a selectable marker. *Plant Cell Rep.* doi:10.1007/s00299-016-2019-6.

Do, P. T., Lee, H., Nelson-Vasilchik, K., Kausch, A., and Zhang, Z. J. (2018). Rapid and Efficient Genetic Transformation of Sorghum via Agrobacterium-Mediated Method. *Curr. Protoc. plant Biol.* doi:10.1002/cppb.20077.

Drew, M. C., He, C. J., and Morgan, P. W. (2000). Programmed cell death and aerenchyma formation in roots. *Trends Plant Sci.* doi:10.1016/S1360-1385(00)01570-3.

Grandis, A., Leite, D. C. C., Tavares, E. Q. P., Arenque-Musa, B. C., Gaiarsa, J. W., Martins, M. C. M., et al. (2019). Cell wall hydrolases act in concert during aerenchyma development in sugarcane roots. *Ann. Bot.* doi:10.1093/aob/mcz099.

Justin, S. H. F. W., and Armstrong, W. (1991). Evidence for the involvement of ethene in aerenchyma formation in adventitious roots of rice (Oryza sativa L.). *New Phytol.* doi:10.1111/j.1469-8137.1991.tb00564.x.

Kahlon, T. S., Chow, F. I., Knuckles, B. E., and Chiu, M. M. (1993). Cholestrol-Lowering Effects in Hamsters of β-Glucan-Enriched Barley Fraction, Dehulled Whole Barley, Rice Bran, and Oat Bran and Their Combinations. *Cereal Chem.* 70, 435–440.

Karrer, P., Staub, M., Weinhagen, A., and Joos, B. (1924). Polysaccharide XXII. Zur Kenntnis der Lichenase und Reservecellulose (Lichenin). *Helv. Chim. Acta.* doi:10.1002/hlca.19240070116.

Leite, D. C. C., Grandis, A., Tavares, E. Q. P., Piovezani, A. R., Pattathil, S., Avci, U., et al. (2017). Cell wall changes during the formation of aerenchyma in sugarcane roots. *Ann. Bot.* 120, 693–708. doi:10.1093/aob/mcx050.

Little, A., Schwerdt, J. G., Shirley, N. J., Khor, S. F., Neumann, K., O'donovan, L. A., et al. (2018). Revised phylogeny of the cellulose synthase gene superfamily: Insights into cell wall evolution. *Plant Physiol.* 177, 1124–1141. doi:10.1104/pp.17.01718.

Liu, G., Li, J., and Godwin, I. D. (2019). "Genome editing by CRISPR/Cas9 in sorghum through biolistic bombardment," in *Methods in Molecular Biology* (Humana Press Inc.), 169–183. doi:10.1007/978-1-4939-9039-9_12.

Liu, G., Massel, K., Tabet, B., and Godwin, I. D. (2020). "Biolistic DNA Delivery and Its Applications in Sorghum bicolor," in *Methods in Molecular Biology* (Humana Press Inc.), 197–215. doi:10.1007/978-1-0716-0356-7_10.

Loqué, D., Scheller, H. V., and Pauly, M. (2015). Engineering of plant cell walls for enhanced biofuel production. *Curr. Opin. Plant Biol.* doi:10.1016/j.pbi.2015.05.018.

Morgan, A. H., and Gothard, P. G. (1977). A rapid, simple viscometric technique for indirect estimation of soluble β-glucan content of raw barley. *J. Inst. Brew.* 83, 37–38. doi:10.1002/j.2050-0416.1975.tb03790.x.

Müller, J. J., Thomsen, K. K., and Heinemann, U. (1998). Crystal structure of Barley 1,3-1,4-β-glucanase at 2.0-Å resolution and comparison with Bacillus 1,3-1,4-β-glucanase. *J. Biol. Chem.* 273, 3438–3446. doi:10.1074/jbc.273.6.3438.

Pauly, M., and Hake, S. (2011). Maize variety and method of production. *US Pat. 20,110,302,669*. Available at: http://www.freepatentsonline.com/y2011/0302669.html.

Planas, A. (2000). Bacterial 1,3-1,4-β-glucanases: structure, function and protein engineering. *Biochim. Biophys. Acta - Protein Struct. Mol. Enzymol.* 1543, 361–382. doi:10.1016/S0167-4838(00)00231-4.

Promkhambut, A., Polthanee, A., Akkasaeng, C., and Younger, A. (2011). Growth, yield and aerenchyma formation of sweet and multipurpose sorghum (Sorghum bicolor L. Moench) as affected by flooding at different growth stages. *Aust. J. Crop Sci.*

Stone, B. A. (2009). "Chapter 2.1 - Chemistry of β-Glucans," in, eds. A. Bacic, G. B. Fincher, and B. A. B. T.-C. Stone Biochemistry, and Biology of 1-3 Beta Glucans and Related Polysaccharides (San Diego: Academic Press), 5–46. doi:https://doi.org/10.1016/B978-0-12-373971-1.00002-9.

Thirugnanasambandam, P. P., Hoang, N. V., and Henry, R. J. (2018). The challenge of analyzing the sugarcane genome. *Front. Plant Sci.* 9, 616. doi:10.3389/fpls.2018.00616.

Vega-Sánchez, M. E., Loqué, D., Lao, J., Catena, M., Verhertbruggen, Y., Herter, T., et al. (2015). Engineering temporal accumulation of a low recalcitrance polysaccharide leads to increased C6 sugar content in plant cell walls. *Plant Biotechnol. J.* doi:10.1111/pbi.12326.

2. MIXED-LINKAGE GLUCAN HYDROLYSIS AND THE AERENCHYMA DEVELOPMENT IN PRIMARY ROOTS OF SORGHUM

ABSTRACT

The aerenchyma is a network of longitudinal interconnected gas spaces that promotes the diffusion of gases within roots. The lysigenous aerenchyma is inducible or constitutive and comprises two remarkable phases: programmed cell death and cell wall degradation. Although important discoveries of these two stages were obtained from studies with rice and maize, sugarcane roots stood out as a model for elucidating cell wall degradation mechanisms during the development of constitutive lysigenous aerenchyma. In the course of this process, a notable event is the degradation of the mixed-linkage (1,3;1,4)-β-D-glucan (MLG), a hemicellulosic polymer composed solely of glucose units. In plants, this polysaccharide is hydrolyzed by enzymes encoded by *endo-(1,3; 1,4)-β-D-glucanases* of the family glycosyl hydrolases 17 (GH17) and synthesized by proteins encoded by *cellulose synthase-like F*, *H*, and *J* (*CslF*, *CsH*, and *CslJ*). Although sugarcane has been established as a reference for aerenchyma cell wall modification, the complexity and polyploidy of its genome hinder robust inferences upon phylogenetic reconstructions. Phylogenetically close to sugarcane, *Sorghum bicolor*, on the other hand, is diploid and has been recognized for the quality of its genome sequencing. Moreover, the species has a rich germplasm collection and recent improvements in genetic transformation. It is highly adaptable to semi-arid regions, and all parts of the plant are usable, especially the grains. At the beginning of its development, the seeds germinate and develop a single primary root that has constitutive aerenchyma. Considering those essential features, we have used sorghum's primary roots to search genes and enzymes related to MLG hydrolysis during aerenchyma development. High-resolution tomography's anatomical characterization enabled the division of the root in three segments (S1, S2, and S3) from the apex towards the root base. At the root apex (S1), there is no aerenchyma. Subsequently, the gas spaces start to form (S2) and continue developing towards the base (S3). Phylogenetic inferences pointed out that *CslHs* are not monocot-restricted but encompass magnoliids. However, the GH17 *endo-(1,3;1,4)-β-D-glucanases* are Poaceae-specific and have three sorghum *endo-(1,3;1,4)-β-D-glucanases* (*Sblic1*, *Sblic2*, and *Sblic3*). The data suggest that *Sblic1* has accumulated more genetic divergence than *Sblic2* and *Sblic3,* both in a distinct clade. The gene expression analyzes showed low and continuous expression for *Sblic2* (S1=S2=S3), whereas *Sblic1* increased tenfold (S1<S3). Furthermore, there was a decrease in expression for *SbCslF6* (S1> S2), an MLG synthase. The enzymatic assays using crude extracts showed an increase in enzyme activities of endo-(1,3; 1,4)-β-D-glucanases (S1<S2), eventually SBLIC1 and SBLIC acting together. Concurrently, there was a decrease in the relative MLG quantity (S1> S2=S3) and a decline in glucose from structural polysaccharides (S1> S3), presumably associated with the reduction of MLG amount, a glucose polymer. Therefore, the gene expression, enzyme activity, MLG quantification, and glucose level are interconnected. Thus, we conclude that MLG is degraded in roots and eventually associated with gas spaces formation. We emphasize that the plant material's fast acquisition and simplicity facilitated the anatomical characterization and subsequent analysis. Finally, we affirm that sorghum's primary roots are an up-and-coming model for understanding the MLG hydrolysis throughout aerenchyma development.

Keywords: sorghum; primary roots; aerenchyma; lichenan; β-glucan; mixed-linkage glucan; mixed-linkage β-glucan; mixed-linkage (1,3;1,4)-β-D-glucan; mixed-linkage (1,3),(1,4)-β-D-glucan; lichenase; mixed-linkage glucanases; endo-(1,3;1,4)-β-D-glucanases; glycosyl hydrolysis 17; cellulose synthases-like F, H, and J

2.1. INTRODUCTION

2.1.1. Sorghum

Botanists, evolutionists, and archaeologists have debated about the origin and domestication of C_4 cereal sorghum for many years. Anthropological records suggest that hunter-gatherers already had contact and used wild and landraces of sorghum varieties around 8,000 BC (Venkateswaran et al., 2019). The domestication of the sorghum genus may have taken place near 4,000 BC in Sudan's western savannah, sorghum's center of origin (Smith, C.W; Frederiksen, 2000). Archaeological evidence shows that sorghum has been cultivated in the far Easter Sahel at the beginning of the second millennium BC and perhaps even earlier, before being migrated to India (Winchell et al., 2018), the second center of origin (Hariprasanna and Patil, 2015).

Sorghum spp. comprise about 22 species (Dillon et al., 2007) and solely *Sorghum bicolor* (L.) Moench contributes to the majority of cultivated sorghum (Venkateswaran et al., 2019). Economically, *S. bicolor*, here mentioned as sorghum, belongs to one of the important angiosperm families: Poaceae (Schmid et al., 2007; Simpson, 2010).

Agronomically, sorghum can be classified as grain sorghum, biomass sorghum, forage sorghum, and sweet sorghum (Rooney, 2014). Despite this variable and non-taxonomic classification, "grain sorghum" has been used as food and biofuel production in the United States and "sweet sorghum" as a sweetener and forage sorghums for animal grazing hay or silage. Moreover, its production can be mechanized from planting to harvest, using equipment already used in other crops, such as soybeans, wheat, and rice (Brandão, 2007).

Sorghum is the fifth most important cereal crop, following wheat, rice, maize, and barley in both total production and acreage in the world (Stutts and Vermerris, 2020). The high productivity of this plant is related to the high efficiency in carbon fixation via C_4 photosynthesis, nitrogen acquisition (Olson et al., 2013), and resistance to stress from heat and drought (Rosenow et al., 1983; Kebede et al., 2001; Sleper and Poehlman, 2006). Besides, plant breeders' extensive work gave rise to cultivars that are resistant to flood (Promkhambut et al., 2011), temperate climates (Zegada-Lizarazu and Monti, 2012), lodging (Sleper and Poehlman, 2006), moderate tolerance to salt stress (Hassanein and Azab, 1993), and aluminum toxicity (Sleper and Poehlman, 2006).

Among grasses, *stricto sensu*, sorghum stands out due to the lower inputs required for bioethanol production implementation (Reddy et al., 2005). Another advantage of this plant vis-à-vis the socio-economic impacts is land use since distinct organs of sorghum can be used for food production (grains) and biofuels (stalk) (Reddy et al., 2008).

2.1.2. Developmental stages of sorghum

According to Vanderlip and Reeves (1972), after germination, sorghum development is separated into three stages: vegetative, reproductive, and grain filling, totaling 95 days. They are shown in Table 1.

Table 1. Identifying characteristics and approximate time intervals among stages of sorghum growth.

Growth stage	Approximate days after emergence *	Identifying characteristic
0	0	Emergence. Coleoptile visible at the soil surface
1	10	The collar of the third leaf is visible
2	20	The collar of the fifth leaf is visible
3	30	Growing point differentiation. Approximately eight leaf stage by previous criteria
4	40	Final leaf visible in the whorl
5	50	Boot. Head extended into flag leaf sheath.
6	60	Half-bloom. Half of the plants at some stage of bloom
7	70	Soft dough
8	85	Hard dough
9	95	Physiological maturity. Maximum dry matter accumulation

*Approximate days required for hybrids of RS 610 maturity grown at Manhattan, Kansas. Adapted from Vanderlip and Reeves (1972).

2.1.3. Germination

Germination of sorghum seeds starts with the seed imbibing water held in its surroundings and culminate with the seed coat's radicle protrusion. Several variables affect the rate at which germination occurs, and water and temperature are the most important ones (Roozeboom et al., 2016). Brar and Stewart (1994) reported that seeds of hybrid sorghum generally take seven days to germinate at 15.5 °C and one day to germinate at 37.5 °C. Although

there is a broad temperature range for seed germination, germination's optimal temperature ranges from 21 °C to 35 °C (Mortlock and Vanderlip, 1989; Brar and Stewart, 1994).

2.1.4. Primary root development

The development of sorghum's primary roots may vary among cultivars (Singh et al., 2010; Hariprasanna and Patil, 2015). After germination, sorghum produces a single primary root and a coleoptile (Figure 1). The latter originates two leaves approximately in seven days, and the former develops lateral branches. The primary root gets longer and becomes vertically orientated, especially from the second to third leaf stage. At this point, higher-order lateral branches are more evident and increase during plant growth, and lateral roots start to appear when four to five leaves have fully expanded (Singh et al., 2010).

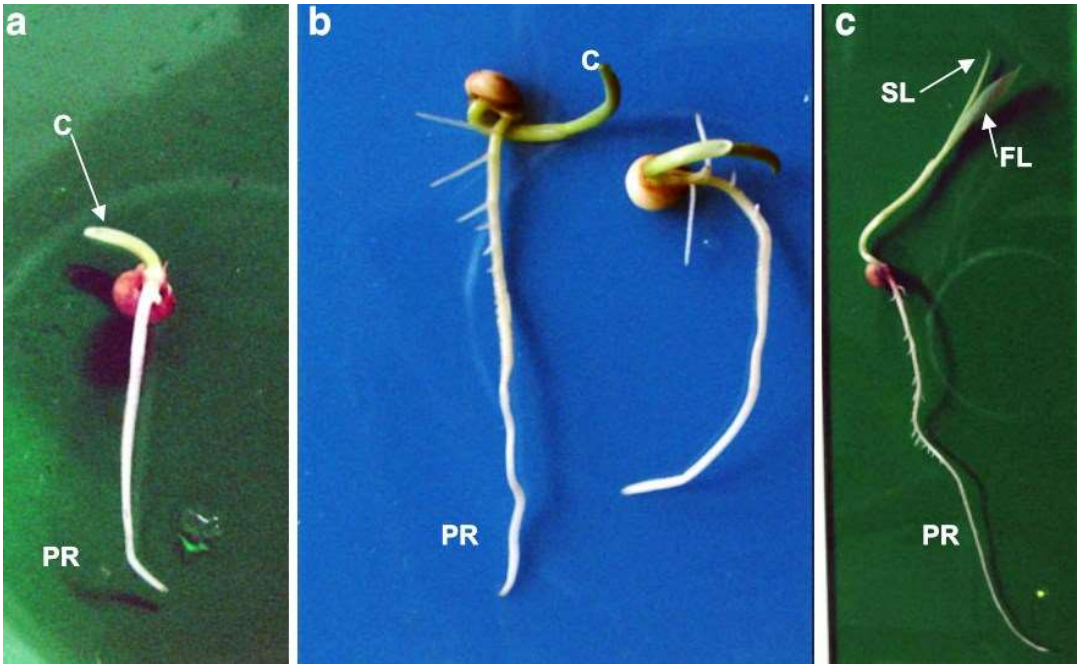

Figure 1. Primary root of sorghum seedling. (a) 3 days, (b) 4 days, and (c) 7 days after germination. C, coleoptile; FL, first leaf; PR, primary root; SL, second leaf. (Singh et al., 2010).

2.1.5. Plant cell wall and mixed-linkage glucan

Extracellular matrices are complexes of polymers that surround most cells of living beings. These matrices are arranged in an encoded fashion, where different polymers (mainly polysaccharides, with lower proportions of proteins, phenolic compounds, and others) are

arranged distinctively, resulting in different biological functions. These distinctive arrangements are named the glycomic code (Buckeridge, 2018).

In plants, the glycomic code gives rise to at least three types of cell walls: I, II, and III (Gibeaut and Carpita, 1993; Silva et al., 2011). In general, the glycomic code displayed by plant cell walls contains five main classes of polymers: cellulose, hemicellulose, pectin, proteins, and lignin. They vary in composition and are combined to form the cell wall types I, II, and III. Although extraordinarily complex and diverse, pectins have not been used to distinguish cell wall types. Conversely, hemicelluloses have been used to distinguish cell wall types. Type I walls stand out by xyloglucan's presence as the main hemicellulose, type II by arabinoxylan, and mixed-linkage (1,3;1,4)-β-D-glucan (MLG), and type III by a higher proportion of mannans in their walls.

Cellulose, being an ancient extracellular matrices polymer, can be found in practically all groups of living organisms, except for Archaea (McNamara et al., 2015). During evolution, it became central to the extracellular matrices mechanical properties of photosynthetic organisms (plants, green and red algae), differing from heterotrophic groups of organisms (bacteria, fungi, and animals), which produce polysaccharides containing nitrogen (Buckeridge, 2018). Although plant cellulose synthase complexes produce most of the cellulose on the planet, the enzyme has a bacterial origin (Römling and Galperin, 2015).

Ancestral organisms, like bacteria, have homologous genes to the cellulose synthases encoding enzymes capable of producing MLG (Pérez-Mendoza et al., 2015, 2017; Baena et al., 2019). In monocots, MLG's synthesis is associated with *cellulose synthase-like* (*Csl*) *F, H,* and *J* (*CslF*, *CslH,* and *CslJ*) families (Burton et al., 2006; Doblin et al., 2009; Ermawar et al., 2015; Little et al., 2018). By contrast, enzymes concerning MLG's hydrolysis in plants are found within two families of glycosyl hydrolases (GH): GH16 and GH17 (Høj and Fincher, 1995; Planas, 2000; Eklöf et al., 2013; McGregor et al., 2017; Tamura et al., 2017).

2.1.6. MLG occurrence

In monocots, Poales is the taxon in which MLG has been studied the most and, nonetheless, researchers are not unanimous regarding MLG's presence or absence in different subgroups within this order (Smith and Harris, 1999; Trethewey et al., 2005). Dissension apart, Harris and Fincher (2009a) have considered the MLG presence in the following families of Poales: Poaceae, Cyperaceae, Xyridaceae, Ecdeiocolaceae, Juncaceae, Flagellariaceae, Joinvilleaceae, and Restionaceae. More recently, Little and coworkers (2018) have shown a more

widespread MLG distribution across monocots, including *Anthurium amnicola* (Alismatales), *Acorus americanus* (Acorales), *Musa acuminata* (Musaceae), and *Ananas comosus* (Bromeliaceae).

The wide distribution of MLG is beyond monocots, and, surprisingly, the polymer has been found in bacteria, like *Sinorhizobium meliloti* (Pérez-Mendoza et al., 2015, 2017; Baena et al., 2019) and "MLG-like oligomers" in *Sarcina ventriculi* (Lee and Hollingsworth, 1997), gram-positive coccus.

In ancestral eukaryotes, the hemicellulose has been discovered in one dinoflagellate (Nevo and Sharon, 1969), xanthophyte (Ford and Percival, 1965), red alga (Lechat et al., 2000), several brown algae (Salmeán et al., 2017), and green algae as well (Popper and Fry, 2003; Eder et al., 2008). In Viridiplantae, in addition to green algae, the polymer exists in liverwort (Popper and Fry, 2003), lycophyte (Fry et al., 2008b; Harholt et al., 2012), and basal tracheophytes, such as horsetails and Aspleniaceae (Fry et al., 2008b; Sørensen et al., 2008).

In organisms closer to the Animalia kingdom, like fungus, MLG was detected in lichen *Cetraria islandica* by the early 20th century (Karrer et al., 1924; Pringsheim and Kusenack, 1924) and other groups of fungi (Honegger and Haisch, 2001; Pettolino et al., 2009).

2.1.7. MLG fine structure

Mixed-linkage glucans, sometimes nonspecifically named as β-glucans, are unbranched linear polymers consisting of β(1,3) and β(1,4)-glycosyl residues. Staudte and coworkers (1983) stated that two or three blocks of β(1,4)-glycosyl residues in a row are randomly arranged, indicating that β(1,3)-glycosyl residues are irregularly spaced in the polymer chain. These "irregular" insertions would kink the polysaccharide along its chain (Figure 2). Consequently, the angular inclination would make the polymer chains interact less and, ultimately, more water-soluble. On the other hand, linearity composed of adjacent sequences of β(1,4)-glycosyl residues would confer to the chain a "cellulose conformation resemblance" and less solubility in water (Buckeridge et al., 2004; Stone, 2009).

MLG's fine structure and identification can be assessed by enzymes able to hydrolyze it. The enzymes used the most are the "lichenases" (EC 3.2.1.73). "Lichenases" may have their etymology from lichenan, a type of MLG (Iakiviak et al., 2011) discovered in the early 20th (Karrer et al., 1924; Pringsheim and Kusenack, 1924). The lichenases are non-specific names for bacterial, fungal, and plant endo-(1,3;1,4)-β-D-glucanases (EC3.2.1.73), which cleave specifically β(1,4) bonds that immediately follow a β(1,3) bond within the MLG polymer. This reaction yields oligomers with different degrees of polymerization (DP), such as trisaccharide (DP3) and

tetrasaccharide (DP4). Eventually, exo-β-glucanases (EC 3.2.1.74) hydrolyzes DP3 and DP4, thus, producing disaccharides (DP2) (Kuge et al., 2015).

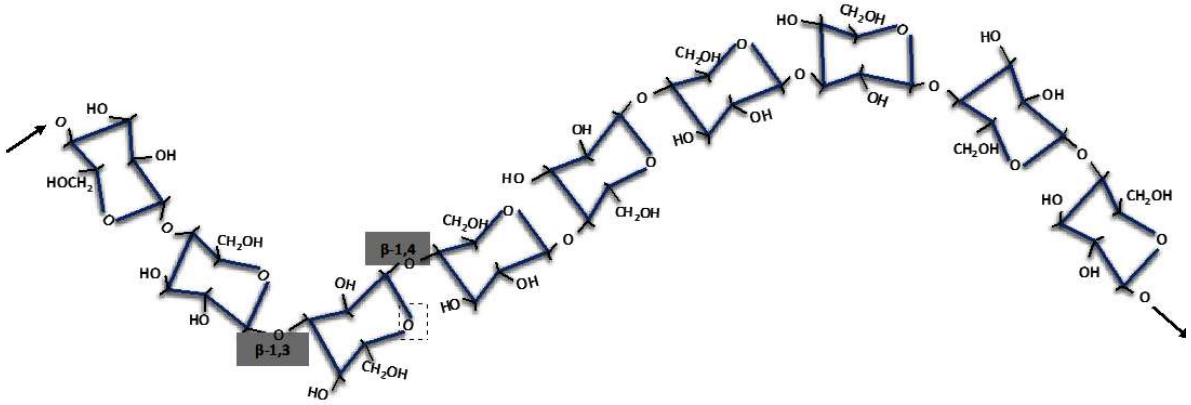

Figure 2. Primary structure of mixed-linkage (1,3;1,4)-β-D-glucan in Poaceae. MLG is a linear homopolymer composed mainly of (1,4)-linkages and less (1,3)-linkages. A single (1,3)-linkage insertion breaks up the chain's regularity, turning it into a more soluble-water polysaccharide. Adapted from Buckeridge and de Souza (2014)

More recently, some researchers have used the term mixed-linkage glucanases (MLGase) for any enzyme capable of modifying the polymer's structure (Görlach et al., 1998). Nonetheless, other scholars employ the word with addenda (Kim et al., 2001; Behar et al., 2018). In this work, we employ MLGase for any glucanases capable of modifying MLG.

Burton and coworkers (2011) reported that MLG's fine structure could be related to gene expression variation from different MLG synthases (*CslFs* and *CslHs*) or the combination of these synthases. Despite the poor knowledge of MLG tailored structure, researchers have been using the DP3:DP4 ratios to assess MLG's fine structure (Burton and Fincher, 2012) and have found that this ratio is highly diverse among species and within tissues of the same species (Lazaridou et al., 2004; Doblin et al., 2009; Burton and Fincher, 2012; Xue and Fry, 2012).

In prokaryotes, MLG has been reported in the bacterium *Sinorhizobium meliloti* (Pérez-Mendoza et al., 2015, 2017; Baena et al., 2019) and upon MLGase digestion, the polymer generated disaccharide repeating units (Pérez-Mendoza et al., 2015), an unusual form. Moreover, the gram-positive bacterium *Sarcina ventriculi* has shown the presence of oligosaccharides of β-glucopyranose, a β-glucose, made up of (1,3) and (1,4) linkages (Lee and Hollingsworth, 1997), resembling MLG in composition.

In the fungi kingdom, MLG has been detected mainly in species that are "lichens," such as *Cetraria islandica*. This fungus has lichenin or lichenan, a polymer known to be a type of MLG (Iakiviak et al., 2011). It highly differs from those in grasses, having a much higher proportion of DP3 to DP4 units (20.2–24.6:1) (Lazaridou et al., 2004). This proportion, in which there is a

greater abundance of DP3, makes the polymer chain much more regular than the poalean MLG chains and favors the formation of viscous solutions gel-like matrices (Tosh et al., 2004). This same chain regularity can occur by low ratios of DP3:DP4, where the DP4 value is high (Harris and Fincher, 2009b). In the fungus *Rhynchosporium secalis*, the hydrolysis of MLG by bacterial MLGases leads primarily to the formation of DP3, with small amounts of laminaribiose, a disaccharide composed of glucosyl residues attached by a β(1,3) linkage (Pettolino et al., 2009).

In algae, *latu sensu*, a sulfated-MLG has been found in one red alga. The sulfated polymer occurs mainly on 4-linked glucose residues (Lechat et al., 2000). On the other hand, in brown algae, MLG has been identified in many species within the Phaeophycean family and is composed mainly of DP3 units, resulting in MLG's higher aggregation and water (Salmeán et al., 2017). In green algae, MLG has been reported in *Ulva lactuca* and *Micrasterias denticulate*. The former is a chlorophyte, whose cell wall yielded pentasaccharides to decasaccharides when subjected to bacterial MLGase digestion (Popper and Fry, 2003). The latter is a desmid, whose secondary cell walls and pores have MLG, and upon MLGase digestion yielded more DP3 than DP4 (Eder et al., 2008).

In the Equisetum genus, MLG consists predominantly of DP4 blocks with a low DP3:DP4 ratio (0.1 or less) (Fry et al., 2008b; Sørensen et al., 2008). Moreover, the polymer MLG has been detected throughout *Equisetum arvense* stem cell walls, exempting vascular tissues (Sørensen et al., 2008).

Poaceae is the family in which MLG has been studied the most. This hemicellulose is widely distributed in primary and secondary walls of grasses. Besides, there is a higher proportion of DP3 than DP4 generated upon bacterial MLGases digestion (Burton and Fincher, 2012). Lazaridou and Biliaderis (2007) compiled data regarding molecular-structural features of cereal MLG. The authors stated the relative percentage amount of DP3 decreases from wheat (67–72%) to barley (52–69%) and oats (53–61%). DP4, on the other hand, increases from wheat (21–24%) to barley (25–33%) and oats (34–41%). So, DP3:DP4 ratios decrease from wheat (3.0–4.5) to barley (1.8–3.5), rye (1.9–3.0), and oats (1.5–2.3). This ratio is considered the fingerprint of the structure of cereal MLG. In the context of poalean MLG, higher solubility exists with DP3:DP4 ratios ranging from 1:1 to 2.5:1 (Burton and Fincher, 2012).

MLG's fine structure diversity seems to be a crucial determinant for its physicochemical properties. It influences its capacity of interaction with other polysaccharides and sets the cell wall's mechanical properties. Thus, the assessment of MLG evolution and its fine structures will need further investigation to unveil their glycomic codes resulting in the identification of the structure-function relationship.

2.1.8. MLG biosynthesis

There is some controversy regarding the site of MLG synthesis. While it has been stated that it occurs at the plasma membrane (Wilson et al., 2015), many authors have argued that MLG is synthesized in the Golgi (Buckeridge et al., 1999; Carpita and McCann, 2010; Kim et al., 2015, 2018). Dissension apart, researchers have found that the bacterium *Sinorhizobium meliloti* synthesizes MLG by glycosyltransferases, whose *BgsA*/*BgsB* genes are homologous to bacterial cellulose synthases A (*BcsA*) (Pérez-Mendoza et al., 2015, 2017; Baena et al., 2019). Phylogenetic inferences suggested that other bacteria, such as *Agrobacterium* and *Methylobacterium*, can also produce MLG (Pérez-Mendoza et al., 2015), considered they may have those synthases. The brown alga *Ectocarpus siliculosus*, which has MLG, contains *cellulose synthases* (*Csls*) closer to *BcsA* than to plants *Csls* (Michel et al., 2010). However, the lycophyte *Selaginella moellendorffi* has orthologous sequences to plant *Csls*, the *CslA*, *CslC*, and *CslD* (Harholt et al., 2012), although they have not been associated with MLG synthesis, remaining unclear the whereabouts of MLG synthases.

In monocots, the *CslFs*, *CslHs*, and *CslJs* are responsible for MLG synthesis (Burton et al., 2006; Doblin et al., 2009; Ermawar et al., 2015; Schwerdt et al., 2015; Little et al., 2018). *CslHs* and *CslJs* have been found throughout monocots, and *CslFs* are Poaceae-restricted (Little et al., 2018). So far, *CslFs* and *CslHs* have not been reported in eudicots. Intriguingly, rice *CslsF* and barley *CslHs* were expressed in *Arabidopsis thaliana* (eudicot), and both experiments showed MLG production (Burton et al., 2006; Doblin et al., 2009), indicating that *A. thaliana* could have additional machinery interacting with the heterologously expressed proteins to produce MLG (Vogel, 2008; Scheller and Ulvskov, 2010). Another similar approach has shown that the overexpression of two *Hordeum vulgare CslFs* genes (*HvCslF3* and *HvCslF10*) in *Nicotiana benthamiana* (eudicot) resulted in the synthesis of a linear glucoxylan, consisting of (1,4)-β-linked glucose and xylose units (Little et al., 2019), thus, putting at stake the previous findings of *CslH*, *CslH*, and *CslJ* as exclusive genes in synthesizing MLG.

2.1.9. MLG rearrangement

MLG remodeling occurs through hydrolysis or transglycosylation by various families of glycosyl hydrolases: GH3, GH16, GH17, GH55, GH64, GH81, and GH128. Most of these families are found in microorganisms, and only a few subgroups within each family are associated with MLG remodeling (Chaari and Chaabouni, 2019).

2.1.10. GH17 and GH16 MLGases

GH17 are plant hydrolases encompassing endo-(1,3;1,4)-β-D-glucanases (EC 3.2.1.73) and β(1,3)-glucanases (Akiyama et al., 2009). The latter is associated with callose hydrolases and gives rise to the former (Høj and Fincher, 1995). The GH17 endo-(1,3;1,4)-β-glucanases and some GH16 glucanases hydrolyze the β(1,4) bonds that immediately follow β(1,3), both are then acting similarly (EC 3.2.1.73) (Müller et al., 1998). However, both MLGases (EC 3.2.1.73) have neither similarity in their amino acid sequences nor their proteins' three-dimensional structure (Planas, 2000). They are an example of convergent evolution towards a single substrate specificity (Müller et al., 1998; Planas, 2000).

GH16 is a large and taxonomically diverse family of β-jelly-roll proteins whose enzymes are associated with hydrolysis and transglycosylation of terrestrial and marine polysaccharides (Viborg et al., 2019). The GH16 concerning MLG hydrolysis falls into three main subgroups: bacterial endo-(1,3;1,4)-β-D-glucanases, endo-glucanases of GH16 (EG16), and xyloglucan endotransglucosylase/hydrolases (XTH). Some studies have shown that bacterial endo-(1,3;1,4)-β-D-glucanases probably gave rise to EG16s and XTHs (Eklöf et al., 2013; McGregor et al., 2017; Behar et al., 2018). Then the ancient EG16s have been considered the evolutionarily link between bacterial endo-(1,3;1,4)-β-D-glucanases and XTHs (Eklöf et al., 2013; McGregor et al., 2017; Viborg et al., 2019). Moreover, EG16s are structurally and functionally similar to bacterial endo-(1,3;1,4)-β-D-glucanases and xyloglucan endo-transglycosylases (XETs), a group within XTHs that contains a catalytic "promiscuity" for MLG and xyloglucan hydrolysis (Behar et al., 2018). Intriguingly, two eudicots EG16s - *Vitis vinifera* (XP_002273975.1) and *Populus trichocarpa* (PtEG16) (Eklöf et al., 2013) - catalyze MLG backbones and xyloglucan (Eklöf et al., 2013; McGregor et al., 2017), despite the MLG's absence in eudicots.

Most XTHs graft part of donor polymer, a xyloglucan, to other acceptor polysaccharides, usually another xyloglucan (Simmons et al., 2015). The XTH family encodes XETs (EC 2.4.1.207) and xyloglucan endo-hydrolases (XEHs) (EC 3.2.1.151) (Behar et al., 2018). The vast majority of XTHs "cut" and "rejoin" xyloglucan by XET activity, whereas some XTHs hydrolyses xyloglucan by XEH (EC 3.2.1.151) action (Rose et al., 2002; Baumann et al., 2007; Ibatullin et al., 2009).

More than a decade ago, Fry and coworkers (2008a) characterized an *Equisetum fluviatile* MLG: xyloglucan endotransglucosylase (MXE) capable of grafting MLG or xyloglucan (donors) to xyloglucan oligosaccharides (acceptor). Later, this MXE was termed as hetero-trans-β-glucanase (HTG) (Simmons et al., 2015; Simmons and Fry, 2017) since the *EfHTG* acts not only on MLG and xyloglucan as donors but also on cellulose as a donor to xyloglucan (receptor.). The

EfHTG is phylogenetically considered a subfamily member of the XTHs (GH16) (Simmons et al., 2015; Simmons and Fry, 2017). Additionally, a *Brachypodium distachyon* XTH8 (*BdXTH8*) has shown MXE activity (Fan et al., 2018).

2.1.11. MLG roles

Our work classifies MLG functions into two main categories: structural and storage, although there may exist overlapping functions between them. To frame the functional categories, we assume that MLGs went through a transference of function processes similar to what has been proposed for other cell wall polysaccharides (Buckeridge, 2010; Buckeridge and de Souza, 2014).

2.1.12. The transient and permanent structure

MLG has been hypothesized as a structural transient polysaccharide in grasses due to its transitory accumulation in the primary cell walls of young tissues in the process of elongation, such as in the coleoptiles of maize. Although Carpita (1984) was the first to demonstrate the accumulation of MLG in coleoptiles of maize up to 4 days of development, it was Luttenegger and Nevins in 1985 who demonstrated the true transitory nature of MLG accumulation in this system, following the presence of the polysaccharide up to 10 days. The authors demonstrated that after maximal cell wall elongation, MLG is rapidly degraded. Similarly, other researchers' observations accounted for corroborating the hypothesis that the MLG could be a transient polysaccharide (Carpita, 1984; Luttenegger and Nevins, 1985; Kim et al., 2000; Carpita et al., 2001; Gibeaut et al., 2005). This same transient role has been discussed by Slakeski and coworkers (1990), who proposed that MLG represents a physical barrier between hydrolytic enzymes secreted from peripheral tissues and their substrates within the cell of the starchy endosperm of barley grain.

Nonetheless, Vega-Sanchez and coworkers (2012) found MLG in older leaves of rice. A year later, Vega-Sánchez and coworkers (2013) observed MLG's appearance in old tissues and some species' secondary cell walls and proposed that MLG's presence at maturity might indicate a strengthening reinforcement role in some organs, such as stems and leaves. They argued that the polymer does not play an exclusive role as a transient polymer but plays other roles that should be considered.

The possibility of MLG as a physical reinforcement was also verified by Kido and coworkers (2015). When they overexpressed rice *endo-(1,3;1,4)-β-D-glucanase 1* (*OsEgl1*), experiments detected a decrease in cell wall resistance linked to the lower MLG amount and ensuing silica distribution profile in leaves. The cell fractionation experiments unveiled the polymer's presence mainly in Equisetum shoots' secondary cell walls, and its contents were associated with an age-dependent process. A few years before, Fry and coworkers (2008b) had proposed that MLG could be a template for silica deposition in Equisetum.

In algae, Herburger and coworkers (2017) also raised the possibility of MLG accumulation in the thickened secondary cell wall of some green algae. Based on their work, it has been argued that the MLG accumulation, especially on secondary cell walls of some green algae, could be an age-dependent process. In brown algae, MLG is associated with alginates in cortex cell walls (most inner and outer cells) and insolubility in water (Salmeán et al., 2017). The authors argued that the regular conformation could allow long stretches of the molecule to align and form microfibrils that may have a structural role.

Indeed, many experiments indicated a structural role for MLG. In a red alga, Lechat and coworkers (2000) detected a sulfated MLG composed mainly of sulfated β(1,4) bonds. The sulfated polymer's cell wall extraction pattern indicated it is probably linked to the algal fibrillar cell wall and interaction with other polysaccharides. Therefore, Lechat and coworkers (2000) speculated that the sulfated MLG could contribute to red alga's overall cell wall cohesion.

In prokaryotes, MLG may have a crucial role in the structure of exopolysaccharide from the Rhizobial bacterium *Sinorhizobium meliloti* 8530, which does not contain cellulose synthase genes (Pérez-Mendoza et al., 2015). According to the author, the polymer is vital to the formation and aggregation of biofilms and, thus, necessary for the bacterium's attachment to the alfalfa plant's roots. Moreover, the scientists suggested that MLG is a surface polymer that helps rhizobia and other plant-associated bacteria grow and develop in the soil (Pérez-Mendoza et al., 2015).

In the lichen *Cetraria islandica*, "the lichenin," or MLG-like, is primarily a structural element of the fungal wall, with essential functions in thalline water relations, rather than a storage compound of lichen-forming ascomycetes" (Honegger and Haisch, 2001).

Some researchers have suggested an association between MLG and aerenchyma development (Slakeski et al., 1990). Given the high level of MLG and *EI endo-(1,3;1,4)-β-glucanase* mRNA in young leaves of barley, Slakeski and coworkers (1990) conjectured that if the elevated level of *EI endo-(1,3;1,4)-β-glucanase* mRNA is proportional to the enzymatic activity, then a rapid degradation of the cell wall or turnover would happen in the leaves. The plausible explanation for

the high levels of an MLGase, according to the authors, is that the enzyme would be involved in the formation of intercellular airspaces that are necessary for the diffusion of gases and water vapor in young leaves. The gas spaces, initially, do not have direct access to the atmosphere. Since these intercellular airspaces develop through a selective dissolution of the cell (lysogeny) or frequently by separation of cells (schizogeny), they suggested the possible involvement of *EI endo-(1,3;1,4)-β-glucanase* in aerenchyma formation of paddy rice.

Other pieces of evidence involving MLG's relationship in the development of aerenchyma in grasses have been reported (Leite et al., 2017; Grandis et al., 2019). Leite and coworkers (2017) clearly demonstrated the retrieval of MLG from the cell wall of sugarcane roots along with the aerenchyma formation (Figure 3). In this case, the transient accumulation seems to be part of the process. Whereas other polymers such as arabinoxylan, xyloglucan, and cellulose remain and form a composite that forms the gas channels, MLG disappears completely. Later on, Grandis and coworkers (2019) showed an increase in an *endo-(1,3;1,4)-β-D-glucanase,* the respective MLGase protein, and its enzyme activity during aerenchyma development, thus, suggesting that MLG's retrieval being essential in the process.

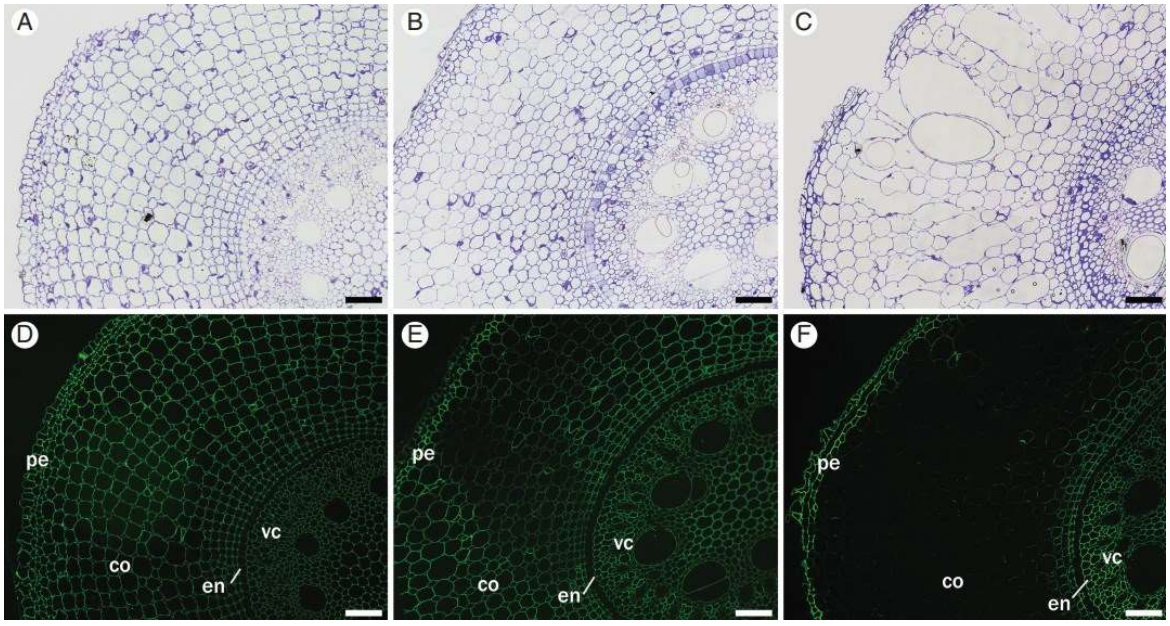

Figure 3. Mixed-linkage glucan and aerenchyma development in sugarcane roots. The cross-sections (A, B, and C) correspond with the same developmental phases of the immunolabeled ones (D, E, and F). There is no aerenchyma at the root apex (A and D), and the MLG signals are noticeable in cell walls. Towards the root base, the aerenchyma formation begins (B, E), and MLG signals fade (E) slightly in the cortex (co). In the final phase (C, F) the aerenchyma is utterly developed, comprising many gas spaces. MLG's disappearance is prominent in the cortex (F), although the polymer remains in the vascular cylinder (vc) and peripheral tissues (pe): epidermis, exodermis, and sclerenchymatous cylinder. Controls (A-C) were stained with toluidine blue and immunolabeled (D-E) deployed MLG-directed antibody. (en) means endoderm. Scale bar represents 100 mm. (Leite et al., 2017).

2.1.13. Storage

Most grass seeds are rich in starch. However, in species such as oat, barley, and Brachypodium, MLG constitutes a significant proportion of the endosperm walls (Buckeridge et al., 2004; Burton and Fincher, 2012). Grasses can use MLG as an endosperm storage polymer and degrade it during germination to provide additional energy supply for early seedling development (Meier and Reid, 1982). Almost twenty years after this statement, Roulin and Feller (2001) found in wheat leaves a relationship between the level of sugar availability for growth and the activity and quantity of an endo-(1,3,1,4)-β-glucanase protein. They showed an increase in the activity and quantity of an MLGase when the leaves were submitted to periods of lack of sugar (e.g., extended periods of darkness, voluntary withdrawal of sugar). Later on, Roulin and coworkers (2002) found a similar pattern in barley leaves subjected to an extended period of darkness: the concomitant increase of an endo-(1,3,1,4)-β-glucanase protein level with the decrease of MLG content. Thus, they suggested that the polysaccharide could also serve as a source of energy during sugar shortage periods (Roulin and Feller, 2001; Roulin et al., 2002; Wälti et al., 2002).

Further evidence of the MLG storage role is the inverse correlation of MLG and starch content in Pooideae grains. *Brachypodium distachyon*, for instance, contains low amounts of starch and a high quantity of MLG. Conversely, little MLG and a high amount of starch in rice grains have been found (Trafford et al., 2013).

A few other indications exhibited high MLG levels in barley lines carrying a mutation on starch biosynthesis genes, suggesting, therefore, a regulatory link between the MLG content level and starch (Munck et al., 2004; Houston et al., 2014). Starch and MLG are synthesized from nucleotide sugars (ADP-glucose and UDP-glucose, respectively) in developing endosperm cells from sucrose breakdown (Kleczkowski, 1996). The cytosolic UDP-glucose pool is common to both pathways and could be "hijacked" for starch and MLG synthesis, eventually diverting the substrate to either pathway (Trafford et al., 2013).

In sorghum's vegetative tissue, Ermawar and coworkers (2015) noticed that the MLG level varies according to tissue age or developmental stage. The mature leaves have low MLG levels compared to young leaves, and the younger internodes have a more significant amount of MLG compared to older ones. By contrast, there is a higher MLG quantity in mature roots compared to seedling roots. Sorghum is a ratoon crop, then, the harvest is based mainly on cutting most of the above-ground part and leaving the roots intact, so the plant can recover and grow for the next season. Based on this premise, the authors suggested that MLG can be a source of energy by new growing shoots recovering from roots.

2.1.14. Other roles

Kim and coworkers (2017) found a negative correlation between the amount of MLG and heat stress-treated seeds in the early development stage of *B. distachyon*. Besides the smaller MLG amount, they argued that MLG plays an essential role in the *B. distachyon* seed development. Nevertheless, further investigation is necessary to know the exact MLG's purpose during the *B. distachyon* seed development.

All evidence mentioned above points to corroboration of the hypothesis that MLG went through a process of transference of function during evolution in plants. As proposed for other cell wall polysaccharides (Buckeridge, 2010), MLG's primary function seems to be the structural one. A secondary function has probably appeared later as storage in seeds and also in leaves of grasses.

2.1.15. MLG biotechnology

MLG technology relies on increasing or decreasing this hemicellulose for bioenergy, brewing, and food industry. On the one hand, plants containing higher MLG levels are advantageous because the polymer displays hypoglycemic effects. Furthermore, high MLG content in plants could also be valuable to produce cosmetics and bioenergy. On the other hand, lower MLG amounts are desirable for some processes since the polymer has negative effects on beer production and animal feeding.

2.1.16. Increasing MLG content: application in bioenergy and human nutrition

The easy accessibility and high MLG content in grasses make the polysaccharide an excellent source for human nutrition and biofuel production. Therefore, this polymer's use has gained attention and been explored for bioenergy research (Burton and Fincher, 2009; Pauly and Hake, 2011; de Souza et al., 2013; Loqué et al., 2015; Vega-Sánchez et al., 2015).

For biofuel production, one step to produce second-generation ethanol is the pre-treatment followed by hydrolysis with cocktails containing mainly hydrolases. However, pre-treatment such as steam explosion may lead to loss of some highly soluble hemicelluloses, such as MLG, which represents ca. 10% of sugarcane biomass (de Souza et al., 2013). Eventually, researchers could control the MLGases temporally and spatially, avoiding the waste of such a high glucose content. Significantly, Pauly and Hake (2011) obtained a maize mutant line for the

candy-leaf 1 (*cal-1*) gene, *MLGase* encoding an *endo-(1,3;1,4)-β-glucanase*. The authors verified that the mutant displayed higher MLG amounts, which showed increased saccharification compared to the wildtype, resulting in a 250% rise in glucose content. According to them, this may occur because the point mutation triggers a loss of MLGase activity.

Members of the *CslF* and *CslH* families have gained attention because they synthesize MLG. Overexpression of these genes in transgenic *A. thaliana* led to the MLG synthesis (Doblin et al., 2009), and, in another work, there was a 42% increase in saccharification through *CslF6* expression (Vega-Sánchez et al., 2015). Burton and coworkers (2011) elaborated a meticulous work in which they obtained numerous lines expressing the different barley synthases (*CslF*) containing a constitutive promoter (Pro35S) coupled to an endosperm specific promoter (ProASGLO). Most lines showed a significant increase in the content of MLG, with variations in the different tissues. Nevertheless, *HvCslF6* overexpression driven by constitutive expression of Pro35S caused lethality in some plants.

The high content level of MLG is a desirable feature in human food as well. Several studies showed its effect in lowering blood glucose and reducing cholesterol in animals and humans (Kahlon et al., 1993; Bourdon et al., 1999; Behall et al., 2004; De Paula et al., 2005). Yokoyama and coworkers (1997) showed that MLG's addition to pasta made from wheat flour, an MLG-poor food, has a hypoglycemic effect in humans. Brennan and Cleary (2005) commented that there is an attempt to extract pure MLG and adding it into MLG-deficient food. However, the cost of such extractions makes the procedure impracticable. A more plausible approach would be expressing the MLG synthases in wheat to obtain flour with hypoglycemic properties and higher nutritional value. This strategy was adopted by researchers who succeeded in increasing MLG content upon overexpressing barley synthases (*HvCslF6* and *HvCslF9*) in wheat plants (Cseh et al., 2013). Despite the results, further research is necessary to verify humans' potential hypoglycemic effects from the transgenic lines.

2.1.17. Decreasing MLG content: application in the brewing industry and animal feed

Unlike the desirable elevated MLG levels for bioenergy and human food, the large amount of MLG in the brewing industry and animal feeding is problematic. MLG's primary concern in the industrial field is in the beer industry because the polymer tends to form highly viscous aqueous solutions, which causes lower yields of malt extract from grains, resulting in lower nutrient availability for fermentative yeast growth (Ramesh and Tharanathan, 2003). In the

fermentation process, those obstacles lead to a reduced rate of beer filtration. Even after fermentation, MLG appears to persist and precipitate at low temperatures, contributing to haze formation and affecting beer's shelf life (Morgan and Gothard, 1977).

The presence of MLG is also problematic for animal nutrition. Some researchers suggested that the ingestion of MLG-rich foods forms a viscous layer and decreases the diffusion rates of specific compounds within the digestive tract (Ramesh and Tharanathan, 2003), impacting body weight gain (Brennan and Cleary, 2005). The polymer seems to have low digestibility, acting as fiber content. Furthermore, MLG-abundant food also causes poultry to excrete sticky droppings that affect bedding, considering some species do not have bacterial MLGases (GH16) to degrade the MLG in their digestive tract (Mrízová et al., 2014). The farmers then use MLG-poor grains, like maize, for poultry feed. Researchers have been trying to circumvent this obstacle by lowering MLG content in foods. For instance, scientists added exogenous bacterial MLGases (GH16) to animal food in order to degrade the polymer (Ouhida et al., 2000; Mathlouthi et al., 2002) or expressed bacterial *endo-(1,3;1,4)-β-D-glucanases* in barley (Von Wettstein et al., 2000, 2003; Mrízová et al., 2014).

Moreover, bacterial *endo-(1,3;1,4)-β-D-glucanases* (GH16) have been designed to improve their thermostability and efficiency during beer process production (Chen et al., 2015; Yang et al., 2015). More recently, Han and coworkers (2017) overexpressed an *EII* barley *endo-(1,3;1,4)-β-glucanase* (GH17) to decrease the MLG content. They achieved a 95.73% decrease in MLG content and increased starch level compared to the wild type. Some researchers have found new alleles from wild-type barley *EII endo-(1,3;1,4)-β-D-glucanases,* whose activity and thermostability are significantly higher than those used in industry (Lauer et al., 2017a, 2017b). Interestingly, Woodwar and Fincher, in 1982, had already reported a more significant barley EII protein's thermostability than the EI enzyme. Back then, both researchers argued that EII is a glycoprotein, whereas EI has only traces of carbohydrates, which would give it less thermostability. Although the researchers have not explored it, another approach could be inserting an MXE gene from Equisetum into grasses and, therefore, eventually remodeling MLG decreases its amount (Simmons and Fry, 2017).

Another strategy explores decreasing MLG synthases levels. Taketa and coworkers (2012) found a loss-of-function mutation in *HvCslF6*. The natural mutant had reduced agronomic features, probably due to the drastic reduction of MLG content. Nevertheless, Hu and coworkers (2014) obtained a viable *HvCslF6* mutant, but in this case, the MLG content was not drastically reduced. Another approach used the *Triticum aestivum CslF6* gene downregulation in wheat grain,

resulting in decreased MLG levels in the endosperm. This methodology has been reported as an industrial application to modulate MLG levels (Nemeth et al., 2010)

All those things considered, it seems reasonable we assume that MLG is essential in several biotechnological applications. The finding of mutants and mainly the genetic manipulation of its synthesis and degradation are valuable tools for improvement of plant-growth performance on the one hand. On the other hand, the capacity to increase the proportion of MLG both in the whole plant and in seeds can lead to a source of the polymer for industrial production. One aspect that has not been discussed here but could be pretty crucial in the future is manipulating the MLG fine structure (i.e., the glycomic code) to obtain designed molecular properties for specific usage in the industry.

2.1.18. Aerenchyma development

The aerenchymas originate from the parenchymal tissues and are characterized by large interconnected, gas-filled intercellular spaces (Evans, 2003). They appear on leaves (Parlanti et al., 2011; Liu et al., 2019b), petioles (Schussler and Longstreth, 1996), stems (Casto et al., 2018; Ni et al., 2019), and roots (Arber, 1920) of plants. Some researchers believe that the gas spaces' function might improve water absorption and respiration, thus providing an internal pathway for oxygen circulation and reducing the number of cells consuming this gas (Drew et al., 2000).

According to their developmental mechanism, researchers established two types of aerenchyma: lysigenous and schizogenous (Arber, 1920; Gunawardena et al., 2001a; Leite et al., 2017). The former develops primarily by cell separation and programmed cell death (PCD) that causes the gas spaces (Gunawardena et al., 2001a; Rajhi et al., 2011; Leite et al., 2017) and has been found in a broad diversity of plants (Jackson et al., 1985; Drew et al., 2000; Aschi-Smiti et al., 2003; Colmer, 2003; Fan et al., 2003; Shimamura et al., 2010; Yamauchi et al., 2013; Abiko and Miyasaka, 2020). The latter is found mainly in wetland plants and is characterized by pre-existing spaces through cell separation and expansion (Du et al., 2018).

Schizogenous aerenchyma has been reported in the genus Rumex, which develops the gas spaces in its adventitious and primary root (Justin and Armostrong, 1987; Colmer et al., 2004). Intriguingly, *Sagittaria lancifolia* has been reported to contain schizogenous aerenchyma in petioles and lysigenous aerenchyma in their roots (Schussler and Longstreth, 1996).

Lysigenous aerenchyma can be constitutive or inducible by external and internal stimuli (Evans, 2003). External stimuli include mechanical impedance, nitrate, phosphate (Drew et al., 1989), and sulfate deficiency (Bouranis et al., 2003). Moreover, it comprises a response to

drought, high temperature, and hypoxia (Evans, 2003). In maize, an environmental inducer is necessary to initiate the aerenchyma development (Rajhi et al., 2011), whereas no external inducer is required at constitutive aerenchyma in plants like sorghum (Promkhambut et al., 2011), sugarcane (Begum et al., 2013; Leite et al., 2017) and rice (Justin and Armstrong, 1991), although the constitutive aerenchyma can be further induced by hypoxia (Yamauchi et al., 2016). Despite the differences, the two subtypes have similar developmental pathways, which have been extensively studied in rice and maize, although other species significantly contributed to understanding this process.

Flooding mains' effect is an energy disruption caused by the absence of oxygen necessary to respiratory metabolism (Hofmann et al., 2020). Oxygen deprivation then interferes with the oxidative phosphorylation metabolic pathway and leads to nitric oxide (NO) production by several oxidative and reductive pathways (Gupta et al., 2011; Astier et al., 2018), especially by nitrate reductase (Wany et al., 2017).

Accumulating evidence has shown that NO and low oxygen concentration are required to suppress group VII ethylene response factors (ERFVIIs). Gibbs and coworkers (2014) found that ERFVIIs are destabilized in the presence of NO and stabilized in its absence by the N-end rule pathway of targeted proteolysis. Vicente and coworkers (2017) attested that nitrate reductase downregulation in *A. thaliana* led to lower NO concentration and higher stability of ERFVIIs. Wany and coworkers (2017) demonstrated that hypoxically induced NO upregulated ethylene biosynthetic genes encoding *ACC synthase* and *ACC oxidase* in wheat roots. Besides, the NO scavenger-treatment compromised PCD events and, ultimately, gas spaces development. Evidence suggests that low oxygen concentration is associated with ERFVIIs stability by the N-end rule pathway (Hinz et al., 2010; Gibbs et al., 2011, 2015; Licausi et al., 2011). Therefore, compelling data indicate that NO and low oxygen concentration are related to ERFVIIs stability (Vicente et al., 2017; Gibbs et al., 2018; Gupta et al., 2020).

The hormone ethylene is an example of internal stimuli and plays an essential role in the aerenchyma development of grasses (Jackson and Armstrong, 1999; Drew et al., 2000; Evans, 2003). When this hormone's rate decreases in maize roots, this organ becomes more responsive to the hormone, culminating in aerenchyma formation (Drew et al., 1989). Maize roots subjected to inhibitors of ethylene action or ethylene biosynthesis have their PCD prevented (He et al., 1996b) and aerenchyma development compromised (Drew et al., 1981; Jackson et al., 1985). In rice under aerated conditions, ethylene inhibitor's usage also inhibited aerenchyma development, although some aerenchyma was developed (Yamauchi et al., 2016). The authors suggested that

constitutive aerenchyma formation is regulated by ethylene-dependent and ethylene-independent pathways.

Plant burst oxidase homologs (RBOHs) are major producers of reactive oxygen species (ROS), which are involved in several cellular signaling pathways in plants, such as PCD (Wang et al., 2018). Some RBOHs are directly activated via phosphorylation by (Ca^{2+})-dependent protein kinases (CDPKs/CPKs) (Kurusu et al., 2015). Yamauchi and coworkers (2017) reported that rice under oxygen-deficient conditions induced one *RBOH* and two *CDPKs* in the cortex of rice roots. The knockout of an RBOH reduced the ROS accumulation and the ensuing inducible aerenchyma in rice. Furthermore, ROS production increased by coexpression of RBOH and CDPK in *N. benthamiana* leaves.

In maize and wheat, ROS and ethylene showed to be essential for the inducible lysigenous aerenchyma process (Rajhi et al., 2011; Yamauchi et al., 2014). In ethylene-treated rice roots, the PCD of the epidermis is H_2O_2-mediated and regulated by RBOHs (Steffens and Sauter, 2009). Besides, ethylene showed to downregulate a *metallothionein-2B* (*MT2b*) gene encoding a ROS scavenger, thereby amplifying the signal and the accumulation of H_2O_2 produced by RBOH. Thus, the submergence of rice roots releases ethylene inhibiting *MT*. Then, ROS accumulates. In maize, *MT* is constitutively expressed in all the cortical cells, the stellar cells, and the outer cell layers of roots (Yamauchi et al., 2011). On the other hand, under hypoxia, *MT* is not expressed in the roots' cortex, although its expression remains high in stellar and outer layer cells. The results suggest that MT constitutively scavenges H_2O_2 and other ROS in the cortex, stellar cells, and outer cell layers. Conversely, the low expression of *MT* in the cortex prevents ROS's hijacking and, consequently, leads to ROS accumulation which, ultimately, activates the subsequent process involved in aerenchyma formation in maize roots: programmed cell death.

Programmed cell death is a remarkable phase of lysigenous aerenchyma. Along with the aerenchyma development, ethylene stimulates PCD by producing ROS that initiate lysigenous aerenchyma in grasses (He et al., 1996a; Drew et al., 2000; Parlanti et al., 2011; Yamauchi et al., 2011, 2014; Leite et al., 2017). During early developmental stages, PCD takes place in the cortex of roots (Evans, 2003; Leite et al., 2017) and is followed by the subsequent cellular processes: DNA fragmentation, chromatin condensation, plasma membrane invagination, and vesicle formation (Gunawardena et al., 2001b; Leite et al., 2017). In the final stage, the cell walls are degraded in the cortex enzymatically. The cell wall disassembly occurs by a coordinated action of pectinases, xylanases, xyloglucan endotransglucosylases, and cellulases (Saab and Sachs, 1996; Evans, 2003).

Despite the fundamental role of ethylene for aerenchyma development, Tavares and coworkers (2018) suggested that the sensitivity to ethylene and the crosstalk between ethylene-auxin may play a crucial role in developing the constitutive aerenchyma in sugarcane roots. Furthermore, they proposed that auxin could be involved in the expression of genes related to cell wall expansion, an event that preceded the formation of the aerenchyma in the sugarcane roots. One year later, Yamauchi and coworkers (2019) found an *iaa33* rice mutant containing reduced constitutive aerenchyma and lateral roots. They reported that auxin/indole-3-acetic acid protein (AUX/IAA; IAA) and auxin response factor (ARF)-mediated signaling are both important for constitute aerenchyma and lateral roots formation in rice. Besides, the authors proposed a model in which there may be an optimal auxin concentration to form lateral roots and constitutive aerenchyma, thereby reinforcing the important role of auxin.

Maize and rice have been used as a model to understand the lysigenous aerenchyma formation of roots. However, sugarcane roots have been standing out vis-à-vis cell wall hydrolysis during aerenchyma development. Tavares and coworkers (2018) suggested that the *endopolygalacturonanase 1* (*ScEPG1*) and an *ethylene transcriptor factor* (*ScRAV1*) may play essential roles in initiating hydrolyses of pectin from middle lamella, resulting in cell wall disassembly (Leite et al., 2017; Grandis et al., 2019). Subsequently, cell wall modification would affect arabinoxylan, xyloglucan, xyloglucan–cellulose interactions, with further partial hydrolysis of cellulose (Grandis et al., 2019). Concomitantly, MLG has been reported as the most degraded polysaccharide (Leite et al., 2017) by an endo-(1,3;1,4)-β-glucanase (Grandis et al., 2019). More recently, Tavares and coworkers (2020) reported several miRNAs associated with cell wall hydrolysis in sugarcane aerenchyma formation. Thirteen miRNAs have been predicted to target ethylene perception and signaling molecules like the miR156 targeting the *ScRAV1* promoter and possibly negatively regulating pectin degradation.

Among all mechanisms involving aerenchyma development, cell wall modifications are undoubtedly significant. One of the first steps is endogenous signaling by hormones and environmental signals. The subsequent changes in gene expression induce programmed cell death and lead to cell wall modification. The final step of cell wall changes forms a "composite" that constitutes the inner part of the channels through which oxygen can flow and improve respiration of the root cells (Leite et al., 2017; Grandis et al., 2019; Tavares et al., 2020)

A remarkable feature of lysigenous aerenchyma development in sugarcane is the disappearance of MLG. In this work, we have chosen sorghum as a model to investigate further MLG's role in aerenchyma formation. Our choice was based on the quality of sorghum's genome and its similarity to the sugarcane. Besides, before branching, the single primary root of sorghum

has a less complex anatomy and is quickly obtained. Its architecture is similar to most cereal embryonic roots, and most importantly, it has constitutive lysigenous aerenchyma. Since sorghum aerenchyma is a less known model system than rice and maize, we decided to investigate the anatomical and molecular aspects of MLG-related genes (synthesis and degradation). The main focus of the work, withal, was the characterization of the MLG hydrolases present in the sorghum genome.

2.2. GOAL

Use of sorghum seedling's primary roots to obtain biochemical and molecular data related to MLG hydrolysis during aerenchyma formation.

Objectives

- MLG systematic review to construct a cladogram containing all organisms which have the polymer
- Anatomical characterization of aerenchyma in sorghum primary roots
- Phylogenetic reconstruction of overall MLG hydrolases and synthases
- Gene expression profile of sorghum *endo-(1,3;1,4)-β-D-glucanases* and *cellulose synthase-like F* and *H*
- Enzymatic assays with crude extracts to detect *endo-(1,3;1,4)-β-D-glucanases-like* activities
- MLG relative quantification

2.3. MATERIAL AND METHODS

2.3.1. Plant material

Seeds of sorghum (*Sorghum bicolor* 'BRS 330') were obtained from EMBRAPA (Maize and Sorghum) and germinated in pots with moist vermiculite for seven days at 25 °C. The entire primary roots of seedlings were divided into five segments, each containing 15 mm in length, exempting the fifth one that is 14.2 mm in length. Our group analyzed only the first three segments (S1, S2, and S3). Given the remarkably similar anatomical pattern of the third, fourth, and fifth segments, we did the molecular and biochemical analysis only for S1, S2, and S3.

Although the S3 onward has the same arrangement and pattern of the gas spaces in their aerenchyma, we anatomically characterized all the five segments (Figure 19 to Figure 23 in Appendix B).

Harvest of leaves, roots, and culm were obtained from sixty-day-old sorghum grown in 40 L pots containing soil and vermiculite. Mature sorghum grew at the beginning of the São Paulo summer in 2017.

2.3.2. Anatomical characterization

2.3.2.1. High-resolution microtomography

We analyzed four *in vivo* primary roots of sorghum seedlings (7 to 12 cm length). We took just one entire primary root for in-depth analysis, considered all four roots showed similar patterns of aerenchyma development.

We used the high-resolution computerized SkyScan 1176 X-ray Microtomography (Bruker) and the software CT-Analyser v.1.13 (Bruker-microCT, 2013) for reconstructing the images. The X-ray beams were set up to get photos of 9 μm in thickness. Roughly 9,000 photos were taken from the entire primary root.

We initially divided the seedling aerenchyma into five segments (Appendix B) according to their developmental stage from the root apex towards the base. Considering that the anatomical pattern of seedlings is repeated in the third, fourth, and fifth segments, in-depth analyzes were performed with only the first three segments (S): S1 (no aerenchyma); S2 (aerenchyma initiation); S3 (aerenchyma under development). In Appendix B (Figure 19, Figure 20, Figure 21, Figure 22, and Figure 23), there are 28 pictures for each segment. The 28 photos are distributed equidistantly within each segment by 540 μm.

2.3.2.2. Histological cross-sections

Samples corresponding to the pattern of three segments were kept to obtain histological sections. We followed the protocol previously used in our group (Leite et al., 2017).

2.3.3. Phylogenetic reconstructions

Characterized amino acid sequences from GH17 endo-(1,3;1,4)-β-D-glucanases (Akiyama et al., 2009; Pauly and Hake, 2011; Lombard et al., 2014) were used as baits with the Blastp algorithm on *Phytozome 12* platform (https://phytozome.jgi.doe.gov/pz/portal.html) (e-value cutoff of 1e–3) to search for similar sequences of *S. bicolor*. GH17 endo-(1,3)-β-D-glucanases (Akiyama et al., 2009) were used for rooting (Høj and Fincher, 1995).

Sobic.003G421900.1 ID was named as *Sorghum lichenase 1* (*Sblic1*), Sobic.009G119400.1 as *Sorghum lichenase 2* (*Sblic2*), and Sobic.009G119200.1 as *Sorghum lichenase 3* (*Sblic3*).

Phytozome 12 platform (https://phytozome.jgi.doe.gov/pz/portal.html) was used to obtain the following sequences: (*Sorghum bicolor*), maize (*Zea mays*), *Setaria viridis*, switchgrass (*Panicum virgatum*), *Setaria italica*, rice (*Oryza sativa*), *Brachypodium distachyon*, wheat (*Triticum aestivum*), barley (*Hordeum vulgare*), *Miscanthus sinensis*, *Oropetium thomaeum*, *Musa acuminata*, *Ananas comosus*, *Populus trichocarpa* and *Aquilegia coerulea*. NCBI GenBank database (https://www.ncbi.nlm.nih.gov/genbank/) was used to obtain the following sequences: oat (*Avena sativa*), *Elaeis guineensis*, *Cocus nucifera*, *Piper nigrum*, *Phoenix dactylifera*, *Asparagus officinalis*, *Anthurium amnicola*, *Persea americana*, *Cinnamomum micranthum, Paenibacillus macerans, Bacillus subtilis, Bacillus licheniformis*, *Ruminococcus albus* and the genus *Dioscorea*. All other sequences were obtained from the *China National GeneBank DataBase 1KP Project* website (https://db.cngb.org/onekp/). The sorghum sequences were used to find the sugarcane ESTs from the SUCEST EST database (Vettore et al., 2003).

All alignments were performed on the online tool *MAFFT VERSION 7* using default parameters (Kuraku et al., 2013; Katoh et al., 2018): https://mafft.cbrc.jp/alignment/server/. Phylogenetic reconstructions were performed using the online tool *IQTREE Webserver* (http://iqtree.cibiv.univie.ac.at) (Nguyen et al., 2015), which uses ultrafast bootstrap values (Minh et al. 2013) and generates the best-fit model through *ModelFinder* (Kalyaanamoorthy et al., 2017). All inferences were performed with 1000 replicates and the maximum likelihood method. The software *FigTree v1.4.3* was used as a graphical viewer of phylogenetic trees (http://tree.bio.ed.ac.uk/software/figtree/). *IQTREE Webserver's ModelFinder* generated (WAG+G4) as the best model for the GH17 family and (JTT+F+I+G4) for MLGase synthases.

The cladograms were generated in PhyloT (Letunic and Bork, 2007) with NCBI taxonomic data (Sayers et al., 2019; Schoch et al., 2020). There are groups with polytomy which are unranked. The name of some clades was placed according to the data of PhyloT.

2.3.4. Quantitative real-time PCR

Total RNA was extracted by (TRIzol - Invitrogen) according to the manufacture's booklet. RNA integrity was confirmed by 1% (w/v) agarose gel. Total RNA was treated with DNAse Amplification Grade (Thermo-Fisher) and used for cDNA synthesis with SuperScript® III Reverse Transcriptase (Thermo-Fischer). The absence of gDNA contamination was verified by using primers designed to amplify exons between introns. Dilution curve tests were performed for all primers, and their efficiency verified as established by Thermo-Fisher's protocol (Real-Time PCR Handbook). The concentrations of the primers were also standardized. The melting curves were analyzed to ensure the specific amplification of each pair of primers. qRT-PCR reactions were performed in QuantStudio ™ 6 Flex Real-Time PCR System (Thermo-Fisher), and the SYBR® Green PCR Master Mix (Thermo Fisher) was used with reactions of final volume of 20 μL, and primer concentration of 0.3 μM.

The *peptidylprolyl isomerase* (*CYP*), *serine/threonine-protein phosphatase* (*PP2A*), and *eukaryotic initiation factor 4A* (*EIF4a*) genes (Sudhakar Reddy et al. 2016) were used as references to calculate the relative expression of genes of interest (Table 5 in Appendix A). Primers for MLG synthases (Table 5 in Appendix A) were taken from the literature (Ermawar et al., 2015). On the other hand, GH17 *endo-(1,3;1,4)-β-D-glucanases* primers were designed using online software *Primer3Plus* (https://primer3plus.com/cgi-bin/dev/primer3plus.cgi) (Table 5 in Appendix A).

Relative expression of these genes was obtained using the 2^-ΔΔ C.T. method (Livak and Schmittgen, 2001) and qbase+ software, v. 3.0 (Biogazelle, Zwijnaarde, Belgium – www.qbaseplus.com). Standard melting curves were performed for all reactions to confirm primer specificity. Additionally, standard curves were performed for all primers used in this work to check for efficiency.

2.3.5. Enzymatic activity assays

Fry (2004) distinguishes between enzymatic activity and enzymatic action. The former is an in vitro assay under optimized conditions after the solubilization of an enzyme. The latter detects the product of an enzyme reaction in the crude extract. Nonetheless, we use the most scientific community's generic term: enzymatic activity, even for assays using crude extracts.

The tissues were crushed in liquid nitrogen with a mortar and pestle. The macerated tissue (g)/ [50 mM Tris-HCl pH 8 (mL)] was used in 5.5/4.0 (w/v) ratio to a final concentration of 1 mM phenylmethanesulfonylfluoride (PMSF). The material was again macerated and

centrifuged at 15,000 g for 10 min at 2 °C. The supernatant was collected, frozen, lyophilized, and stored at - 85 °C. The lyophilized material was resuspended in water to 1/10 of the initial crude extract supernatant volume, named resuspended material for determining enzyme activity.

The MLG used in all experiments was the barley β-glucan (Low Viscosity from Megazyme). The method of MLG dissolution was performed according to Megazyme's booklet.

The positive control has 0.001 U/μL of endo-(1,3;1,4)-β-D-glucanase from *B. subtilis* (Megazyme) in water/MLG 0.2% (w/v)/ 1 M pH 5 ammonium acetate (1:2:1 by volume) to a final concentration of 1 mM PMSF (Crivellari, 2012). We have prepared the following solutions for negative controls: (1) pre-boiled resuspended material (10 min)/ MLG 0.2% (w/v)/ 1 M pH 5 ammonium acetate (1:2:1 by volume) to a final concentration of 1 mM PMSF; (2) water/ MLG 0.2% (w/v)/ 1 M pH 5 ammonium acetate (1:2:1 by volume) to a final concentration of 1 mM PMSF; (3) non-boiled resuspended material/ water/ 1 M pH 5 ammonium acetate (1:2:1 by volume) to a final concentration of 1 mM PMSF. We used solution (1) for TLC and all three solutions for HPLC.

All samples were incubated at 40 °C for 24 h with stirring on a thermoblock at 330 rpm. Three volumes (3X) of 99% (v/v) ethanol proportional were added to those samples and remained at -20 °C for two hours. All samples were centrifuged at 15,000 g, 2 °C for 15 min. The supernatant was collected and left at room temperature under vacuum in the Vacuum-Concentrator (Eppendorf) for 5 h. The material was resuspended in 1/20 of the initial volume of the supernatant from the crude extract.

2.3.6. Cell wall preparation

We used four biological replicates of the first three segments for cell fractionation. They were frozen, freeze-dried, and macerated in liquid nitrogen. Twenty-five milligrams of each grounded sample was subjected to five successive extractions with 80 % (v/v) ethanol at 80 °C for 20 min. The supernatants were collected as soluble sugars. The pellets, residual alcohol-insoluble residue (AIR), were washed with distilled water and dried at 60 °C for 24 h (de Souza et al., 2013).

The starch removal was performed according to Amaral and coworkers (2007). Starch extraction was performed by treating AIR with 120 U/mL of *Bacillus licheniformis* α-amylase (E.C. 3.2.1.1) (Megazyme® Inc., Australia).

2.3.6.1. MLG quantification

Oligosaccharides profiles were obtained upon hydrolysis of 1% de-starched AIR fraction (w/v), containing 50 mM pH 5.0 sodium acetate buffer and 0.5 U of endo-(1,3;1,4)-β-glucanase from *B. subtilis* (Megazyme®). The mixture was placed at 30 °C for 24 h.

2.3.6.2. Monosaccharide composition

Two mg of de-starched AIR was hydrolyzed upon 1 mL of 2M trifluoroacetic acid for 1 h at 100 °C, dried under vacuum, resuspended in 1 mL deionized water, and filtered on 0.22 μ (Merck Millipore®). Subsequently, we analyzed the samples by HPAEC-PAD by injecting 10 μL of hydrolysate into a CarboPac SA10 column (ICS 5.000 system, Dionex-Thermo®). Fucose, arabinose, galactose, rhamnose, glucose, xylose, and mannose were used as standards.

2.3.7. Chromatographic procedures

2.3.7.1. Oligosaccharide profile by HPAEC-PAD

The oligosaccharides were analyzed by High-Performance Anion Exchange Chromatography with Pulsed Amperometric Detection (HPAEC-PAD) on a CarboPac PA-100 (ICS-3000 system, Dionex®) using 88 mM NaOH and 200 mM sodium acetate as eluent (0.9 mL min^{-1}) for 45 min (de Souza et al., 2013).

2.3.7.2. Oligosaccharide profile by thin-layer chromatography

Oligosaccharides produced by enzyme assays were separated on Merck silica-gel 60'. TLC plates developed (twice) in butan-1-ol/ acetic acid/ water (2:1:1 by volume) (Fry et al., 2008b). Plates were sprayed with a developer containing 5% (v/v) of H_2SO_4 in 95% (v/v) ethanol.

The positive control is the product of barley MLG hydrolysis upon *B. subtilis endo-(1,3;1,4)-β-D-glucanase* (Megazyme), generating DP3 and DP4. Negative controls, on the other hand, are pre-boiled crude extracts.

2.3.7.3. Chromatogram data analysis

The chromatograms were printed on a squared photographic A4 180g paper at fixed scales. Each resolved peak area, reasonably close to the baseline, was cut off and individually weighed for quantitative analyses. The peak area is proportional to the weight and to the concentration of that component. For the enzymatic action, we used the sum of the masses of DP3 and DP4 cut-out areas. To measure the relative amount of MLG, we summed DP3, DP4, and DP5 masses, obtained by weighted peak area.

Despite being a method no longer used because we use computers, it is a very reliable method the chemists used to employ. We used this method because the analysis started during the pandemic scenario where we could not access the computer from the University of São Paulo.

2.3.8. Statistical analysis

The data were subjected to normality and homogeneity tests and were statistically validated by analyzing variance ($p < 0.05$). When there was a significant difference, Tukey's test ($p < 0.05$) was used. The experimental data that did not show a normal distribution were transformed into ($\sqrt{x}$) (Bartlett, 1936; Zar, 1999). Statistical analyses were performed using the *Sisvar 5.6 software* (Ferreira, 2011). For all experiments, except for cell fractionation, we used three biological replicates containing roughly 400 roots. For cell fractionation, we used four biological replicates containing approximately 400 roots.

2.4. RESULTS

2.4.1. Anatomical characterization of aerenchyma

The anatomical characterization by microtomography and histological cross-sections enabled the establishment of a precise division of primary roots into five segments. In a two-month-old sorghum root (Figure 4), the white arrows indicate the gas spaces occupying a large area of the parenchyma. Figure 5 is a combination of histology with microtomography. It indicates the first segment (Figures 5A and 5E) as absent from gas spaces, the second segment with some gas spaces (5B and 5F), and the third segment, onwards, containing developing aerenchyma of root seedling (5C and 5G). Thus, this similar developmental pattern of the third has been found in the fourth and fifth segments as well (Figure 21, Figure 22, and Figure 23 in

Appendix B). Figure 5D is the primary root used in this microtomography, which is 74.1 mm in length. The letters (E, F, and G in 3D) are the exact positions from which the 5E, 5F, and 5G images were taken, respectively.

Appendix B (Figure 19, Figure 20, Figure 21, Figure 22, and Figure 23) contains a set of images for each segment. In the first segment, there is no aerenchyma. In the second, the formation of gas spaces begins, and in the third, there are the developing gas spaces. Thus, Figures 5E, 5F, and 5G represent a gradient shown in Appendix B. In the fourth and fifth segments (Figure 22 and Figure 23 in Appendix B), the gas spaces' distribution patterns are similar to the third. Moreover, pictures' compilation shows regions of primary roots where the aerenchyma is not continuous and has interruptions as aerenchyma develops in seedlings.

Figure 4. Freehand cross-section from roots of mature sorghum. The aerenchyma is comprised of gas spaces, and some of them are indicated by white arrows. The dye used was Safrablau. Magnification of 20X.

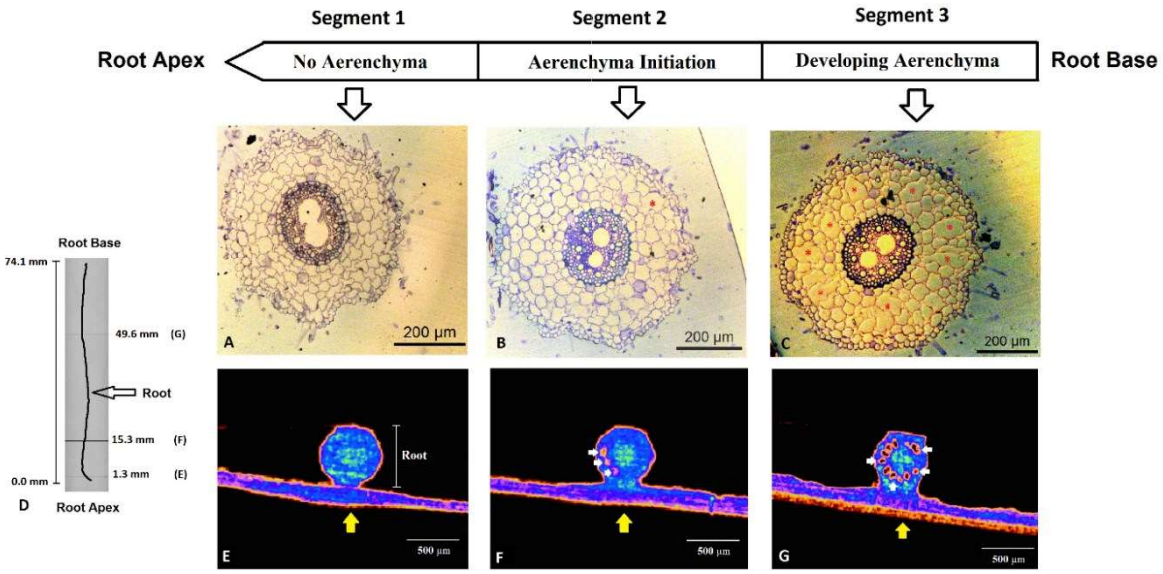

Figure 5. Microtomography of roots of sorghum seedlings. The top image is a root scheme divided into three segments: no aerenchyma, aerenchyma initiation, and aerenchyma under development. Each segment has nearly 1.5 cm. This same arrangement (apex towards the root base) was adopted for the histological (A, B, and C) and X-Ray (E, F, and G) tomographic images. Figure D is an X-Ray image of the root used in the microtomography, whose total length is 74.1 mm. Figure A shows the root apex without aerenchyma. Figure B is the beginning of aerenchyma formation (asterisk in red showing an enlarged cell). Figure C is the aerenchyma at a further developmental stage, containing several enlarged cells. In D, the letters along the root's length (E, F, G) are the exact locations where cross-sections E, F, and G were taken from, respectively. The yellow arrow is an artifact and constitutes the foam material on which the roots were placed for analysis. The white arrows indicate the position of the gas spaces during the formation of the aerenchyma. Images were subjected to color density range using software CT-Analyzer. E is the root apex with no aerenchyma near the root tip (see the position in D). F is the beginning of aerenchyma formation, while G the aerenchyma is under development. Figures A and E are apical regions without aerenchyma. In contrast, Figures C and G are aerenchymas under development at the root base. Figures B and F, the root's intermediate region, are the gas spaces still at the beginning of its formation. Each section from micrography represents 9 µm.

2.4.2. Cladograms and phylogenetic inferences

Following Leite and coworkers' finding (2017), who found that the mixed linkage-glucan (MLG) is degraded during aerenchyma formation in sugarcane, here we sought to verify this hypothesis for sorghum.

We first analyzed the occurrence of MLG in living beings. The systematic review of manuscripts enabled us the assembling the cladogram (Figure 6), which shows the presence of MLG in the following organisms: dinoflagellate from genus *Peridinium* (Nevo and Sharon, 1969); the bacterium *Sinorhizobium meliloti* (Pérez-Mendoza et al., 2015, 2017; Baena et al., 2019); fungi (Honegger and Haisch, 2001; Olafsdottir and Ingólfsdottir, 2001; Carbonero et al., 2005; Pettolino et al., 2009); the xantophyte alga *Monodus subterraneus* (Ford and Percival, 1965), the

brown algae (Phaeophyceae) (Salmeán et al., 2017); two green algae, *Micrasterias denticulata* (charophyte) (Eder et al., 2008), and *Ulva lactuca* (Chlorophyta) (Popper and Fry, 2003); the red alga *Kappaphycus alvarezii* (Lechat et al., 2000); the lycophyte such as *Selaginella moellendorffii* (Fry et al., 2008b; Harholt et al., 2012); Equisetum species (Fry et al., 2008b; Sørensen et al., 2008), and monocots (Smith and Harris, 1999; Trethewey et al., 2005; Little et al., 2018). The eudicot group is indicated by dashed lines and has no MLG.

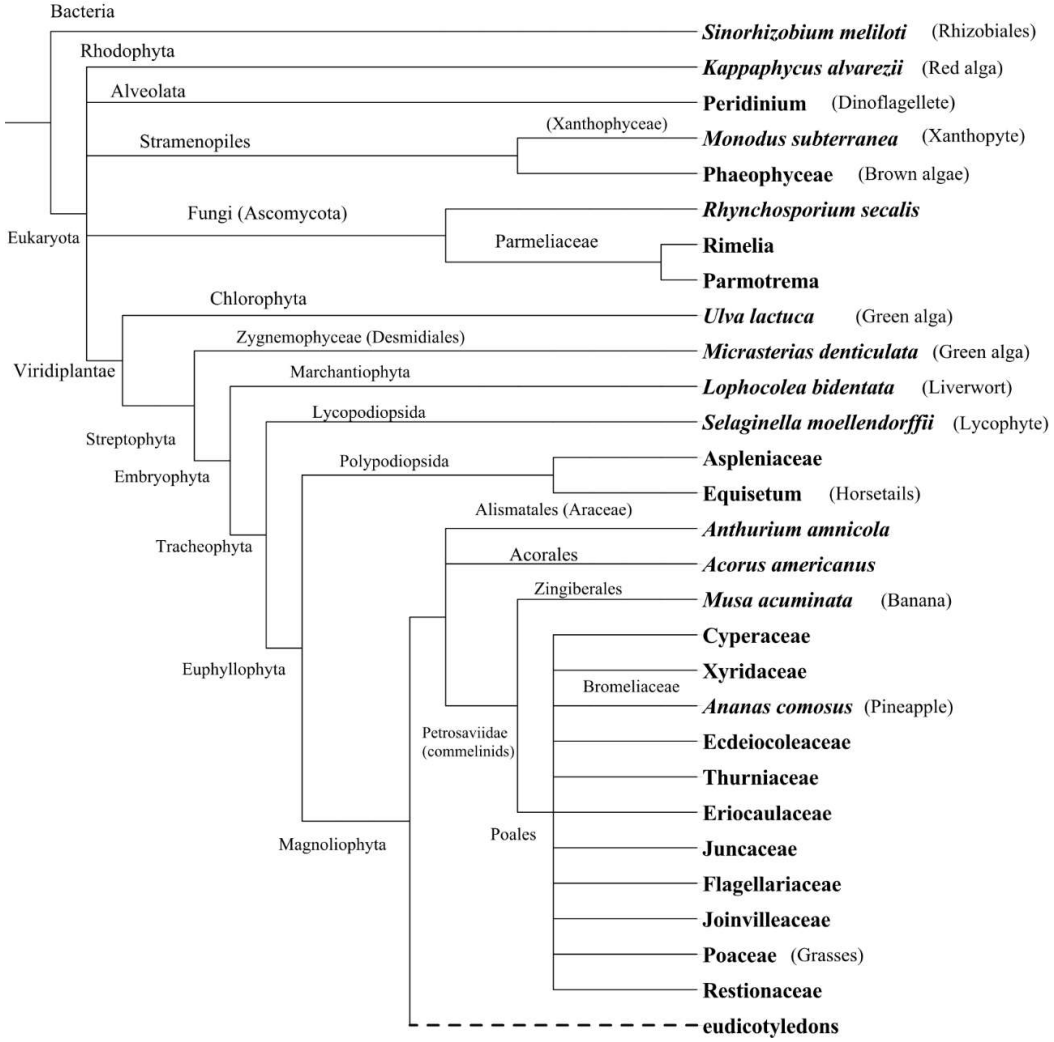

Figure 6. MLG occurrence in living organisms. MLG is found in a bacterium, many fungi, some algae groups, and throughout plants, exempting the eudicots indicated by the dashed lines. The cladogram was generated in PhyloT (Letunic and Bork, 2007) with NCBI taxonomic data. There are groups with polytomy, which are still unranked. This figure was adapted from PhyloT. The names of some clades were placed according to the data of PhyloT and NCBI taxonomic databank.

2.4.3. MLG biosynthesis

The *CslHs*, *CslFs,* and *CslJs* are shown in Figure 7. Sorghum genes have already been studied (Ermawar et al., 2015). The *CslF*s are Poaceae-specific, already mentioned by Little and co-works (2018), and encompass the *SbCslF6*. Moreover, our inferences indicate *CslHs* comprising monocots (Little et al., 2018) and the Magnoliids, a clade never reported being in the *CslHs* family.

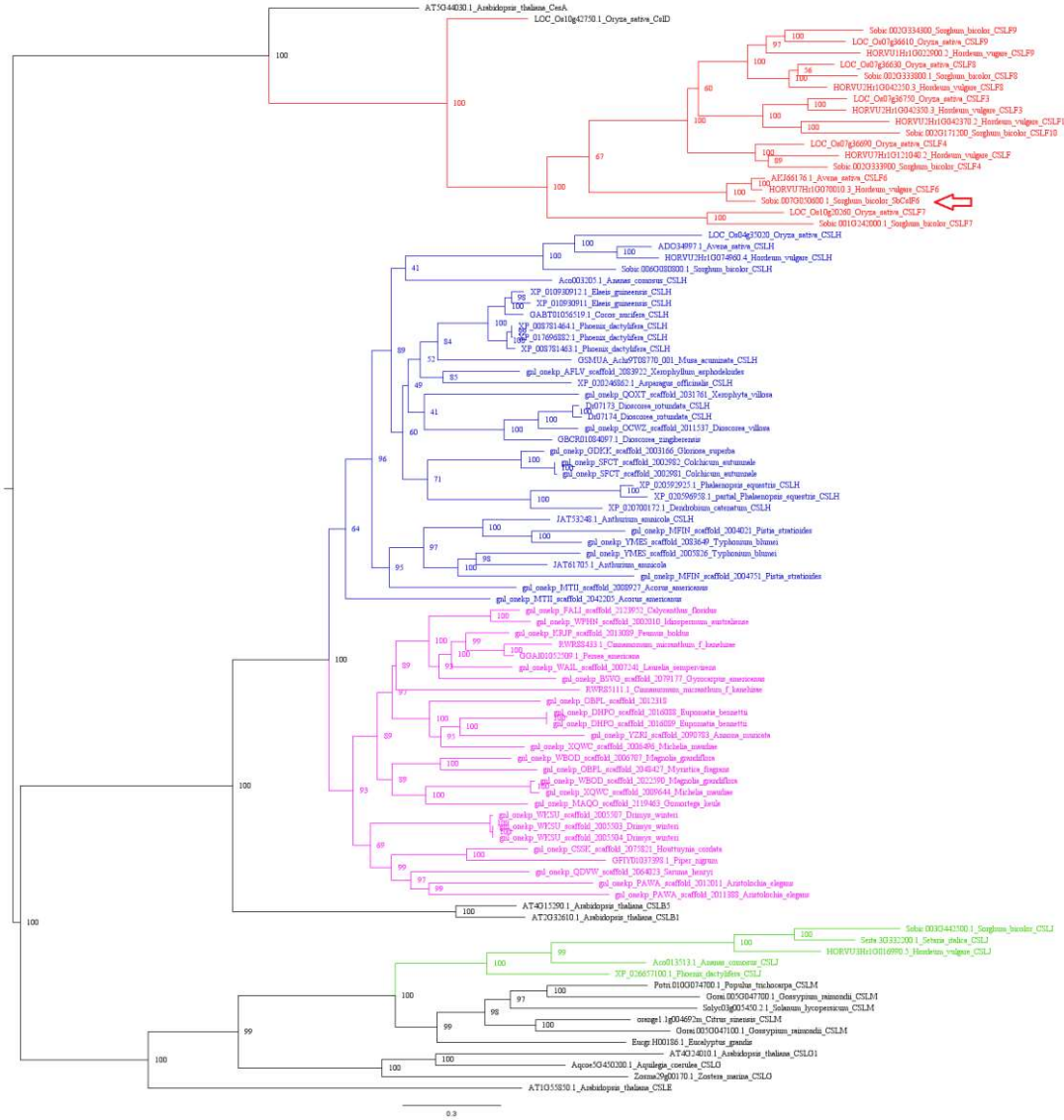

Figure 7. Phylogeny of *CslFs*, *CslHs*, and *CslJs*. The *CslFs* clade are Poaceae-specific genes (red color), and *CslJs* are in green color. The *CslHs* family encompasses monocots (blue) and the magnoliid clade (lilac color). The red arrow indicates *SbCslF6*. The tree is rooted at the midpoint.

2.4.4. MLG hydrolysis

The work's main focus was to study the events related to MLG hydrolysis in sorghum and rice, both species belonging to Poaceae. We used genomic databanks to evaluate the presence of GH17 glycosyl hydrolases. Here we determined GH17 phylogeny (Figure 8) showing *endo-(1,3)-β-D-glucanases* (merged into red triangles) and Poaceae-specific *endo-(1,3;1,4)-β-D-glucanases*.

Sorghum *endo-(1,3;1,4)-β-D-glucanases* are indicated by black arrows (*Sblic1*, *Sblic2,* and *Sblic3*) and rice genes by blue ones (*OsEgl1* and *OsEgl2*). Generally, this phylogeny's nesting pattern resembles a nesting pattern of Poaceae species tree (Figure 24 in Appendix B), especially the α clade, to where *Sblic1* belongs (Figure 8). Also, *Sblic1*, according to its ID number, is in the first chromosome. On the other hand, *Sblic2*/*Sblic3* belongs to the β clade (Figure 8). They are closer to each other in the ninth chromosome and have similar amounts of genetic changes (Figure 25 in Appendix B). Moreover, branch length and clades' split suggest evolutionary divergence between both clades.

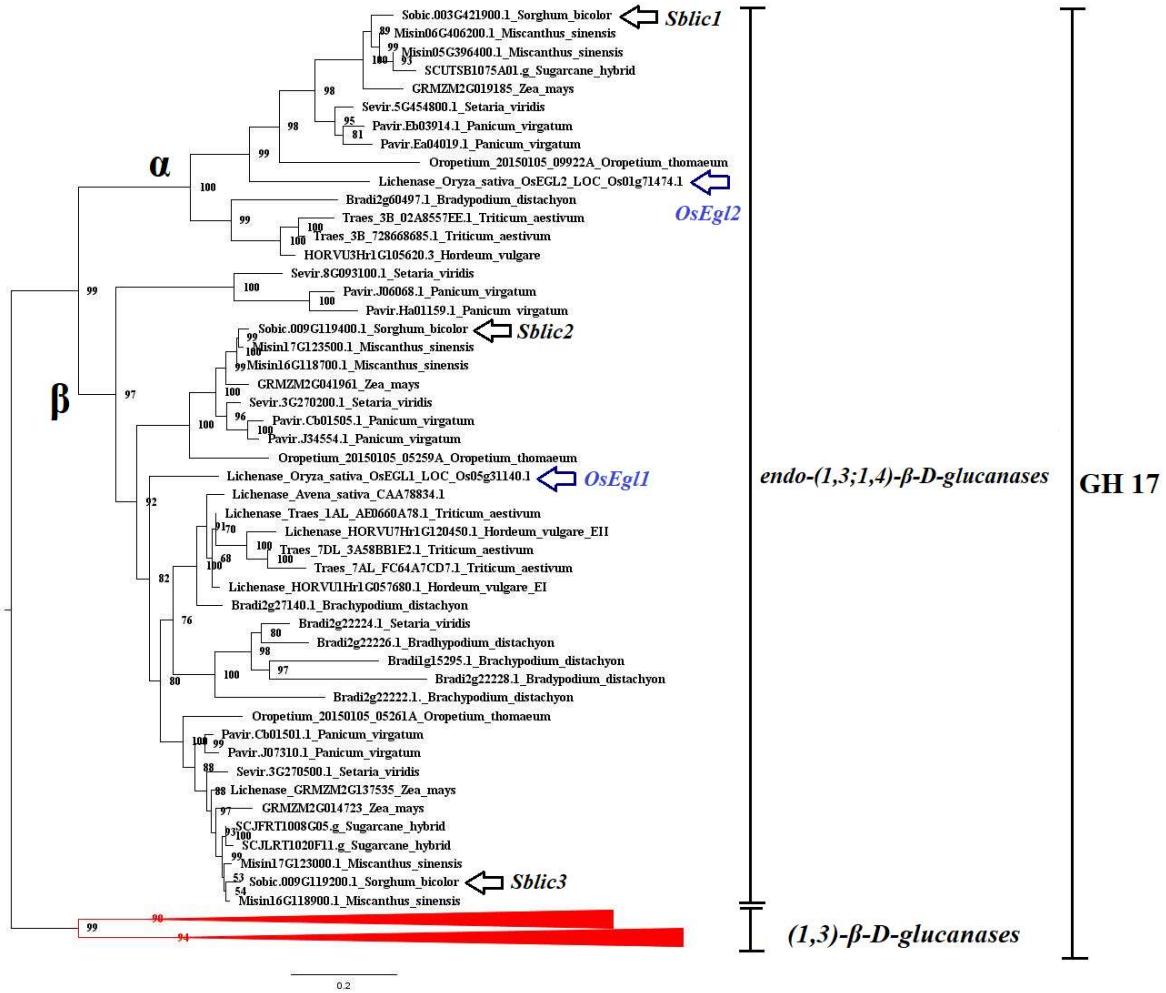

Figure 8. Phylogeny of GH17 *endo-(1,3;1,4)-β-D-glucanases*. The GH17 encompass the Poaceae-specific *endo-(1,3;1,4)-β-D-glucanases* and the *endo-(1,3)-β-glucanases,* which were used for rooting (Høj and Fincher, 1995) and merged into red triangles. IDs starting by "lichenase" indicate characterized endo-(1,3;1,4)-β-D-glucanases. Black arrows indicate sorghum genes, and blue arrows rice genes. *Sblic1* belongs to α clade and *Sblic2*/*Sblic* to the β one. The two rice genes (*OsEgl1* and *OsEgl2*) are shown in blue.

2.4.5. Expression profile of *Sblic1*, *Sblic2*, and *SbCslF6*

We detected the expression solely for three genes regarding MLG metabolism (Figure 9; Figure 26 in Appendix B). Two are hydrolases (*Sblic1*, *Sblic2*) and one is a synthase (*SbCslF6*). While the expression of *Sblic2* did not vary during aerenchyma development of seedlings, *Sblic1* increased almost 10-fold from segment 1 to segment 3 (Figure 9). Besides, *Sblic2* is highly expressed in young leaves of mature sorghum (Figure 26 in Appendix B). Regarding biosynthesis, we observed a slight decrease in the expression of *SbCslF6* (Figure 9). Our results suggest that

Sblic2 might be pretty important in young leaves (Figure 26 in Appendix B)., whereas *Sblic1* seems to be more relevant in roots (Figure 9).

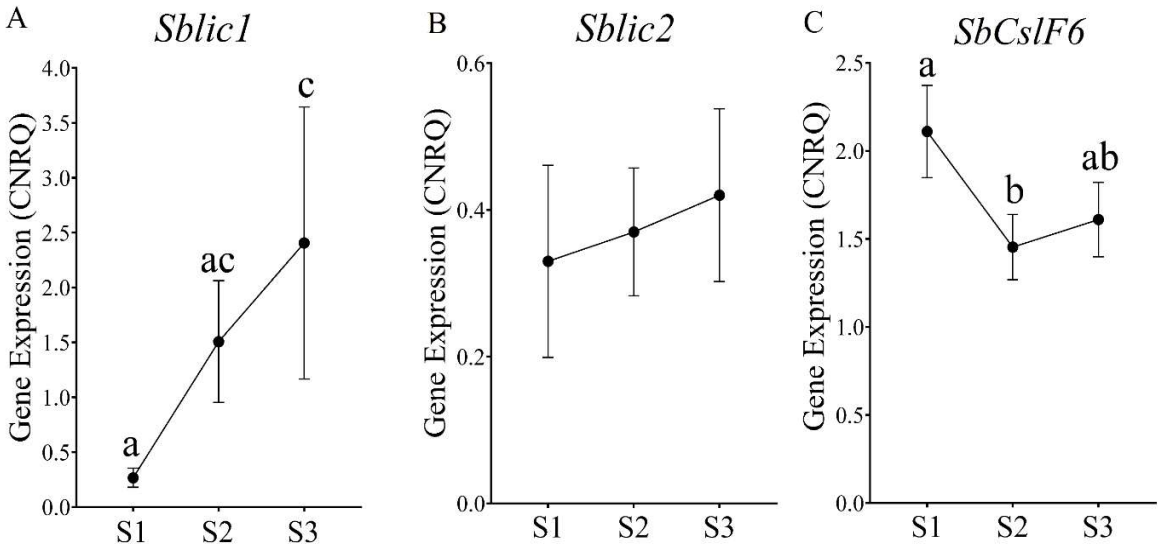

Figure 9. Expression profile of *Sblic1*, *Sblic2*, and *SbCslF6* during aerenchyma development. MLG hydrolases (A and B) and synthase (C). *Sblic1*(A) increases significantly from S1 to S3, while *Sblic2* (B) barely changes its expression. *SbClsF6* expression (C) slightly decreases from S1 to S2. S1 to S3 corresponds to segments from apex to base (1.5 cm each). Values are given as calibrated normalized relative quantities (CNRQ Values are means (n=3) ± standard errors, and letters represent the statistical difference among segments according to Tukey's test ($p < 0.05$).

2.4.6. Enzymatic activity

2.4.6.1. Detection of enzyme activity by thin-layer chromatography (TLC)

TCL was the first chromatographic technique used to evaluate the presence of MLGase activity in crude extracts of segments (Figure 10). Figure 10 corroborates the data of *Sblic1* expression (Figure 9), showing progressively higher MLGase activity from segments 1 to 3. There are no bands of DP3 and DP4 oligosaccharides in the first segment, indicating no MLGase activity from crude extracts. The second and third segments do have DP3 and DP4, indicating MLGase activity (Figure 10).

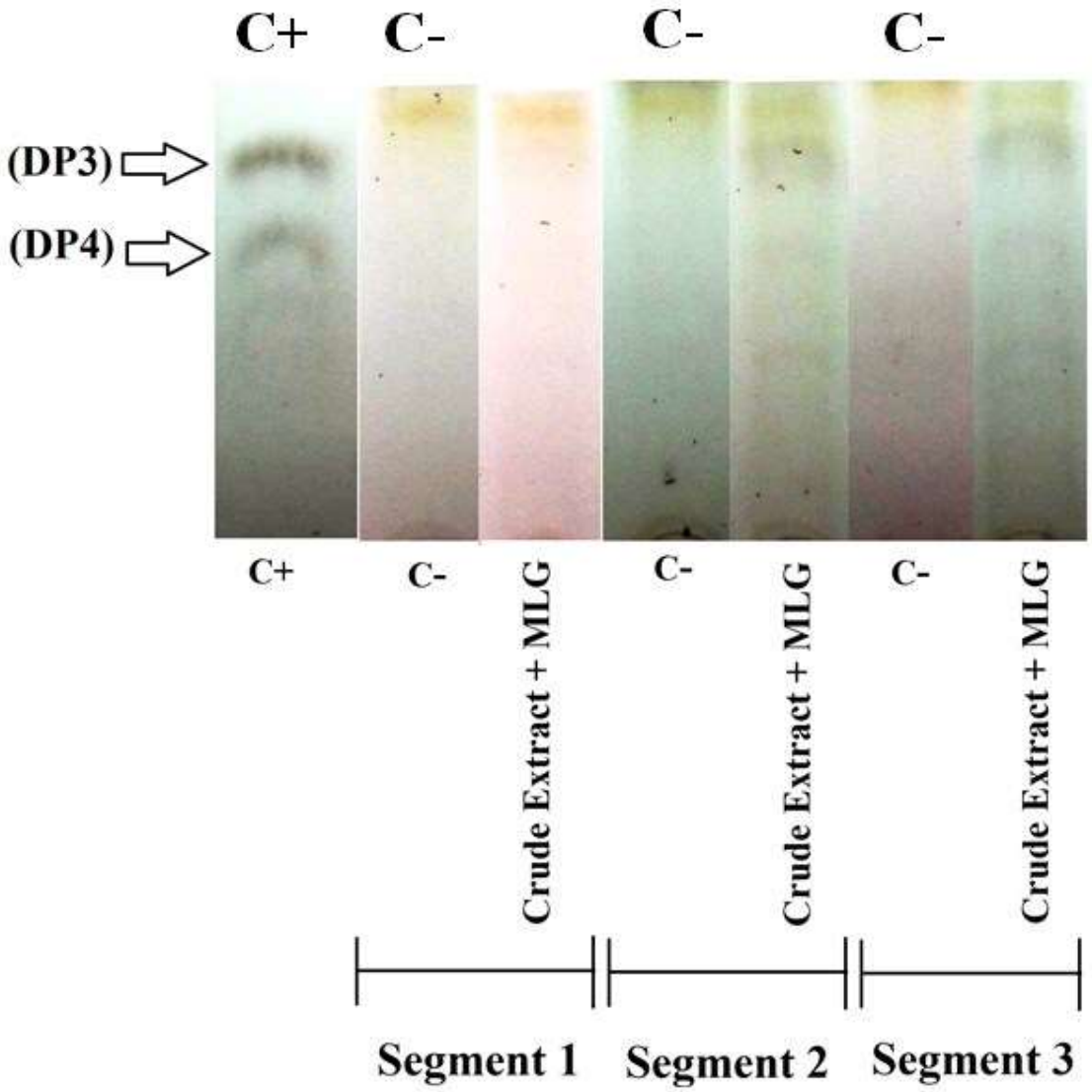

Figure 10. Detection of DP3 and DP4 by thin-layer chromatography. Products of positive control (C+) are DP3 and DP4, indicated by arrows. Negative controls (C-) are pre-boiled crude extracts with barley MLG. The first segment has no bands, whereas the second and third segments display DP3 and DP4 bands, indicating MLGase activity.

2.4.6.2. Detection of enzyme activity using HPAEC-PAD

We used HPAEC-PAD to detect MLG oligosaccharides as this technique is more sensitive and produces more precise results. Thus, we analyzed specifically the presence and the amounts of DP3 and DP4 in the three segments. The experiment was stoichiometrically adjusted for a fair comparison among the extracts. However, this sensitivity also produces small peaks that are unknown.

Unlike the TLC analysis (Figure 10), HPAE-PAD detected the presence of DP3 and DP4 in all the segments (Figure 11). The positive control is in blue (secondary axis) and was generated using purchased MLGase and barley MLG, generating specifically DP3 and DP4, but

not at the 8 min peak as we observed in the crude extract. Negative controls are named as C- and segments as (S). At elution time 8.0, an unknown oligosaccharide was observed, which could be a disaccharide (cellobiose or laminaribiose) produced by further degradation of DP3 and DP4 by the exo-glucosidases presence (Kuge et al., 2015). Table 2 shows that the enzymatic activity level of the three segments. The second segment has a significantly higher activity than other segments. The correlation with gene expression (*Sblic1*), as seen in Figure 9, suggests that a peak of activity in segment 2 could be correlated with the process of aerenchyma formation.

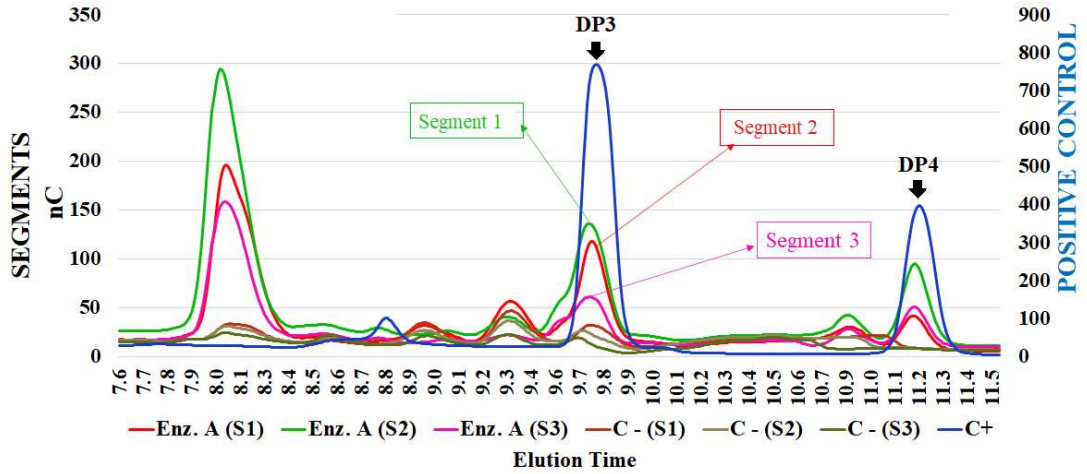

Figure 11. Enzymatic assays' chromatogram with crude extracts. The positive control (blue) is on the secondary axis (y) on the right side. The first segment is in green color, the second in red, and the third in lilac color. Arrows indicate DP3 and DP4 metabolites upon MLG hydrolysis using commercial MLGase. At 8.0 min elution time, an unknown oligosaccharide could be cellobiose (DP2), a disaccharide produced by further hydrolysis of DP3 and DP4 by exo-β-glucanases (Kuge et al., 2015).

Table 2. Enzymatic activity as aerenchyma develops.

Segments	Enzymatic activity
S1	**0.06±0.05 c**
S2	**0.08±0.01 b**
S3	**0.06±0.02 bc**
C+	**0.47±0.01 a**
Average Mean	0.17
CV (%)	4.93
p-value	0.0001

Mean values (n=3) ± standard errors indicate enzymatic action. Original data were transformed into √X for statistical analysis. Distinct letters indicate statistically significant differences by Tukey's test ($p<0.05$) and are in bold. C.V. (%) = coefficient of variation.

2.4.7. Cell wall fractionation

2.4.7.1. MLG quantification

In this experiment, the MLG is extracted from the segments' cell wall and, subsequently, subjected to MLGase digestion. This reaction generates DP3 and DP4. Table 3 shows that the first segment has the highest relative amount of MLG, while the second and third segments still contain MLG but do not differ significantly.

Table 3. MLG relative quantity and DP3:DP4 ratios.

Segments	MLG relative quantity	DP3:DP4 ratio
S1	**0.64±0.11 a**	**1.44±0.08 b**
S2	**0.34±0.02 c**	**1.67±0.04 a**
S3	**0.31±0.05 c**	**1.73±0.14 a**
C+	**0.49±0.04 b**	**1.59±0.08 ab**
Average mean	0.44	1.61
CV (%)	14.93	5.55
p-value	0.0001	0.0034

Mean values indicate MLG relative quantity and DP3:DP4 ratio per segment (n = 4) ± standard error. Original data were transformed into √X for statistical analysis. Distinct letters indicate statistically significant differences by Tukey's ($p<0.05$) and are in bold. CV (%) = coefficient of variation

2.4.7.2. Profile of structural carbohydrates

Table 4 shows no statistical differences in fucose, arabinose, galactose, and xylose among segments. Xylose, however, represents 15% of structural polysaccharides, an expected value found in grasses. Glucose and mannose significantly decreased from segment 1 to segment 3. The finding of a decrease in glucose, the monosaccharide that composes MLG, is another indication that the polymer is degraded during aerenchyma development.

Table 4. Percentage of neutral monosaccharides extracted from the alcohol-insoluble residue.

Samples	Fucose	Arabinose	Galactose	Glucose	Xylose	Mannose
S1	0.24±0.10	7.42±3.09	4.03±1.70	**3.75±1.48 a**	16.35±6.26	**0.99±0.40 a**
S2	0.14±0.02	6.08±0.54	3.63±0.35	**2.35±0.31 ab**	13.87±1.39	**0.50±0.05 b**
S3	0.17±0.01	6.12±0.48	3.74±0.30	**2.11±0.40 b**	14.61±1.73	**0.50±0.04 b**
General Average	0.18	6.54	3.8	2.74	14.95	0.66
CV (%)	13.23	12.53	12.44	14.06	11.74	13.86
p-value	0.0633	0.5624	0.9065	0.0405	0.6953	0.0082

Mean values indicate the percentage of neutral monosaccharides (n=4) ± standard error. Original data were transformed into √X for statistical analysis. Distinct letters indicate statistically significant differences by Tukey's ($p<0.05$) and are in bold. CV (%) = coefficient of variation.

2.5. DISCUSSION

2.5.1. Anatomical characterization

The primary roots are a convenient model system to study the aerenchyma development and MLG hydrolysis. Seven-day-old primary roots are quickly obtained, do not branch, and have less complex anatomy to characterize. Thus, this type of root enabled us to analyze four seedlings' entire primary roots, subsequently dividing them into three segments based on their aerenchyma development: S1 (no aerenchyma), S2 (aerenchyma initiation). S3 (developing aerenchyma). The micrographs indicated a similar pattern in the distribution of the gas spaces in the third, fourth, and fifth segments. They are displayed in a scattered and discontinuous fashion in the cortex as aerenchyma develops. Consequently, this anatomical pattern differs from the mature roots of sorghum (Figure 4) and sugarcane (Figure 3), in which the last segments are mainly filled by gas spaces (Leite et al., 2017).

The cell wall changes during aerenchyma formation in sugarcane have been studied by Leite and coworkers (2017). One of the highlights of the cell wall transformations observed was the disappearance of MLG signal (using BG1 antibody) from the cortex walls as aerenchyma develops (Figure 3). However, the authors also noted that if MLG is followed by quantitative detection (using *B. subtilis* MLGase), not all the polymer disappears. It could be possible that the quantitative analysis detected the remaining MLG in the epidermic walls and the vascular system,

like in Figure 3 (Leite et al., 2017). Based on these findings, the authors suggested the presence of endo-(1,3;1,4)-β-D-glucanases as the enzymes responsible for MLG hydrolysis in the cortex.

Later on, Grandis and coworkers (2019) measured enzyme activity, proteomics, and gene expression to assess sugarcane aerenchyma development. They detected the expression of three GH17 genes and respective proteins that correlated with aerenchyma formation in roots. The authors proposed that the MLG's primary function in aerenchyma development could be structural.

MLG has basically two functions: structural and another as a storage polysaccharide (Buckeridge et al., 2004). Carpita (1996) proposed that MLG is a transition polysaccharide in coleoptiles of maize. Moreover, the polymer can act as a scaffold for arabinoxylan (the main hemicellulose of grasses), and when it is retrieved, it may cause a collapse of the cell walls, helping to form progressive larger spaces within the root. Grandis and coworkers (2019) do not discard MLG's possibility of interfering with cell wall porosity. In this case, the retrieval of MLG from the walls of the cortex would open the way for other hydrolases (e.g., xylanases, xyloglucanases, and cellulases), leading to the modifications on the walls observed by Leite and coworkers (2017).

Here, we observed rather similar events in the roots of sorghum seedlings. The aerenchyma formed similarly as in sugarcane, and the chemical transformation in the cell walls is like those observed in sugarcane (Leite et al., 2017). As observed by these authors, the glucose levels in the roots decreased as aerenchyma developed. Simultaneously, the detection of MLG using purchased MLGase showed that the polysaccharide decreases during the process. An alteration in MLG fine structure has also been observed. The ratio DP3/DP4 increased during aerenchyma development (Table 3), suggesting that progressively more β-1,3 linkages are present in the MLG left in the wall, probably out of the cortex as demonstrated for sugarcane. Concurrently, it can be suggested that relatively more MLG containing β-1,4 linkages are retrieved from the wall.

MLG's alternative hypothesis could function as a storage carbohydrate is not favored by the observation that glucose does not increase in roots while MLG is degraded. On the other hand, the structural function (scaffold and porosity determination) is likely, although our data cannot be used to support this hypothesis.

2.5.2. Cladogram and phylogenetic inferences

The cladogram shows the existence of MLG in some clades and its alleged absence in other groups. Therefore, this scattered distribution tempts scientists to suggest MLG multiple

independent origins, although a broader taxonomic sampling is necessary to state this hypothesis. Furthermore, the systematic collection and analysis from the literature suggested MLG as a structural polymer in all clades, exempting Poaceae, in which the polymer has gained multiple functions.

Many researchers annotated GH17 *endo-(1,3;1,4)-β-glucanases* as *endo-(1,3)-β-D- glucanases* and vice versa (McKinley et al., 2016; Grandis et al., 2019). However, those data were not subject to phylogenetic reconstruction methods and may lead to misconceptions. Then, our phylogeny contributes to a better distinction between subgroups within GH17 and, ultimately, MLG hydrolysis mechanisms. The phylogeny of GH17 *endo-(1,3;1,4)-β-glucanases*, which are Poaceae-specific, has two major phylogenetic subgroups: α and β. The α group, to which *Sblic1* belongs, has the traditional nesting pattern of a species tree of Poaceae, and the β group, comprising *Sblic2* and *Sblic3*, has a more complex nesting pattern, although it still resembles a nesting pattern of a species tree. *Sblic1* accumulates fewer genetic changes during evolution. On the other hand, *Sblic2* and *Sblic3* accumulate similar genetic changes and are close to each other in the ninth chromosome. Despite their closer evolutionary proximity, *Sblic3* showed no gene expression by real-time analysis. Besides, it could be that *Sblic2* and *Sblic3* originated from gene duplication, and *Sblic3* lost its function. Nonetheless, further investigation of *Sblic3* should be done to assert possible loss of function.

Contrasting to insufficient information associated with MLG remodeling, the MLG synthesis has been intensively studied by the US and Australian institutions. Our inferences are in accordance with the restriction of *CslFs* to the Poaceae family and the presence of *CslHs* throughout monocots (Little et al., 2018). However, our data suggest the presence of *CslHs* within Magnoliidae, something not previously reported.

Due to the diversity of genes associated with MLG metabolism, we suggest that the multiple roles of MLG in Poaceae may be associated with the diversity of families for its synthesis (*CslFs*, *CslHs,* and *CslJs*) and remodeling (GH16 and GH17).

2.5.3. MLG hydrolysis in sorghum primary roots

Plant cell wall expansion occurs mainly by expansion and elongation. In this scenario where cellular elasticity is vital, it is plausible that in young sorghum leaves, which have abundant MLG (Ermawar et al., 2015), the high-level expression of *Sblic2* is correlated to polymer hydrolysis. Another piece of evidence was reported by Slakeski and coworkers (1990). They

observed a more significant amount of barley *endo-(1,3;1,4)-β-glucanase* mRNA in younger leaves compared to mature leaves.

During aerenchyma development in sorghum roots, the expression of *Sblic2* does not change, whereas we observed an increase of *Sblic1* (10-fold from segment 1 to segment 3). On the other hand, the MLG synthase *SbCslF6* tends to decrease its expression. These observations suggest that while MLG is being degraded, its biosynthesis is partially arrested. Some synthesis may continue in the roots because MLG is still present in tissues other than the cortex, although this assumption remains to be investigated.

The analysis of the fragments (using TLC and HPAEC-PAD) after assays with crude enzyme extracts and segments 1, 2, and 3 showed that endo-(1,3;1,4)-β-glucanases-like enzymes are present in roots. The activity progressively increases with aerenchyma development, suggesting a possible correlation between gene expression, enzyme activity, and the decrease in MLG in the roots. A similar scenario was observed in the development of aerenchyma in sugarcane roots, in which there is a concomitant increase in MLG hydrolysis (Leite et al., 2017) and *endo-(1,3;1,4)-β-glucanase* protein level (SCJFRT1008G05.g) (Grandis et al., 2019), although the authors considered SCJFRT1008G05.g as an *endo-(1,3)-β-glucanase*.

Based on the molecular phylogenetics, gene expression profile, enzyme activity assays, and MLG quantification, our group suggests SBLIC1 and SBLIC2 as conceivable MLGases associated with MLG's hydrolysis during aerenchyma development in seedlings. Nonetheless, the data do not allow inferences about the MLG's role in aerenchyma development of primary roots seedlings.

2.6. CONCLUSION

The sorghum's primary roots can be obtained quickly (approximately 7 days), and their diameter allows clear visualization of the gas spaces by microtomography, a fundamental technique for aerenchyma characterization and its division into three fundamental stages. Additionally, the sequenced genome enabled the construction of robust molecular phylogenies, revealing the sequences of the selected genes *Sblic1, Sblic2,* and *SbCslF6*, which afforded the evaluation of the levels of gene expression associated with hydrolysis and biosynthesis of MLG in different segments of the sorghum roots.

The finding of expression of only two genes associated with hydrolases, with only one of them varying *pari passu* with aerenchyma formation, led us to measure enzyme activities using

crude extracts, which ultimately led us to conclude that MLG hydrolysis indeed takes place in sorghum roots and suggests a possible association with aerenchyma formation. We further conclude that primary sorghum roots are a promising model for studying the mechanisms related to mixed-linkage glucan hydrolysis during the aerenchyma development.

REFERENCES

Abiko, T., and Miyasaka, S. C. (2020). Aerenchyma and barrier to radial oxygen loss are formed in roots of Taro (Colocasia esculenta) propagules under flooded conditions. *J. Plant Res.* 133, 49–56. doi:10.1007/s10265-019-01150-6.

Akiyama, T., Jin, S., Yoshida, M., Hoshino, T., Opassiri, R., and Ketudat Cairns, J. R. (2009). Expression of an endo-(1,3;1,4)-β-glucanase in response to wounding, methyl jasmonate, abscisic acid and ethephon in rice seedlings. *J. Plant Physiol.* 166, 1814–1825. doi:10.1016/j.jplph.2009.06.002.

Amaral, L. I. V. do, Gaspar, M., Costa, P. M. F., Aidar, M. P. M., and Buckeridge, M. S. (2007). Novo método enzimático rápido e sensível de extração e dosagem de amido em materiais vegetais. *Hoehnea*. doi:10.1590/s2236-89062007000400001.

Arber, A. (1920). *Water plants, a study of aquatic angiosperms*. Cambridge, UK: Cambridge University Press.

Aschi-Smiti, S., Chaïbi, W., Brouquisse, R., Ricard, B., and Saglio, P. (2003). Assessment of enzyme induction and aerenchyma formation as mechanisms for flooding tolerance in Trifolium subterraneum "Park." *Ann. Bot.* doi:10.1093/aob/mcf022.

Astier, J., Gross, I., and Durner, J. (2018). Nitric oxide production in plants: An update. *J. Exp. Bot.* doi:10.1093/jxb/erx420.

Baena, I., Pérez-Mendoza, D., Sauviac, L., Francesch, K., Martín, M., Rivilla, R., et al. (2019). A partner-switching system controls activation of mixed-linkage β-glucan synthesis by c-di-GMP in Sinorhizobium meliloti. *Environ. Microbiol.* doi:10.1111/1462-2920.14624.

Bartlett, M. S. (1936). The Square Root Transformation in Analysis of Variance. *Suppl. to J. R. Stat. Soc.* 3, 68–78. doi:10.2307/2983678.

Baumann, M. J., Eklöf, J. M., Michel, G., Kallas, Å. M., Teeri, T. T., Czjzek, M., et al. (2007). Structural evidence for the evolution of xyloglucanase activity from xyloglucan Endo-transglycosylases: Biological implications for cell wall metabolism. *Plant Cell.* doi:10.1105/tpc.107.051391.

Begum, M. K., Alam, M. R., and Islam, M. S. (2013). Adaptive mechanisms of sugarcane genotypes under flood stress condition. *World J. Agric. Sci.*

Behall, K. M., Scholfield, D. J., and Hallfrisch, J. (2004). Diets containing barley significantly reduce lipids in mildly hypercholesterolemic men and women. *Am. J. Clin. Nutr.* 80, 1185–1193. doi:10.1016/S0084-3741(08)70311-1.

Behar, H., Graham, S. W., and Brumer, H. (2018). Comprehensive cross-genome survey and phylogeny of glycoside hydrolase family 16 members reveals the evolutionary origin of EG16 and XTH proteins in plant lineages. *Plant J.* doi:10.1111/tpj.14004.

Bouranis, D. L., Chorianopoulou, S. N., Siyiannis, V. F., Protonotarios, V. E., and Hawkesford, M. J. (2003). Aerenchyma formation in roots of maize during sulphate starvation. *Planta.* doi:10.1007/s00425-003-1007-6.

Bourdon, I., Yokoyama, W., Davis, P., Hudson, C., Backus, R., Richter, D., et al. (1999). Postprandial lipid, glucose, insulin, and cholecystokinin responses in men fed barley pasta enriched with β-glucan. *Am. J. Clin. Nutr.* 69, 55–63.

Brandão, R. (2007). Transformação genética de Sorghum bicolor (L. Moench) visando tolerância ao AL3+.

Brar, G. S., and Stewart, B. A. (1994). Germination under controlled temperature and field emergence of 13 sorghum cultivars. *Crop Sci.* 34, 1336–1340. doi:10.2135/cropsci1994.0011183X003400050036x.

Brennan, C. S., and Cleary, L. J. (2005). The potential use of cereal (1→3,1→4)-β-d-glucans as functional food ingredients. *J. Cereal Sci.* 42, 1–13. doi:10.1016/j.jcs.2005.01.002.

Buckeridge, M. S. (2010). Seed cell wall storage polysaccharides: Models to understand cell wall biosynthesis and degradation. *Plant Physiol.* 154, 1017–1023. doi:10.1104/pp.110.158642.

Buckeridge, M. S. (2018). The evolution of the Glycomic Codes of extracellular matrices. *BioSystems*. doi:10.1016/j.biosystems.2017.10.003.

Buckeridge, M. S., and de Souza, A. P. (2014). Breaking the "Glycomic Code" of Cell Wall Polysaccharides May Improve Second-Generation Bioenergy Production from Biomass. *Bioenergy Res.* doi:10.1007/s12155-014-9460-6.

Buckeridge, M. S., Rayon, C., Urbanowicz, B., Tiné, M. A. S., and Carpita, N. C. (2004). Mixed Linkage (1→3),(1→4)-β- d -Glucans of Grasses. *Cereal Chem.* 81, 115–127. doi:10.1094/CCHEM.2004.81.1.115.

Buckeridge, M. S., Vergara, C. E., and Carpita, N. C. (1999). The Mechanism of Synthesis of a Mixed-Linkage (1→3),(1→4)β-d-Glucan in Maize. Evidence for Multiple Sites of Glucosyl Transfer in the Synthase Complex. *Plant Physiol.* 120, 1105–1116. doi:10.1104/pp.120.4.1105.

Burton, R. A., Collins, H. M., Kibble, N. A. J., Smith, J. A., Shirley, N. J., Jobling, S. A., et al. (2011). Over-expression of specific HvCslF cellulose synthase-like genes in transgenic barley increases the levels of cell wall (1,3;1,4)-β-d-glucans and alters their fine structure. *Plant Biotechnol. J.* doi:10.1111/j.1467-7652.2010.00532.x.

Burton, R. A., and Fincher, G. B. (2009). (1,3;1,4)-β-D-glucans in cell walls of the poaceae, lower plants, and fungi: A tale of two linkages. *Mol. Plant*. doi:10.1093/mp/ssp063.

Burton, R. A., and Fincher, G. B. (2012). Current challenges in cell wall biology in the cereals and grasses. *Front. Plant Sci.* doi:10.3389/fpls.2012.00130.

Burton, R. A., Wilson, S. M., Hrmova, M., Harvey, A. J., Shirley, N. J., Medhurst, A., et al. (2006). Cellulose synthase-like CslF genes mediate the synthesis of cell wall (1,3;1,4)-β-D-glucans. *Science (80-.).* 311, 1940–1942. doi:10.1126/science.1122975.

Carbonero, E. R., Montai, A. V., Mellinger, C. G., Eliasaro, S., Sassaki, G. L., Gorin, P. A. J., et al. (2005). Glucans of lichenized fungi: Significance for taxonomy of the genera Parmotrema and Rimelia. *Phytochemistry*. doi:10.1016/j.phytochem.2005.02.020.

Carpita, N. C. (1984). Cell wall development in maize coleoptiles. *Plant Physiol.* 76, 205–212. doi:10.1104/pp.76.1.205.

Carpita, N. C. (1996). Structure and biogenesis of the cell walls of grasses. *Annu. Rev. Plant Physiol. Plant Mol. Biol.* doi:10.1146/annurev.arplant.47.1.445.

Carpita, N. C., Defernez, M., Findlay, K., Wells, B., Shoue, D. a, Catchpole, G., et al. (2001). Cell wall architecture of the elongating maize coleoptile. *Plant Physiol.* 127, 551–565. doi:10.1104/pp.010146.

Carpita, N. C., and McCann, M. C. (2010). The Maize Mixed-Linkage (1→3),(1→4)-β-d-Glucan Polysaccharide Is Synthesized at the Golgi Membrane. *Plant Physiol.* 153, 1362 LP – 1371.

Casto, A. L., McKinley, B. A., Yu, K. M. J., Rooney, W. L., and Mullet, J. E. (2018). Sorghum stem aerenchyma formation is regulated by SbNAC_D during internode development. *Plant Direct*. doi:10.1002/pld3.85.

Chaari, F., and Chaabouni, S. E. (2019). Fungal β-1,3-1,4-glucanases: production, proprieties and biotechnological applications. *J. Sci. Food Agric.* doi:10.1002/jsfa.9491.

Chen, C. C., Huang, J. W., Zhao, P., Ko, T. P., Huang, C. H., Chan, H. C., et al. (2015). Structural analyses and yeast production of the β-1,3-1,4-glucanase catalytic module encoded by the licB gene of Clostridium thermocellum. *Enzyme Microb. Technol.* doi:10.1016/j.enzmictec.2015.01.002.

Colmer, T. D. (2003). Aerenchyma and an inducible barrier to radial oxygen loss facilitate root aeration in upland, paddy and deep-water rice (Oryza sativa L.). *Ann. Bot.* doi:10.1093/aob/mcf114.

Colmer, T. D., Peeters, A. J. M., Wagemaker, C. A. M., Vriezen, W. H., Ammerlaan, A., and Voesenek, L. A. C. J. (2004). Expression of α-expansin genes during root acclimations to O 2 deficiency in Rumex palustris. *Plant Mol. Biol.* doi:10.1007/s11103-004-3844-5.

Crivellari, A. C. (2012). Caracterização estrutural das hemiceluloses de paredes celulares de cana-de-açúcar. doi:10.11606/D.41.2012.tde-10102012-084959.

Cseh, A., Soõs, V., Rakszegi, M., Türkösi, E., Balázs, E., and Molnár-Láng, M. (2013). Expression of HvCslF9 and HvCslF6 barley genes in the genetic background of wheat and their influence on the wheat β-glucan content. *Ann. Appl. Biol.* doi:10.1111/aab.12043.

De Paula, A. C. C. F. F., Sousa, R. V., Figueiredo-Riberio, R. C. L., and Buckeridge, M. S. (2005). Hypoglycemic activity of polysaccharide fractions containing β-glucans from extracts of Rhynchelytrum repens (Willd.) C.E. Hubb., Poaceae. *Brazilian J. Med. Biol. Res.* 38, 885–893. doi:10.1590/S0100-879X2005000600010.

de Souza, A. P., Leite, D. C. C., Pattathil, S., Hahn, M. G., and Buckeridge, M. S. (2013). Composition and Structure of Sugarcane Cell Wall Polysaccharides: Implications for Second-Generation Bioethanol Production. *Bioenergy Res.* 6, 564–579. doi:10.1007/s12155-012-9268-1.

Dillon, S. L., Lawrence, P. K., Henry, R. J., and Price, H. J. (2007). Sorghum resolved as a distinct genus based on combined ITS1, ndhF and Adh1 analyses. *Plant Syst. Evol.* doi:10.1007/s00606-007-0571-9.

Doblin, M. S., Pettolino, F. A., Wilson, S. M., Campbell, R., Burton, R. A., Fincher, G. B., et al. (2009). A barley cellulose synthase-like CSLH gene mediates (1,3;1,4)- -D-glucan synthesis in transgenic Arabidopsis. *Proc. Natl. Acad. Sci.* 106, 5996–6001. doi:10.1073/pnas.0902019106.

Drew, M. C., He, C.-J., and Morgan, P. W. (1989). Decreased Ethylene Biosynthesis, and Induction of Aerenchyma, by Nitrogen- or Phosphate-Starvation in Adventitious Roots of Zea mays L. . *Plant Physiol.* doi:10.1104/pp.91.1.266.

Drew, M. C., He, C. J., and Morgan, P. W. (2000). Programmed cell death and aerenchyma formation in roots. *Trends Plant Sci.* doi:10.1016/S1360-1385(00)01570-3.

Drew, M. C., Jackson, M. B., Giffard, S. C., and Campbell, R. (1981). Inhibition by silver ions of gas space (aerenchyma) formation in adventitious roots of Zea mays L. subjected to exogenous ethylene or to oxygen deficiency. *Planta.* doi:10.1007/BF00383890.

Du, X. M., Ni, X. L., Ren, X. L., Xin, G. L., Jia, G. L., Liu, H. D., et al. (2018). De novo transcriptomic analysis to identify differentially expressed genes during the process of aerenchyma formation in Typha angustifolia leaves. *Gene.* doi:10.1016/j.gene.2018.03.099.

Eder, M., Tenhaken, R., Driouich, A., and Lütz-Meindl, U. (2008). Occurrence and characterization of arabinogalactan-like proteins and hemicelluloses in Micrasterias (Streptophyta). *J. Phycol.* 44, 1221–1234. doi:10.1111/j.1529-8817.2008.00576.x.

Eklöf, J. M., Shojania, S., Okon, M., McIntosh, L. P., and Brumer, H. (2013). Structure-function analysis of a broad specificity Populus trichocarpa endo-β-glucanase reveals an evolutionary link between bacterial licheninases and plant XTH gene products. *J. Biol. Chem.* 288, 15786–15799. doi:10.1074/jbc.M113.462887.

Ermawar, R. A., Collins, H. M., Byrt, C. S., Betts, N. S., Henderson, M., Shirley, N. J., et al. (2015). Distribution, structure and biosynthetic gene families of (1,3;1,4)-β-glucan in Sorghum bicolor. *J. Integr. Plant Biol.* 57, 429–445. doi:10.1111/jipb.12338.

Evans, D. E. (2003). Aerenchyma formation. *New Phytol.* 161, 35–49. doi:10.1046/j.1469-8137.2003.00907.x.

Fan, M., Herburger, K., Jensen, J. K., Zemelis-Durfee, S., Brandizzi, F., Fry, S. C., et al. (2018). A Trihelix Family Transcription Factor Is Associated with Key Genes in Mixed-Linkage Glucan Accumulation. *Plant Physiol.* doi:10.1104/pp.18.00978.

Fan, M., Zhu, J., Richards, C., Brown, K. M., and Lynch, J. P. (2003). Physiological roles for aerenchyma in phosphorus-stressed roots. *Funct. Plant Biol.* doi:10.1071/FP03046.

Ferreira, D. F. (2011). Sisvar: a computer statistical analysis system. *Ciência e Agrotecnologia.* doi:10.1590/s1413-70542011000600001.

Fincher, G. B. (2009). Revolutionary Times in Our Understanding of Cell Wall Biosynthesis and Remodeling in the Grasses. *Plant Physiol.* 149, 27–37. doi:10.1104/pp.108.130096.

Ford, C. W., and Percival, E. (1965). 551. Polysaccharides synthesised by Monodus subterraneus. Part II. The cell-wall glucan. *J. Chem. Soc.* doi:10.1039/JR9650003014.

Fry, S. C. (2004). Primary cell wall metabolism: Tracking the careers of wall polymers in living plant cells. *New Phytol.* doi:10.1111/j.1469-8137.2004.00980.x.

Fry, S. C., Mohler, K. E., Nesselrode, B. H. W. A., and Franková, L. (2008a). Mixed-linkage β-glucan: Xyloglucan endotransglucosylase, a novel wall-remodelling enzyme from Equisetum (horsetails) and charophytic algae. *Plant J.* doi:10.1111/j.1365-313X.2008.03504.x.

Fry, S. C., Nesselrode, B. H. W. A., Miller, J. G., and Mewburn, B. R. (2008b). Mixed-linkage (1→3,1→4)-β-D-glucan is a major hemicellulose of Equisetum (horsetail) cell walls. *New Phytol.* 179, 104–115. doi:10.1111/j.1469-8137.2008.02435.x.

Gibbs, D. J., Bacardit, J., Bachmair, A., and Holdsworth, M. J. (2014). The eukaryotic N-end rule pathway: Conserved mechanisms and diverse functions. *Trends Cell Biol.* doi:10.1016/j.tcb.2014.05.001.

Gibbs, D. J., Conde, J. V., Berckhan, S., Prasad, G., Mendiondo, G. M., and Holdsworth, M. J. (2015). Group VII Ethylene Response Factors Coordinate Oxygen and Nitric Oxide Signal Transduction and Stress Responses in Plants. *Plant Physiol.* 169, 23 LP – 31. doi:10.1104/pp.15.00338.

Gibbs, D. J., Lee, S. C., Md Isa, N., Gramuglia, S., Fukao, T., Bassel, G. W., et al. (2011). Homeostatic response to hypoxia is regulated by the N-end rule pathway in plants. *Nature.* doi:10.1038/nature10534.

Gibbs, D. J., Tedds, H. M., Labandera, A. M., Bailey, M., White, M. D., Hartman, S., et al. (2018). Oxygen-dependent proteolysis regulates the stability of angiosperm polycomb repressive complex 2 subunit VERNALIZATION 2. *Nat. Commun.* doi:10.1038/s41467-018-07875-7.

Gibeaut, D. M., and Carpita, N. C. (1993). Synthesis of (1-->3), (1-->4)-beta-D-glucan in the Golgi apparatus of maize coleoptiles. *Proc. Natl. Acad. Sci. U. S. A.* 90, 3850–3854.

Gibeaut, D. M., Pauly, M., Bacic, A., and Fincher, G. B. (2005). Changes in cell wall polysaccharides in developing barley (Hordeum vulgare) coleoptiles. *Planta* 221, 729–738. doi:10.1007/s00425-005-1481-0.

Görlach, J. M., Van Der Knaap, E., and Walton, J. D. (1998). Cloning and targeted disruption of MLG1, a gene encoding two of three extracellular mixed-linked glucanases of Cochliobolus carbonum. *Appl. Environ. Microbiol.* doi:10.1128/aem.64.2.385-391.1998.

Grandis, A., Leite, D. C. C., Tavares, E. Q. P., Arenque-Musa, B. C., Gaiarsa, J. W., Martins, M. C. M., et al. (2019). Cell wall hydrolases act in concert during aerenchyma development in sugarcane roots. *Ann. Bot.* doi:10.1093/aob/mcz099.

Gunawardena, A. H. L. A. N., Pearce, D. M. E., Jackson, M. B., Hawes, C. R., and Evans, D. E. (2001a). Rapid changes in cell wall pectic polysaccharides are closely associated with early stages of aerenchyma formation, a spatially localized form of programmed cell death in roots of maize (Zea mays L.) promoted by ethylene. *Plant, Cell Environ.* doi:10.1046/j.1365-3040.2001.00774.x.

Gunawardena, A. H. L. A. N., Pearce, D. M., Jackson, M. B., Hawes, C. R., and Evans, D. E. (2001b). Characterisation of programmed cell death during aerenchyma formation induced by ethylene or hypoxia in roots of maize (Zea mays L.). *Planta*. doi:10.1007/s004250000381.

Gupta, K. J., Fernie, A. R., Kaiser, W. M., and van Dongen, J. T. (2011). On the origins of nitric oxide. *Trends Plant Sci.* doi:10.1016/j.tplants.2010.11.007.

Gupta, K. J., Mur, L. A. J., Wany, A., Kumari, A., Fernie, A. R., and Ratcliffe, R. G. (2020). The role of nitrite and nitric oxide under low oxygen conditions in plants. *New Phytol.* 225, 1143–1151. doi:10.1111/nph.15969.

Han, N., Na, C., Chai, Y., Chen, J., Zhang, Z., Bai, B., et al. (2017). Over-expression of (1,3;1,4)-β-D-glucanase isoenzyme EII gene results in decreased (1,3;1,4)-β-D-glucan content and increased starch level in barley grains. *J. Sci. Food Agric.* 97, 122–127. doi:10.1002/jsfa.7695.

Harholt, J., Sørensen, I., Fangel, J., Roberts, A., Willats, W. G. T., Scheller, H. V., et al. (2012). The glycosyltransferase repertoire of the spikemoss selaginella moellendorffii and a comparative study of its cell wall. *PLoS One* 7. doi:10.1371/journal.pone.0035846.

Hariprasanna, K., and Patil, J. V (2015). "Sorghum: Origin, Classification, Biology and Improvement," in *Sorghum Molecular Breeding*, eds. R. Madhusudhana, P. Rajendrakumar, and J. V Patil (New Delhi: Springer India), 3–20. doi:10.1007/978-81-322-2422-8_1.

Harris, P. J., and Fincher, G. B. (2009a). "Distribution, fine structure and function of (1,3;1,4)----lucans in the grasses and other taxa," in *Chemistry, Biochemistry, and Biology of 1-3 Beta Glucans and Related Polysaccharides* doi:10.1016/B978-0-12-373971-1.00021-2.

Harris, P. J., and Fincher, G. B. (2009b). "Distribution, Fine Structure and Function of (1,3;1,4)-β-Glucans in the Grasses and Other Taxa," in *Chemistry, Biochemistry, and Biology of 1-3 Beta Glucans and Related Polysaccharides* doi:10.1016/B978-0-12-373971-1.00021-2.

Hassanein, A.-H. M., and Azab, A. M. (1993). "Salt tolerance of grain sorghum," in *Towards the rational use of high salinity tolerant plants: Vol. 2 Agriculture and forestry under marginal soil water conditions*, eds. H. Lieth and A. A. Al Masoom (Dordrecht: Springer Netherlands), 153–156. doi:10.1007/978-94-011-1860-6_19.

He, C. J., Finlayson, S. A., Drew, M. C., Jordan, W. R., and Morgan, P. W. (1996a). Ethylene biosynthesis during aerenchyma formation in roots of maize subjected to mechanical impedance and hypoxia. *Plant Physiol.* doi:10.1104/pp.112.4.1679.

He, C. J., Morgan, P. W., and Drew, M. C. (1996b). Transduction of an ethylene signal is required for cell death and lysis in the root cortex of maize during aerenchyma formation induced by hypoxia. *Plant Physiol.* doi:10.1104/pp.112.2.463.

Herburger, K., Ryan, L. M., Popper, Z. A., and Holzinger, A. (2017). Localisation and substrate specificities of transglycanases in charophyte algae relate to development and morphology. *J. Cell Sci.*, jcs.203208. doi:10.1242/jcs.203208.

Hinz, M., Wilson, I. W., Yang, J., Buerstenbinder, K., Llewellyn, D., Dennis, E. S., et al. (2010). Arabidopsis RAP2.2: An Ethylene Response Transcription Factor That Is Important for Hypoxia Survival. *Plant Physiol.* 153, 757 LP – 772. doi:10.1104/pp.110.155077.

Hofmann, A., Wienkoop, S., Harder, S., Bartlog, F., and Lüthje, S. (2020). Hypoxia-responsive class iii peroxidases in maize roots: Soluble and membrane-bound isoenzymes. *Int. J. Mol. Sci.* doi:10.3390/ijms21228872.

Høj, P. B., and Fincher, G. B. (1995). Molecular evolution of plant β-glucan endohydrolases. *Plant J.* 7, 367–379. doi:10.1046/j.1365-313X.1995.7030367.x.

Honegger, R., and Haisch, A. (2001). Immunocytochemical location of the (1⟶3) (1⟶4)-β-glucan lichenin in the lichen-forming ascomycete Cetraria islandica (Icelandic moss). *New Phytol.* 150, 739–746. doi:10.1046/j.1469-8137.2001.00122.x.

Houston, K., Russell, J., Schreiber, M., Halpin, C., Oakey, H., Washington, J. M., et al. (2014). A genome wide association scan for (1,3;1,4)-β- glucan content in the grain of contemporary 2-row Spring and Winter barleys. *BMC Genomics* 15. doi:10.1186/1471-2164-15-907.

Hu, G., Burton, C., Hong, Z., and Jackson, E. (2014). A mutation of the cellulose-synthase-like (CslF6) gene in barley (Hordeum vulgare L.) partially affects the β-glucan content in grains. *J. Cereal Sci.* doi:10.1016/j.jcs.2013.12.009.

Iakiviak, M., Mackie, R. I., and Cann, I. K. O. (2011). Functional Analyses of Multiple Lichenin-Degrading Enzymes from the Rumen Bacterium Ruminococcus albus 8. *Appl. Environ. Microbiol.* doi:10.1128/aem.06088-11.

Ibatullin, F. M., Banasiak, A., Baumann, M. J., Greffe, L., Takahashi, J., Mellerowicz, E. J., et al. (2009). A real-time fluorogenic assay for the visualization of glycoside hydrolase activity in planta. *Plant Physiol.* doi:10.1104/pp.109.147439.

Jackson, M. B., and Armstrong, W. (1999). Formation of aerenchyma and the processes of plant ventilation in relation to soil flooding and submergence. *Plant Biol.* doi:10.1111/j.1438-8677.1999.tb00253.x.

Jackson, M. B., Fenning, T. M., Drew, M. C., and Saker, L. R. (1985). Stimulation of ethylene production and gas-space (aerenchyma) formation in adventitious roots of Zea mays L. by small partial pressures of oxygen. *Planta.* doi:10.1007/BF00398093.

Justin, S. H. F. W., and Armostrong, W. (1987). The anatomical characteristics of roots and plant response to soil flooding. *New Phytol.* 106, 465–495. doi:10.1111/j.1469-8137.1987.tb00153.x.

Justin, S. H. F. W., and Armstrong, W. (1991). Evidence for the involvement of ethene in aerenchyma formation in adventitious roots of rice (Oryza sativa L.). *New Phytol.* doi:10.1111/j.1469-8137.1991.tb00564.x.

Kahlon, T. S., Chow, F. I., Knuckles, B. E., and Chiu, M. M. (1993). Cholestrol-Lowering Effects in Hamsters of β-Glucan-Enriched Barley Fraction, Dehulled Whole Barley, Rice Bran, and Oat Bran and Their Combinations. *Cereal Chem.* 70, 435–440.

Kalyaanamoorthy, S., Minh, B. Q., Wong, T. K. F., Von Haeseler, A., and Jermiin, L. S. (2017). ModelFinder: Fast model selection for accurate phylogenetic estimates. *Nat. Methods.* doi:10.1038/nmeth.4285.

Karrer, P., Staub, M., Weinhagen, A., and Joos, B. (1924). Polysaccharide XXII. Zur Kenntnis der Lichenase und Reservecellulose (Lichenin). *Helv. Chim. Acta.* doi:10.1002/hlca.19240070116.

Katoh, K., Rozewicki, J., and Yamada, K. D. (2018). MAFFT online service: Multiple sequence alignment, interactive sequence choice and visualization. *Brief. Bioinform.* doi:10.1093/bib/bbx108.

Kebede, H., Subudhi, P. K., Rosenow, D. T., and Nguyen, H. T. (2001). Quantitative trait loci influencing drought tolerance in grain sorghum (Sorghum bicolor L. Moench). *Theor. Appl. Genet.* doi:10.1007/s001220100541.

Kido, N., Yokoyama, R., Yamamoto, T., Furukawa, J., Iwai, H., Satoh, S., et al. (2015). The matrix polysaccharide (1;3,1;4)-β-D -glucan is involved in silicon-dependent strengthening of rice cell wall. *Plant Cell Physiol.* 56, 268–276. doi:10.1093/pcp/pcu162.

Kim, H., Ahn, J. H., Görlach, J. M., Caprari, C., Scott-Craig, J. S., and Walton, J. D. (2001). Mutational analysis of β-glucanase genes from the plant-pathogenic fungus Cochliobolus carbonum. *Mol. Plant-Microbe Interact.* doi:10.1094/MPMI.2001.14.12.1436.

Kim, J. B., Olek, a T., and Carpita, N. C. (2000). Cell wall and membrane-associated exo-beta-D-glucanases from developing maize seedlings. *Plant Physiol.* 123, 471–86. doi:10.1104/pp.123.2.471.

Kim, S. J., Zemelis-Durfee, S., Jensen, J. K., Wilkerson, C. G., Keegstra, K., and Brandizzi, F. (2018). In the grass species Brachypodium distachyon, the production of mixed-linkage (1,3;1,4)-β-glucan (MLG) occurs in the Golgi apparatus. *Plant J.* 93, 1062–1075. doi:10.1111/tpj.13830.

Kim, S. J., Zemelis-Durfee, S., Wilkerson, C., and Brandizzi, F. (2017). In Brachypodium a complex signaling is actuated to protect cells from proteotoxic stress and facilitate seed filling. *Planta* 246, 75–89. doi:10.1007/s00425-017-2687-7.

Kim, S. J., Zemelis, S., Keegstra, K., and Brandizzi, F. (2015). The cytoplasmic localization of the catalytic site of CSLF6 supports a channeling model for the biosynthesis of mixed-linkage glucan. *Plant J.* 81, 537–547. doi:10.1111/tpj.12748.

Kleczkowski, L. A. (1996). Back to the drawing board: redefining starch synthesis in cereals. *Trends Plant Sci.* 1, 363–364.

Kuge, T., Nagoya, H., Tryfona, T., Kurokawa, T., Yoshimi, Y., Dohmae, N., et al. (2015). Action of an endo-β-1,3(4)-glucanase on cellobiosyl unit structure in barley β-1,3:1,4-Glucan. *Biosci. Biotechnol. Biochem.* 79, 1810–1817. doi:10.1080/09168451.2015.1046365.

Kuraku, S., Zmasek, C. M., Nishimura, O., and Katoh, K. (2013). aLeaves facilitates on-demand exploration of metazoan gene family trees on MAFFT sequence alignment server with enhanced interactivity. *Nucleic Acids Res.* doi:10.1093/nar/gkt389.

Kurusu, T., Kuchitsu, K., and Tada, Y. (2015). Plant signaling networks involving ca2+ and Rboh/Nox-mediated ROS production under salinity stress. *Front. Plant Sci.* doi:10.3389/fpls.2015.00427.

Lauer, J. C., Cu, S., Burton, R. A., and Eglinton, J. K. (2017a). Variation in barley (1 → 3, 1 → 4)-β-glucan endohydrolases reveals novel allozymes with increased thermostability. *Theor. Appl. Genet.* 130, 1053–1063. doi:10.1007/s00122-017-2870-z.

Lauer, J. C., Yap, K., Cu, S., Burton, R. A., and Eglinton, J. K. (2017b). Novel barley (1→3,1→4)-β-glucan endohydrolase alleles confer increased enzyme thermostability. *J. Agric. Food Chem.* 65, 421–428. doi:10.1021/acs.jafc.6b04287.

Lazaridou, A., and Biliaderis, C. G. (2007). Molecular aspects of cereal b-glucan functionality: Physical properties, technological applications and physiological effects. *J. Cereal Sci.* 46, 101–118. doi:10.1016/j.jcs.2007.05.003.

Lazaridou, A., Biliaderis, C. G., Micha-Screttas, M., and Steele, B. R. (2004). A comparative study on structure-function relations of mixed-linkage (1→3), (1→4) linear β-D-glucans. *Food Hydrocoll.* doi:10.1016/j.foodhyd.2004.01.002.

Lechat, H., Amat, M., Mazoyer, J., Buléon, A., and Lahaye, M. (2000). Structure and distribution of glucomannan and sulfated glucan in the cell walls of the red alga Kappaphycus alvarezii (Gigartinales, Rhodophyta). *J. Phycol.* 36, 891–902. doi:10.1046/j.1529-8817.2000.00056.x.

Lee, J., and Hollingsworth, R. I. (1997). Oligosaccharide β-glucans with unusual linkages from Sarcina ventriculi. *Carbohydr. Res.* doi:10.1016/S0008-6215(97)00204-8.

Leite, D. C. C., Grandis, A., Tavares, E. Q. P., Piovezani, A. R., Pattathil, S., Avci, U., et al. (2017). Cell wall changes during the formation of aerenchyma in sugarcane roots. *Ann. Bot.* 120, 693–708. doi:10.1093/aob/mcx050.

Letunic, I., and Bork, P. (2007). Interactive Tree Of Life (iTOL): An online tool for phylogenetic tree display and annotation. *Bioinformatics*. doi:10.1093/bioinformatics/btl529.

Licausi, F., Kosmacz, M., Weits, D. A., Giuntoli, B., Giorgi, F. M., Voesenek, L. A. C. J., et al. (2011). Oxygen sensing in plants is mediated by an N-end rule pathway for protein destabilization. *Nature*. doi:10.1038/nature10536.

Little, A., Lahnstein, J., Je, D. W., Khor, S. F., Schwerdt, J. G., Shirley, N. J., et al. (2019). A Novel (1,4)- β -Linked Glucoxylan Is Synthesized by Members of the Cellulose Synthase-Like F Gene Family in Land Plants. doi:10.1021/acscentsci.8b00568.

Little, A., Schwerdt, J. G., Shirley, N. J., Khor, S. F., Neumann, K., O'donovan, L. A., et al. (2018). Revised phylogeny of the cellulose synthase gene superfamily: Insights into cell wall evolution. *Plant Physiol.* 177, 1124–1141. doi:10.1104/pp.17.01718.

Liu, H., Hao, N., Jia, Y., Liu, X., Ni, X., Wang, M., et al. (2019). The ethylene receptor regulates Typha angustifolia leaf aerenchyma morphogenesis and cell fate. *Planta*. doi:10.1007/s00425-019-03177-4.

Livak, K. J., and Schmittgen, T. D. (2001). Analysis of Relative Gene Expression Data Using Real- Time Quantitative PCR and the 2 ⁂C T Method. *METHODS* 25, 402–408. doi:10.1006.

Lombard, V., Golaconda Ramulu, H., Drula, E., Coutinho, P. M., and Henrissat, B. (2014). The carbohydrate-active enzymes database (CAZy) in 2013. *Nucleic Acids Res.* doi:10.1093/nar/gkt1178.

Loqué, D., Scheller, H. V., and Pauly, M. (2015). Engineering of plant cell walls for enhanced biofuel production. *Curr. Opin. Plant Biol.* doi:10.1016/j.pbi.2015.05.018.

Luttenegger, D. G., and Nevins, D. J. (1985). Transient Nature of a (1 → 3), (1 → 4)-β-d-Glucan in Zea mays Coleoptile Cell Walls. *Plant Physiol.* 77, 175–178.

Mathlouthi, N., Mallet, S., Saulnier, L., Ouemener, B., and Larbier, M. (2002). Effects of xylanase and β-glucanase addition on performance, nutrient digestibility, and physico-chemical conditions in the small intestine contents and caecal microflora of broiler chickens fed a wheat and barley-based diet. *Anim. Res.* doi:10.1051/animres:2002034.

McGregor, N., Yin, V., Tung, C. C., Van Petegem, F., and Brumer, H. (2017). Crystallographic insight into the evolutionary origins of xyloglucan endotransglycosylases and endohydrolases. *Plant J.* 89, 651–670. doi:10.1111/tpj.13421.

McKinley, B., Rooney, W., Wilkerson, C., and Mullet, J. (2016). Dynamics of biomass partitioning, stem gene expression, cell wall biosynthesis, and sucrose accumulation during development of Sorghum bicolor. *Plant J.* doi:10.1111/tpj.13269.

McNamara, J. T., Morgan, J. L. W., and Zimmer, J. (2015). A Molecular Description of Cellulose Biosynthesis. *Annu. Rev. Biochem.* doi:10.1146/annurev-biochem-060614-033930.

Meier, H., and Reid, J. S. G. (1982). "Reserve Polysaccharides Other Than Starch in Higher Plants," in *Plant Carbohydrates I*, 418–471. doi:10.1007/978-3-642-68275-9_11.

Michel, G., Tonon, T., Scornet, D., Cock, J. M., and Kloareg, B. (2010). The cell wall polysaccharide metabolism of the brown alga *Ectocarpus siliculosus*. Insights into the evolution of extracellular matrix polysaccharides in Eukaryotes. *New Phytol.* 188, 82–97. doi:10.1111/j.1469-8137.2010.03374.x.

Morgan, A. H., and Gothard, P. G. (1977). A rapid, simple viscometric technique for indirect estimation of soluble β-glucan content of raw barley. *J. Inst. Brew.* 83, 37–38. doi:10.1002/j.2050-0416.1975.tb03790.x.

Mortlock, M. Y., and Vanderlip, R. L. (1989). Germination and establishment of pearl millet and sorghum of different seed qualities under controlled high-temperature environments. *F. Crop. Res.* doi:10.1016/0378-4290(89)90092-0.

Mrízová, K., Holasková, E., Öz, M. T., Jiskrová, E., Frébort, I., and Galuszka, P. (2014). Transgenic barley: A prospective tool for biotechnology and agriculture. *Biotechnol. Adv.* doi:10.1016/j.biotechadv.2013.09.011.

Müller, J. J., Thomsen, K. K., and Heinemann, U. (1998). Crystal structure of Barley 1,3-1,4-β-glucanase at 2.0-Å resolution and comparison with Bacillus 1,3-1,4-β-glucanase. *J. Biol. Chem.* 273, 3438–3446. doi:10.1074/jbc.273.6.3438.

Munck, L., Møller, B., Jacobsen, S., and Søndergaard, I. (2004). Near infrared spectra indicate specific mutant endosperm genes and reveal a new mechanism for substituting starch with (1→3,1→4)-β-glucan in barley. *J. Cereal Sci.* 40, 213–222. doi:10.1016/j.jcs.2004.07.006.

Nemeth, C., Freeman, J., Jones, H. D., Sparks, C., Pellny, T. K., Wilkinson, M. D., et al. (2010). Down-regulation of the CSLF6 gene results in decreased (1,3;1,4)-β-D-glucan in endosperm of wheat. *Plant Physiol.* doi:10.1104/pp.109.151712.

Nevo, Z., and Sharon, N. (1969). The cell wall of *Peridinium westii*, a non cellulosic glucan. *BBA - Biomembr.* 173, 161–175. doi:10.1016/0005-2736(69)90099-6.

Nguyen, L. T., Schmidt, H. A., Von Haeseler, A., and Minh, B. Q. (2015). IQ-TREE: A fast and effective stochastic algorithm for estimating maximum-likelihood phylogenies. *Mol. Biol. Evol.* 32, 268–274. doi:10.1093/molbev/msu300.

Ni, X. L., Gui, M. Y., Tan, L. L., Zhu, Q., Liu, W. Z., and Li, C. X. (2019). Programmed cell death and aerenchyma formation in water-logged sunflower stems and its promotion by Ethylene and ROS. *Front. Plant Sci.* doi:10.3389/fpls.2018.01928.

Olafsdottir, E. S., and Ingólfsdottir, K. (2001). Polysaccharides from lichens: Structural characteristics and biological activity. *Planta Med.* doi:10.1055/s-2001-12012.

Olson, S. N., Ritter, K., Medley, J., Wilson, T., Rooney, W. L., and Mullet, J. E. (2013). Energy sorghum hybrids: Functional dynamics of high nitrogen use efficiency. *Biomass and Bioenergy*. doi:10.1016/j.biombioe.2013.04.028.

Ouhida, I., Pérez, J. F., Piedrafita, J., and Gasa, J. (2000). The effects of sepiolite in broiler chicken diets of high, medium and low viscosity. Productive performance and nutritive value. *Anim. Feed Sci. Technol.* doi:10.1016/S0377-8401(00)00148-6.

Parlanti, S., Kudahettige, N. P., Lombardi, L., Mensuali-Sodi, A., Alpi, A., Perata, P., et al. (2011). Distinct mechanisms for aerenchyma formation in leaf sheaths of rice genotypes displaying a quiescence or escape strategy for flooding tolerance. *Ann. Bot.* doi:10.1093/aob/mcr086.

Pauly, M., and Hake, S. (2011). Maize variety and method of production. *US Pat. 20,110,302,669*. Available at: http://www.freepatentsonline.com/y2011/0302669.html.

Pérez-Mendoza, D., Bertinetti, D., Lorenz, R., Gallegos, M. T., Herberg, F. W., and Sanjuán, J. (2017). A novel c-di-GMP binding domain in glycosyltransferase BgsA is responsible for the synthesis of a mixed-linkage β-glucan. *Sci. Rep.* 7. doi:10.1038/s41598-017-09290-2.

Pérez-Mendoza, D., Rodríguez-Carvajal, M. Á., Romero-Jiménez, L., Farias, G. de A., Lloret, J., Gallegos, M. T., et al. (2015). Novel mixed-linkage β-glucan activated by c-di-GMP in Sinorhizobium meliloti. *Proc. Natl. Acad. Sci. U. S. A.* 112, E757-65. doi:10.1073/pnas.1421748112.

Pettolino, F., Sasaki, I., Turbic, A., Wilson, S. M., Bacic, A., Hrmova, M., et al. (2009). Hyphal cell walls from the plant pathogen *Rhynchosporium secalis* contain (1,3/1,6)-β-D-glucans, galacto- and rhamnomannans, (1,3;1,4)-β-D- glucans and chitin. *FEBS J.* doi:10.1111/j.1742-4658.2009.07086.x.

Planas, A. (2000). Bacterial 1,3-1,4-β-glucanases: structure, function and protein engineering. *Biochim. Biophys. Acta - Protein Struct. Mol. Enzymol.* 1543, 361–382. doi:10.1016/S0167-4838(00)00231-4.

Popper, Z. A., and Fry, S. C. (2003). Primary cell wall composition of bryophytes and charophytes. *Ann. Bot.* 91, 1–12. doi:10.1093/aob/mcg013.

Pringsheim, H., and Kusenack, W. (1924). Über Lichenin und die Lichenase. V. Mitteilung über Hemicellulosen. *Hoppe-Seyler´s Zeitschrift für Physiol. Chemie* 137, 265–271. doi:10.1515/bchm2.1924.137.3-6.265.

Promkhambut, A., Polthanee, A., Akkasaeng, C., and Younger, A. (2011). Growth, yield and aerenchyma formation of sweet and multipurpose sorghum (Sorghum bicolor L. Moench) as affected by flooding at different growth stages. *Aust. J. Crop Sci.*

Rajhi, I., Yamauchi, T., Takahashi, H., Nishiuchi, S., Shiono, K., Watanabe, R., et al. (2011). Identification of genes expressed in maize root cortical cells during lysigenous aerenchyma formation using laser microdissection and microarray analyses. *New Phytol.* doi:10.1111/j.1469-8137.2010.03535.x.

Ramesh, H. P., and Tharanathan, R. N. (2003). Carbohydrates—The Renewable Raw Materials of High Biotechnological Value. *Crit. Rev. Biotechnol.* 23, 149–173. doi:10.1080/713609312.

Reddy, B. V., Ramesh, S., Reddy, P. S., Ramaiah, B., Salimath, P., and Kachapur, R. (2005). Sweet Sorghum – A Potential Alternate Raw Material for Bio-ethanol and Bio- energy. *Ismn.*

Reddy, B. V. S., Ramesh, S., Ashok Kumar, A., Wani, S. P., Ortiz, R., Ceballos, H., et al. (2008). Bio-Fuel Crops Research for Energy Security and Rural Development in Developing Countries. *BioEnergy Res.* doi:10.1007/s12155-008-9022-x.

Römling, U., and Galperin, M. Y. (2015). Bacterial cellulose biosynthesis: Diversity of operons, subunits, products, and functions. *Trends Microbiol.* 23, 545–557. doi:10.1016/j.tim.2015.05.005.

Rooney, W. L. (2014). "Sorghum," in *Cellulosic Energy Cropping Systems* (John Wiley & Sons, Ltd), 109–129. doi:10.1002/9781118676332.ch7.

Roozeboom, K. L., Prasad, P. V. V. V., Ciampitti, I., and Prasad, V. (2016). Sorghum Growth and Development. 66506, 1–18. doi:10.2134/agronmonogr58.2014.0062.

Rose, J. K. C., Braam, J., Fry, S. C., and Nishitani, K. (2002). The XTH family of enzymes involved in xyloglucan endotransglucosylation and endohydrolysis: Current perspectives and a new unifying nomenclature. *Plant Cell Physiol.* doi:10.1093/pcp/pcf171.

Rosenow, D. T., Quisenberry, J. E., Wendt, C. W., and Clark, L. E. (1983). Drought tolerant sorghum and cotton germplasm. *Agric. Water Manag.* doi:10.1016/0378-3774(83)90084-7.

Roulin, S., Buchala, A. J., and Fincher, G. B. (2002). Induction of (1→3,1→4)-β-D-glucan hydrolases in leaves of dark-incubated barley seedlings. *Planta* 215, 51–59. doi:10.1007/s00425-001-0721-1.

Roulin, S., and Feller, U. (2001). Reversible accumulation of (1→3,1→4)-β-glucan endohydrolase in wheat leaves under sugar depletion. *J. Exp. Bot.* 52, 2323–2332.

Saab, I. N., and Sachs, M. M. (1996). A flooding-induced xyloglucan endo-transglycosylase homolog in maize is responsive to ethylene and associated with aerenchyma. *Plant Physiol.* doi:10.1104/pp.112.1.385.

Salmeán, A. A., Duffieux, D., Harholt, J., Qin, F., Michel, G., Czjzek, M., et al. (2017). Insoluble (1 → 3), (1 → 4)-β-D-glucan is a component of cell walls in brown algae (Phaeophyceae) and is masked by alginates in tissues. *Sci. Rep.* 7. doi:10.1038/s41598-017-03081-5.

Sayers, E. W., Cavanaugh, M., Clark, K., Ostell, J., Pruitt, K. D., and Karsch-Mizrachi, I. (2019). GenBank. *Nucleic Acids Res.* doi:10.1093/nar/gky989.

Scheller, H. V., and Ulvskov, P. (2010). Hemicelluloses. *Annu. Rev. Plant Biol.* doi:10.1146/annurev-arplant-042809-112315.

Schmid, R., Judd, W., Campbell, C., Kellogg, E., Stevens, P., Donoghue, M., et al. (2007). Plant Systematics: A Phylogenetic Approach. *Taxon* 56, 1316. doi:10.2307/25065934.

Schoch, C. L., Ciufo, S., Domrachev, M., Hotton, C. L., Kannan, S., Khovanskaya, R., et al. (2020). NCBI Taxonomy: A comprehensive update on curation, resources and tools. *Database*. doi:10.1093/database/baaa062.

Schussler, E. E., and Longstreth, D. J. (1996). Aerenchyma develops by cell lysis in roots and cell separation in leaf petioles in *Sagittaria lancifolia* (Alismataceae). *Am. J. Bot.* doi:10.2307/2446110.

Schwerdt, J. G., MacKenzie, K., Wright, F., Oehme, D., Wagner, J. M., Harvey, A. J., et al. (2015). Evolutionary Dynamics of the Cellulose Synthase Gene Superfamily in Grasses. *Plant Physiol.* 168, 968–983. doi:10.1104/pp.15.00140.

Shimamura, S., Yamamoto, R., Nakamura, T., Shimada, S., and Komatsu, S. (2010). Stem hypertrophic lenticels and secondary aerenchyma enable oxygen transport to roots of soybean in flooded soil. *Ann. Bot.* doi:10.1093/aob/mcq123.

Silva, G. B., Ionashiro, M., Carrara, T. B., Crivellari, A. C., Tiné, M. A. S., Prado, J., et al. (2011). Cell wall polysaccharides from fern leaves: Evidence for a mannan-rich Type III cell wall in *Adiantum raddianum*. *Phytochemistry* 72, 2352–2360. doi:10.1016/j.phytochem.2011.08.020.

Simmons, T. J., and Fry, S. C. (2017). Bonds broken and formed during the mixed-linkage glucan : Xyloglucan endotransglucosylase reaction catalysed by Equisetum hetero-trans-β-glucanase. *Biochem. J.* 474, 1055–1070. doi:10.1042/BCJ20160935.

Simmons, T. J., Mohler, K. E., Holland, C., Goubet, F., Franková, L., Houston, D. R., et al. (2015). Hetero-trans-β-glucanase, an enzyme unique to Equisetum plants, functionalizes cellulose. *Plant J.* doi:10.1111/tpj.12935.

Simpson, M. G. (2010). "Plant Systematics," in *Plant Systematics* doi:10.1016/B978-0-12-374380-0.50001-4.

Singh, V., van Oosterom, E. J., Jordan, D. R., Messina, C. D., Cooper, M., and Hammer, G. L. (2010). Morphological and architectural development of root systems in sorghum and maize. *Plant Soil*. doi:10.1007/s11104-010-0343-0.

Slakeski, N., Baulcombe, D. C., Devos, K. M., Ahluwalia, B., Doan, D. N. P., and Fincher, G. B. (1990). Structure and tissue-specific regulation of genes encoding barley (1→3, 1→4)-β-glucan endohydrolases. *MGG Mol. Gen. Genet.* 224, 437–449. doi:10.1007/BF00262439.

Sleper, D., and Poehlman, J. (2006). *Breeding Fild Crops*. Fifht Edit. Wiley-Blackwell.

Smith, C.W; Frederiksen, R. . (2000). *Sorghum: Origin, History, Technology, and Production*. John Wiley. New York, NY.

Smith, B. G., and Harris, P. J. (1999). The polysaccharide composition of Poales cell walls: Poaceae cell walls are not unique. *Biochem. Syst. Ecol.* 27, 33–53. doi:10.1016/S0305-1978(98)00068-4.

Sørensen, I., Pettolino, F. A., Wilson, S. M., Doblin, M. S., Johansen, B., Bacic, A., et al. (2008). Mixed-linkage (1 → 3),(1 → 4)-β-D-glucan is not unique to the Poales and is an abundant component of Equisetum arvense cell walls. *Plant J.* 54, 510–521. doi:10.1111/j.1365-313X.2008.03453.x.

Staudte, R. G., Woodward, J. R., Fincher, G. B., and Stone, B. A. (1983). Water-soluble (1→3), (1→4)-β-d-glucans from barley (Hordeum vulgare) endosperm. III. Distribution of cellotriosyl and cellotetraosyl residues. *Carbohydr. Polym.* 3, 299–312. doi:https://doi.org/10.1016/0144-8617(83)90027-9.

Steffens, B., and Sauter, M. (2009). Epidermal cell death in rice is confined to cells with a distinct molecular identity and is mediated by ethylene and H_2O_2 through an autoamplified signal pathway. *Plant Cell*. doi:10.1105/tpc.108.061887.

Stone, B. A. (2009). "Chapter 2.1 - Chemistry of β-Glucans," in, eds. A. Bacic, G. B. Fincher, and B. A. B. T.-C. Stone Biochemistry, and Biology of 1-3 Beta Glucans and Related Polysaccharides (San Diego: Academic Press), 5–46. doi:https://doi.org/10.1016/B978-0-12-373971-1.00002-9.

Stutts, L. R., and Vermerris, W. (2020). Elucidating Anthracnose Resistance Mechanisms in Sorghum—A Review. *Phytopathology®*. doi:10.1094/phyto-04-20-0132-rvw.

Taketa, S., Yuo, T., Tonooka, T., Tsumuraya, Y., Inagaki, Y., Haruyama, N., et al. (2012). Functional characterization of barley betaglucanless mutants demonstrates a unique role for CslF6 in (1,3;1,4)-β-D-glucan biosynthesis. *J. Exp. Bot.* doi:10.1093/jxb/err285.

Tamura, K., Hemsworth, G. R., Déjean, G., Rogers, T. E., Pudlo, N. A., Urs, K., et al. (2017). Molecular Mechanism by which Prominent Human Gut Bacteroidetes Utilize Mixed-Linkage Beta-Glucans, Major Health-Promoting Cereal Polysaccharides. *Cell Rep.* doi:10.1016/j.celrep.2017.09.049.

Tavares, E., Camara Mattos Martins, M., Grandis, A., Romim, G. H., Rusiska Piovezani, A., Weissmann Gaiarsa, J., et al. (2020). Newly identified miRNAs may contribute to aerenchyma formation in sugarcane roots. *Plant Direct*. doi:10.1002/pld3.204.

Tavares, E. Q. P., Grandis, A., Lembke, C. G., Souza, G. M., Purgatto, E., De Souza, A. P., et al. (2018). Roles of auxin and ethylene in aerenchyma formation in sugarcane roots. *Plant Signal. Behav.* doi:10.1080/15592324.2017.1422464.

Tosh, S. M., Brummer, Y., Wood, P. J., Wang, Q., and Weisz, J. (2004). Evaluation of structure in the formation of gels by structurally diverse (1 → 3)(1 → 4)-β-D-glucans from four cereal and one lichen species. *Carbohydr. Polym.* doi:10.1016/j.carbpol.2004.05.009.

Trafford, K., Haleux, P., Henderson, M., Parker, M., Shirley, N. J., Tucker, M. R., et al. (2013). Grain development in Brachypodium and other grasses: Possible interactions between cell expansion, starch deposition, and cell-wall synthesis. *J. Exp. Bot.* 64, 5033–5047. doi:10.1093/jxb/ert292.

Trethewey, J. A. K., Campbell, L. M., and Harris, P. J. (2005). (1→3),(1→4)-ß-d-Glucans in the cell walls of the Poales (sensu lato): an immunogold labeling study using a monoclonal antibody. *Am. J. Bot.* 92, 1660–1674. doi:10.3732/ajb.92.10.1660.

Vanderlip, R. L., and Reeves, H. E. (1972). Growth Stages of Sorghum [Sorghum bicolor, (L.) Moench.]. *Agron. J.* doi:10.2134/agronj1972.00021962006400010005x.

Vega-Sánchez, M. E., Loqué, D., Lao, J., Catena, M., Verhertbruggen, Y., Herter, T., et al. (2015). Engineering temporal accumulation of a low recalcitrance polysaccharide leads to increased C6 sugar content in plant cell walls. *Plant Biotechnol. J.* doi:10.1111/pbi.12326.

Vega-Sánchez, M. E., Verhertbruggen, Y., Christensen, U., Chen, X., Sharma, V., Varanasi, P., et al. (2012). Loss of Cellulose Synthase - Like F6 Function Affects Mixed-Linkage Glucan Deposition, Cell Wall Mechanical Properties, and Defense Responses in Vegetative Tissues of Rice. *Plant Physiol.* 159, 56–69. doi:10.1104/pp.112.195495.

Vega-Sánchez, M. E., Verhertbruggen, Y., Scheller, H. V., and Ronald, P. C. (2013). Abundance of mixed linkage glucan in mature tissues and secondary cell walls of grasses. *Plant Signal. Behav.* 8. doi:10.4161/psb.23143.

Venkateswaran, K., Elangovan, M., and Sivaraj, N. (2019). "Origin, Domestication and Diffusion of Sorghum bicolor," in *Breeding Sorghum for Diverse End Uses* doi:10.1016/b978-0-08-101879-8.00002-4.

Vettore, A. L., da Silva, F. R., Kemper, E. L., Souza, G. M., da Silva, A. M., Ferro, M. I. T., et al. (2003). Analysis and functional annotation of an expressed sequence tag collection for tropical crop sugarcane. *Genome Res.* doi:10.1101/gr.1532103.

Viborg, A. H., Terrapon, N., Lombard, V., Michel, G., Czjzek, M., Henrissat, B., et al. (2019). A subfamily roadmap of the evolutionarily diverse glycoside hydrolase family 16 (GH16). *J. Biol. Chem.* doi:10.1074/jbc.RA119.010619.

Vicente, J., Mendiondo, G. M., Movahedi, M., Peirats-Llobet, M., Juan, Y. ting, Shen, Y. yen, et al. (2017). The Cys-Arg/N-End Rule Pathway Is a General Sensor of Abiotic Stress in Flowering Plants. *Curr. Biol.* doi:10.1016/j.cub.2017.09.006.

Vogel, J. (2008). Unique aspects of the grass cell wall. *Curr. Opin. Plant Biol.* doi:10.1016/j.pbi.2008.03.002.

Von Wettstein, D., Mikhaylenko, G., Froseth, J. A., and Kannangara, C. G. (2000). Improved barley broiler feed with transgenic malt containing heat-stable (1,3-1,4)-β-glucanase. *Proc. Natl. Acad. Sci. U. S. A.* doi:10.1073/pnas.97.25.13512.

Von Wettstein, D., Warner, J., and Kannangara, G. G. (2003). Supplements of transgenic malt or grain containing (1,3-1,4)-β- glucanase increase the nutritive value of barley-based broiler diets to that of maize. *Br. Poult. Sci.* doi:10.1080/0007166031000085526.

Wälti, M., Roulin, S., and Feller, U. (2002). Effects of pH, light and temperature on (1→3,1→4)-β- glucanase stability in wheat leaves. *Plant Physiol. Biochem.* 40, 363–371. doi:10.1016/S0981-9428(02)01373-6.

Wang, W., Chen, D., Zhang, X., Liu, D., Cheng, Y., and Shen, F. (2018). Role of plant respiratory burst oxidase homologs in stress responses. *Free Radic. Res.* 52, 826–839. doi:10.1080/10715762.2018.1473572.

Wany, A., Kumari, A., and Gupta, K. J. (2017). Nitric oxide is essential for the development of aerenchyma in wheat roots under hypoxic stress. *Plant Cell Environ.* doi:10.1111/pce.13061.

Wilson, S. M., Ho, Y. Y., Lampugnani, E. R., Van de Meene, A. M. L., Bain, M. P., Bacic, A., et al. (2015). Determining the Subcellular Location of Synthesis and Assembly of the Cell Wall Polysaccharide (1,3; 1,4)-β-d-Glucan in Grasses. *Plant Cell* 27, 754–771. doi:10.1105/tpc.114.135970.

Winchell, F., Brass, M., Manzo, A., Beldados, A., Perna, V., Murphy, C., et al. (2018). On the Origins and Dissemination of Domesticated Sorghum and Pearl Millet across Africa and into India: a View from the Butana Group of the Far Eastern Sahel. *African Archaeol. Rev.* doi:10.1007/s10437-018-9314-2.

Woodwar, J. R., and Fincher, G. B. (1982). Purification and Chemical Properties of Two 1,3;1,4-β-Glucan Endohydrolases from Germinating Barley. *Eur. J. Biochem.* doi:10.1111/j.1432-1033.1982.tb05837.x.

Xue, X., and Fry, S. C. (2012). Evolution of mixed-linkage (13, 14)-b-D-glucan (MLG) and xyloglucan in Equisetum (horsetails) and other monilophytes. *Ann. Bot.* doi:10.1093/aob/mcs018.

Yamauchi, T., Rajhi, I., and Nakazono, M. (2011). Lysigenous aerenchyma formation in maize root is confined to cortical cells by regulation of genes related to generation and scavenging of reactive oxygen species. *Plant Signal. Behav.* doi:10.4161/psb.6.5.15417.

Yamauchi, T., Shimamura, S., Nakazono, M., and Mochizuki, T. (2013). Aerenchyma formation in crop species: A review. *F. Crop. Res.* doi:10.1016/j.fcr.2012.12.008.

Yamauchi, T., Tanaka, A., Inahashi, H., Nishizawa, N. K., Tsutsumi, N., Inukai, Y., et al. (2019). Fine control of aerenchyma and lateral root development through AUX/IAA- And ARF-dependent auxin signaling. *Proc. Natl. Acad. Sci. U. S. A.* doi:10.1073/pnas.1907181116.

Yamauchi, T., Tanaka, A., Mori, H., Takamure, I., Kato, K., and Nakazono, M. (2016). Ethylene-dependent aerenchyma formation in adventitious roots is regulated differently in rice and maize. *Plant Cell Environ.* doi:10.1111/pce.12766.

Yamauchi, T., Watanabe, K., Fukazawa, A., Mori, H., Abe, F., Kawaguchi, K., et al. (2014). Ethylene and reactive oxygen species are involved in root aerenchyma formation and adaptation of wheat seedlings to oxygen-deficient conditions. *J. Exp. Bot.* doi:10.1093/jxb/ert371.

Yamauchi, T., Yoshioka, M., Fukazawa, A., Mori, H., Nishizawa, N. K., Tsutsumi, N., et al. (2017). An NADPH oxidase RBOH functions in rice roots during lysigenous aerenchyma formation under oxygen-deficient conditions. *Plant Cell.* doi:10.1105/tpc.16.00976.

Yang, S. Q., Xiong, H., Yang, H. Y., Yan, Q. J., and Jiang, Z. Q. (2015). High-level production of β-1,3-1,4-glucanase by *Rhizomucor miehei* under solid-state fermentation and its potential application in the brewing industry. *J. Appl. Microbiol.* doi:10.1111/jam.12694.

Yokoyama, W. H., Hudson, C. A., Knuckles, B. E., Chiu, M. C. M., Sayre, R. N., Turnlund, J. R., et al. (1997). Effect of barley β-glucan in durum wheat pasta on human glycemic response. *Cereal Chem.* 74, 293–296. doi:10.1094/CCHEM.1997.74.3.293.

Zar, J. (1999). Biostatistical analysis. 4nd. *Prentice Hall USA*, 929.

Zegada-Lizarazu, W., and Monti, A. (2012). Are we ready to cultivate sweet sorghum as a bioenergy feedstock? A review on field management practices. *Biomass and Bioenergy*. doi:10.1016/j.biombioe.2012.01.048.

3. CRISPR-EDITING RICE *ENDO-(1,3;1,4)-B-D-GLUCANASES* TO STUDY ITS INVOLVEMENT IN AERENCHYMA DEVELOPMENT

ABSTRACT

The lysigenous aerenchyma of roots has been studied mainly in rice and maize. As this process develops into gas spaces, two phases are noticeable: programmed cell death and plant cell wall degradation. Unlike the inducible maize roots, rice, sorghum, and sugarcane have constitutive lysigenous aerenchyma. Recently, research into aerenchyma development of sugarcane has stated that the mixed-linkage (1,3;1,4)-β-D-glucan (MLG) is one of the polysaccharides that is degraded during cell wall modification. Composed solely of glucose units, MLG is a hemicellulosic polymer hydrolyzed by endo-(1,3;1,4)-β-D-glucanases of glycosyl family hydrolase 17 (GH17). According to the phylogenetic inferences described in the previous chapter, the GH17 are Poaceae-specific hydrolases, encompassing two rice (*OsEgl1* and *OsEgl2*) and three sorghum (*Sblic1, Sblic2,* and *Sblic2*) *endo-(1,3;1,4)-β-D-glucanases*. Moreover, we also reported a decrease in the relative amount of MLG throughout the aerenchyma development and confirmed that the polymer is degraded in sorghum's primary roots, eventually associated with the rise of enzymatic activity and *Sblic1* expression. Furthermore, we emphasized the importance of having a sequenced genome and the low complexity of dealing with sorghum's primary root. Another advantage is the recent advances in sorghum genetic transformation. All those attributes led us to consider sorghum as a promising model for understanding MLG hydrolysis and its eventual role in aerenchyma formation. However, a more in-depth analysis using sorghum for genetic transformation led us to conclude that sorghum was not adequate for genetic transformation, especially using the modern editing technique CRISPR/Cas9. Conversely, rice, for which tissue culture was established three decades ago, was a much more robust model for genetic engineering. The stability for genetic manipulation and the following criteria were used in our decision to attempt knocking out both rice *endo-(1,3;1,4)-β-D-glucanases* using CRISPR/Cas9. We also considered non-technical issues such as the time of research funding (12 months), requirements for obtaining a double degree by the American University, and above all, the availability of specific rice vectors and the mastery of its tissue culture at Rutgers, The State University of New Jersey. Initially, public microarray data indicated a high expression in roots for *OsEgl1* and *OsEgl2*. Thus, both became target sequences for two gRNAs that we cloned into the psgR-Cas9-Os, a vector driven by an *OsU6* promoter. Subsequently, the cassettes were subcloned into the plant expression vector pCAMBIA1300, which we used to transform calli by gene gun bombardment. When submitted to a selection media culture, the resistant calli developed into seedlings we transplanted to the soil. After gDNA extraction, the genotyping indicated the presence of the Cas9 complex in all samples, although other analyses (RFLP, T7E1 assays, sequencing) suggested off-target mutations. Intriguingly, the plants did not survive. So, we repeated the entire transformation procedure and obtained new plants by the end of our research. Some plants survived and are available for future analysis. After 11 months of waiting to import the transgenic material, we acquired a mutant with a T-DNA insertion within the *OsEgl2* coding region. Unfortunately, the material was not at the end of our funding. In conclusion, the data indicated no on-target mutations, although the Cas9 complex has been detected. Above all, we emphasize that the T-DNA line is a valuable material for understanding the eventual consequences for loss-of-function

mutations in *OsEgl2*, thereby decreasing MLG hydrolysis and compromising the aerenchyma development.

Keywords: CRISPR; mixed-linkage glucan; endo-(1,3;1,4)-β-D-glucanases; aerenchyma; roots

3.1. INTRODUCTION

3.1.1. Rice

The genus Oryza emerged over 130 million years ago and spread across the Gondwana continent as a wild grass. Oryza domestication occurred about 9,000 years ago in Asia, where it was grown on flood-free soils. Later on, flooding and transplanting seedlings generated better cultivars in China, making this species domesticated (Khush, 1997). Oryza genus cultivates mainly two species: *Oryza glaberrima* and *Oryza sativa*. The latter stands out worldwide for agriculture, and its production comprises *indica* and *japonica* subspecies (Kato et al., 1928). Generally, *indica* rice is found in flooded regions in tropical Asia, while *japonica* in highland regions in South Asia (Garris et al., 2003).

Rice varieties have high adaptation and tolerance to biotic and abiotic stresses due to their great genetic diversity combined with good agricultural practices, resulting in high yields (Zong et al., 2007; Zhang et al., 2009). Furthermore, the advancement in genomics allowed a better understanding of rice molecular traits, improved by the plant breeders. (Chauhan et al., 2017). However, not only new technologies enabled scientists to advance knowledge regarding rice biology. Other more straightforward techniques, such as rice tissue culture, have been evolving over the last forty years and, undoubtedly, played a vital role in developing gene-editing tools such as TALENS and CRISPR/Cas9. (Chauhan et al., 2017).

3.1.2. Beginning of CRISPR

The studies of clustered regularly interspaced short palindromic repeats (CRISPR) began in the late 1980s in the salt flats of Santa Pola city in Spain. Dr. Francis Mojica, University of Alicante, aimed to understand salinity's effect on the DNA-cutting mechanism by restriction enzymes in the *Haloferax mediterranei* genome, an extremely salt-tolerant halobacterium (Figure 12). The Spaniard found multiple 30 bp palindromic copies 36 bp spaced in its genome (Ishino et al., 1987; Mojica et al., 1993) and suggested that such repetitions should have some importance in prokaryotes (Mojica et al., 1995, 2000). As DNA database sequences advanced, he analyzed 4,500 spacers, later called protospacers, and found that many sequences could be related to microbial

adaptive immune systems against specific infections (Mojica et al., 2005). In the same year, other scientists in Europe proposed the CRISPR relationship against foreign DNA (Bolotin et al., 2005; Pourcel et al., 2005). The following year, researchers suggested CRISPR as a bacteria and archaea adaptive defense system that uses antisense RNA as "signatures" or "memories" from previous invasions (Makarova et al., 2006). However, this hypothesis was only proven with phage infection on plasmid conjugation assays (Barrangou et al., 2007; Marraffini and Sontheimer, 2008).

Figure 12. Dr. Mojica at Santa Pola's salt flat, Spain. The microbiologist has been invested as Dr. honoris causa from the Complutense University of Madrid due to his contribution to CRISPR technology (Fernández, 2021). One can see a buildup of salt on the lake's edge, located in the Province of Alicante, Valencian Community. Photo by Raúl Belinchón and taken from (Ansede, 2017).

In 2017, the microbiologist Dr. Mojica, who was recently awarded an honoris causa degree (Fernández, 2021), briefly described CRISPR's history in a video published by the *El País* newspaper (Ansede, 2017). I transcribed it and then translated it *ipsis verbis*:

"*In this extreme environment like Santa Pola's salt flats live very few microorganisms capable of tolerating such high salinity. Among them are the Haloferax mediterranei that are prokaryotes in which, by analyzing their genome, we found some repetitions that caught our attention, and later we named them CRISPR. After approximately ten years trying to discover what those replications of bacteria and archaea were for, we found that they were, no more and no less, part of an adaptive immunity system, which microorganisms have and use as a defense for themselves against invaders, mainly viruses. One needs to keep in mind that viruses kill 50% of all bacteria and archaea on this planet every two days. This immune system, which archaea and bacteria have got, turned out to have become nothing but the most powerful tool available to modify the genetic material of any living being, with many applications in agriculture, livestock, and biotechnology. What was discovered in the early 90 in*

the Santa Pola salt flats has led to many possibilities of curing diseases, like cancer. Actually, right now, many have been performed as the first human clinical trials using CRISPR-modified cells to fight cancer. Surely someone in the CRISPR research area will receive a Nobel and probably several others for developing a technology that certainly will change humanity's future. "

3.1.3. CRISPR/Cas9 technology

CRISPR/Cas9 technology is based on the acquired immunity system of bacteria and archaea against viruses and plasmids. This system is a gene-targeting mechanism based on the cluster regularly interspaced short palindromic repeats (CRISPR)-associated nuclease. One of the associate nucleases is Cas9 endonuclease, a type II CRISPR-Cas system from the adaptive immune system in *Streptococcus pyogenes* (Deveau et al., 2010). This system is a complex composed of two short RNA named CRISPR RNA (crRNA) and the transactivating crRNA (transcrCRISPR), whose nuclease guides the cleavage of non-DNA on both strands at a specific site (Gasiunas et al., 2012). The simplicity of the CRISPR nuclease of type II, comprising three components (Cas9, the crRNA, and trRNA), turns it into a tractable system for genome editing. This promising tool was realized in 2012 by the Doudna and Charpentier labs (Jinek et al., 2012). The researchers, who recently were awarded the Nobel Prize in Chemistry (Eva, 2020), created a two-component system based on the CRISPR type II system by combining crRNA and trRNA into a single synthetic guide RNA (sgRNA or gRNA). The gRNA guides endonuclease Cas9 that generates double-strand breaks (DSBs) in the target genome, which are then repaired by homologous recombination (HR) and non-homologous end-joining (NHEJ) (Feng et al., 2013, 2014).

3.1.4. CRISPR/Cas9 and knockout

Several modifications have been made to improve expression and target knockout efficiency in CRISPR-editing tools: Cas9 and promoters' optimization; gRNA sequence extensions and mutations. For instance, those are some techniques among several others that have been employed recently (Dang et al., 2015).

One of the biggest obstacles to knock out plants is somatic tissue mutations, like chimerism (Liu et al., 2017). Wang and coworkers (2015) overcame this setback by employing mutations from germline cells. They circumvented this problem using specific egg-cell promoters, generating a higher frequency of biallelic homozygous mutations in T1.

Problems respecting knockouts are not exceptions from chimerism. The blunt cutting end activity by Cas9 generates one basepair (bp) indel that may not be easily detected and can cause gene loss function neither. One way to overcome this obstacle is by creating two gRNA adjacent to each other, which induce larger deletions that are more convenient to detect (Gasperini et al., 2016). Alternatively, blocking and suppressing NHEJ genes (e.g., Ku70, Ku80) to promote microhomology-based repair have been used. Such approaches have been employed in Arabidopsis through ZFNs and TALENs (Qi et al., 2013). A similar procedure has targeted genes using Cas9/gRNA to inhibit DNA ligase VI, a DNA ligase inhibitor (Ma et al., 2016). In addition to NHEJ inhibition, raising the amount of donor DNA has been shown to increase the HDR event (Čermák et al., 2015). This statement was confirmed on a modified geminiviral virus replicon fused to a donor molecule merged to CRISPR/Cas9 complex. This vector was then cloned into T-DNA for Agrobacterium-mediated transformation. Once delivered into the nucleus, the viral genome amplified into thousands of copies. The high copy number of donor DNA templates increased gene targeting frequency, which was tenfold higher than the classical DNA delivery approaches (Čermák et al., 2015).

The multiplex tool, aiming to target multiple genes at once, has shown to be successful in knockout events, although time-consuming. Furthermore, this technology proved efficient in editing Arabidopsis and maize using two gRNA driven by a U6 promoter (Xing et al., 2014). A similar methodology used six gRNAs driven by different promoters (Zhang et al., 2016). The researchers cloned the sextuple into a single Cas9 and obtained homozygosity after three generations. Although time-consuming, this methodology enabled editing several genes simultaneously.

3.1.5. Gene knock-in and replacement

A significant challenge in eukaryotes is gene replacement or knock-ins by introducing new alleles in the genome. To accomplish gene knock-ins using CRISPR/Cas9, it is necessary that after DBS, the repair occurs through HDR and uses a template as a sequence donor.

This homology-directed repair system was verified by an experiment with the herbicide-resistant rice gene, targeted by two gRNA and a free donor sequence. Both of them were co-bombarded into rice calli. The free DNA source contained mutated target site sequences flanked by identical wild gene sequences for herbicide resistance. According to the authors, the co-bombardment of both sources of DNA templates raised the HDR efficiency (Sun et al., 2016). Although there are cases where substitutions have been made, knock-ins are still tricky and

challenging. However, a CRISPR/Cas9 attached to the HR can overcome this obstacle. Some groups used gene suppression methods associated with NHEJ DNA repair (Liu et al., 2017).

An agile platform for delivering regulatory components is by deactivating the nuclease Cas9 function (dCas9) without affecting its gRNA binding ability. The dCas9 is then fused with general transcriptional activators or repressors at the C-terminal region, and dCas9/gRNA targets a promoter sequence of a gene (Liu et al., 2017). An experiment *in planta* (Piatek et al., 2015) fused dCas9 with potent activators (*dCas9:EDLL* and *dCas9:TAL*) and repressor *dCas9:SDRX*. They aimed to test regulatory patterns from promoter regions of a reporter gene (*Bs3::uidA),* using three gRNA targeting different regions of this promoter. The pattern was measured by qRT-PCR, and they tested the functionality of those gRNAs by targeting an endogenous *Nicotiana benthamiana phytoene desaturase* (*NbPDS*) gene, co-delivering them in different combination. The approach indicated the CRISPR/dCas9 DNA-targeting tools as valuable methodologies for functional genomics and biotechnology *in planta.* Moreover, Woo and coworkers (2015) transfected plant protoplast with Cas9 and protein-rRNA ribonucleoproteins (RNPs), resulting in a higher frequency of edited plants than other techniques.

Although some CRISPR-editing methodologies generate edited crops without introducing foreign DNA into a cell, strict regulations for GMOs and transgene-free gene-edited crops are still obstacles scientists (Woo et al., 2015). One method for screening transgene-free mutants was used in asexual plants whose Mendelian segregation pattern does not exist or takes many years to occur (Chen et al., 2018). The scientists used the gRNA/Cas9 transient expression via Agrobacterium to target the PDS gene, whose mutation generated albino tobacco. They selected albino calli or shoots without selection pressure for high-throughput screening and searched for foreign DNA. Then, they genotyped the edited line to find traces of Agrobacterium T-DNA. Subsequently, mutant plants without T-DNA were selected and subjected to a high-resolution melting and Illumina sequencing. Ultimately, they identified and sequenced simple mutations.

Other scientists used a similar screening methodology and targeted the *ALS* gene of tomato and potato by Agrobacterium transformation (Veillet et al., 2019). However, the researchers used CRISPR/Cas9 cytidine base editors (CEBs), an activation-induced cytidine deaminase (Nishida et al., 2016), to induce C into T and target then *ALS*. The mutation led to transgene-free chlorsulfuron-resistant plants.

Although researchers have developed transgene-free editing tools, the European Court of Justice decided that products derived from plants subjected to genome editing processes are under strict regulation applied for GMOs. This decision triggered frustration in the European

scientific community (Schulman et al., 2020). Nonetheless, the European Group on Ethics in Science and New Technologies recognizes that introducing new genome-edited plants into the agricultural environment may help provide products for an increasing population and face the impact of climate change (European Commission, 2021).

3.1.6. Rice *endo-(1,3;1,4)-β-D-glucanases* and mixed-linkage-glucan

Hemicellulose has been used to distinguish cell wall types, and one of the polysaccharides that stands out in grasses is the mixed-linkage (1,3;1,4)-β-D-glucan (MLG). MLG is degraded by endo-(1,3;1,4)-β-D-glucanases, which hydrolyzes specifically β(1,4) bonds followed by β(1,3) bonds, producing tri and tetrasaccharide blocks (Buckeridge et al., 2004).

From the previous chapter, literature and phylogenies have indicated two rice *endo-(1,3;1,4)-β-D-glucanases* (*OsEgl1* and *OsEgl2*). Studies with GH17 *endo-(1,3;1,4)-β-D-glucanases* were performed mainly in oats, barley, wheat, and rice. Scientists researched MLG's role as a transient structural polysaccharide. They observed increased MLG in young tissues of elongating maize coleoptiles' primary cells (Luttenegger and Nevins, 1985). When elongation reached its maximum, the MLG was rapidly hydrolyzed. Thus, Luttenegger and Nevins suggested MLG as a transient polymer.

Researchers from Swiss Institutions have elegantly demonstrated MLG as an energy source in leaves of wheat and barley. They exposed the leaves to light and then, intentionally, placed them in the dark. They also investigated the *endo-(1,3;1,4)-β-D-glucanases* protein level regarding the presence and absence of sugar level in leaves. The studies found that the increase of MLGase protein was related to low leaf sugar levels. Therefore, they suggested MLG as a source of energy during a sugar shortage (Roulin and Feller 2001; Wälti, Roulin, and Feller 2002).

Pioneering works on rice *endo-(1,3;1,4)-β-D-glucanases* used forward genetics. Akiyama and coworkers (1996) isolated and partially characterized a rice MLGase. Many years later, Akiyama and coworkers (2009) purified, isolated, and characterized both rice *endo-(1,3;1,4)-β-D-glucanase*s. Their northern blots revealed *OsEgl1* expressing in all tissues, whereas RNA blots indicated no expression for *OsEgl2* on analyzed samples, exempting the panicles. Despite their contrasting expression pattern, both MLGases showed endo-(1,3;1,4)-β-D-glucanases activity.

Kido and coworkers (2015) overexpressed *OsEgl1* and noticed an MLG decrease and alteration of silica distribution associated with reduced cell wall resistance. They suggested that MLG would play a physical reinforcement function.

3.1.7. MLG and aerenchyma development

Slakeski and coworkers (1990) were probably the first group of researchers who suggested a possible association between MLG and aerenchyma development. Considering the high level of MLG and *endo-(1,3;1,4)-β-D-glucanase* mRNA in young leaves of barley, they suggested that if the elevated *endo-(1,3;1,4)-β-glucanase* level was proportional to the enzymatic activity, cell wall degradation could then occur in leaves. They mentioned that high levels of an MLGase could be related to the formation of intercellular airspaces necessary for the gas and water vapor diffusion in young leaves. According to the authors, the gas spaces, in the beginning, do not access the atmosphere directly. Also, considering these intercellular airspaces develop by selective dissolution of the cell (lysogeny) or often by separation of cells (schizogeny), they indicated the possible association of *endo-(1,3;1,4)-β-D-glucanases* to aerenchyma development of paddy rice.

Compelling evidence associating MLG's hydrolysis to aerenchyma has recently been reported (Leite et al., 2017; Grandis et al., 2019). Leite and coworkers (2017) reported that MLG is one of the most degraded polysaccharides from sugarcane's cell wall while aerenchyma develops. Later on, Grandis and coworkers (2019) showed an increase in an *endo-(1,3;1,4)-β-D-glucanase* and the subsequent rise of its protein level as aerenchyma develops. Therefore, the authors suggested that MLG's retrieval is associated with aerenchyma development.

Since rice genetic engineering has stood out for its stability over the last decade, the association mentioned above could be in-depth explored by editing the rice *endo-(1,3;1,4)-β-D-glucanases* using CRISPR/Cas9.

3.2. GOAL

Knockout (KO) both rice *endo-(1,3;1,4)-β-D-glucanases* using CRISPR/Cas9 and investigate the eventual decrease in MLG hydrolysis into aerenchyma development.

Objectives

- KO of *OsEgl1* by CRISPR/Cas9
- KO of *OsEgl2* by CRISPR/Cas9
- Phenotypic analysis of aerenchyma in edited lines

3.3. MATERIAL AND METHODS

3.3.1. Plant material

Nipponbare seeds of *O. sativa* were ground with sandpaper to remove the husk, sterilized with 5% (v/v) sodium hypochlorite, and shaken at 100-120 rpm for 40 min. They were rinsed with sterile water five times and plated on callus induction medium 2N6 (Table 6 in Appendix A), then sealed plates were grown at 22 ºC in the dark for 3-4 weeks. The embryogenic calli were collected, transferred to new 2N6 media, and maintained at 22 ºC in the dark. The 2N6 medium was changed to fresh ones every three-four weeks.

3.3.2. Design of *OsEgl1* and *OsEgl2* sgRNA targets

The rice genomic and mRNA sequence of *OsEgl1* and *OsEgl2* were obtained from the Phytozome database (https://phytozome.jgi.doe.gov/pz/portal.html) using LOC_Os05g31140.1 and LOC_Os01g71474.1 accession numbers, respectively.

For target recognition, 20-nt guide oligonucleotides were synthesized (Table 5 in Appendix A) for ligation with sgRNA modules. The gRNAs targeting *OsEgl1* and *OsEgl2* were designed according to standard guidelines. Both being 20 bp and upstream of a proto-spacer adjacent motif (PAM). Moreover, for *OsEgl1,* we chose a *SacII* recognition site and, for *OsEgl2,* an *XmaI* one. Those sites were carefully chosen for restriction fragment length polymorphism (RFLP) analysis.

The sense and antisense primers of *OsEgl1* gRNA and *OsEglII* gRNA (Table 5 in Appendix A) were phosphorylated and annealed under the following condition: 37 °C for 30 min, 95 °C for 5 min, and then ramping down to 25 °C at the rate of 5 °C/min, in a 10 µL reaction (1 µL of 10x T4 ligation buffer, 0.5 µL of T4 PNK, 1 µL of each oligo at 100 µM). The annealed sgRNA oligos were cloned into the *BsI* site of psgR-Cas9-Os vector and driven by the *OsU6* promoter (Mao et al., 2013). The resulting plasmids were confirmed by sequencing, subcloned into the plant expression vector pCAMBIA1300 (https://www.addgene.org/vector-database/5930/), and used to transformed *Escherichia coli* DH5α strain cells. The plasmids were then extracted according to the manufactures' protocol (PureLink™ HiPure Plasmid Miniprep Kit).

Lastly, pCAMBIA1300 containing *OsEgl1* cassette plus Cas9 was named pRD365 and pCAMBIA1300 containing *OsEgl2* cassette plus Cas9 pRD366.

3.3.3. Cloning fragments of *OsEgl1* and *OsEgl2*

The extraction of gDNA in all steps was done according to the Sigma plant genomic DNA isolation kit. We cloned partial fragments of *OsEgl1* and *OsEgl2* as future positive controls. The partial sequences of *OsEgl1* (478 bp) and *OsEgl2* (465 bp) were amplified using GenScript *Taq* DNA polymerase (Table 5 in Appendix A). The resulting products were cloned into pGEM-T-Easy and used to transform *E. coli* DH5α cells. The transformants were plated on solid LB/ampicillin, overnight grown at 37 °C. The resulting single white colonies were put in liquid LB/ampicillin and overnight grown at 37 °C and shaken appropriately. Plasmid DNAs were purified by PureLink plasmid mini-prep kit (Invitrogen).

3.3.4. Biolistic and rice tissue culture

Half a gram of calli was placed on a 5.5 cm filter disk containing 2N6 medium plates (Table 6 in Appendix B). So, 2 mg of gold particles (0.75 μm) were sterilized in 70 % ethanol (v/v) for 10 min and washed with water two times. The particles were resuspended in 15 μL of [10 mM Tris (pH 8.0), 150 mM NaCl]. One microgram of each plasmid (pRD365 and pRD366) was separately added into the resuspended particles and vortexed for 10 seconds. The following mix was added: 20 μL of 0.1 M spermidine, 20 μL 25% PEG (1300 MW), 20 μL 2.5 M $CaCl_2$. The tubes were vortexed for 10 sec, incubated at room temperature for 10 min, centrifuged for 30 sec at 16,000 g. The supernatant was then aspirated off, and the remaining pellets resuspended in 70 % ethanol. Finally, 6 μL of resuspended pellets were aliquoted into four carrier disks for bombardment.

The gene gun bombardment was done at 1100 psi, and the calli were placed 10 cm from the particle holder. The bombarded calli were incubated on the 2N6 medium for three weeks in the dark. They were transferred to hygromycin-containing N6SE medium (Table 6 in Appendix A) and incubated in the dark for more than three weeks. The yellowish-resistant calli were then transferred to a hygromycin-containing MSRE regeneration medium (Table 6 in Appendix A) and incubated in light for three weeks. The resistant calli were transferred to a new MSRE medium, which was replaced after three weeks. The resistant calli were separated from non-resistant brown calli. Those whose roots were visible were transferred to plant pots containing hygromycin MSRT medium (Table 6 in Appendix A). The pots stayed under light for approximately three weeks. Finally, the small plants were transferred to soil and covered with

plastic to maintain the humidity. Some holes were made to drop the humidity, and the plants then adapted to the chamber environment.

3.3.5. Genotyping

Firstly, plant gDNA was extracted and purified. Subsequently, the presence of the Cas9 complex was confirmed by PCR (Table 5 in Appendix A). We used a plasmid containing the Cas9 gene (Feng et al., 2013) as a positive control. Potential edited plants for *OsEgl1* were named RD365 and for *OsEgl2* as RD366. So, the partial sequence of *OsEgl1* (478 bp) and *OsEgl2* (465 bp) was amplified using gDNA from RD365 and RD366. All bands were cut and purified.

OsEgl1 and *OsEgl2* amplicons (bands) were submitted to *SacII* and *XmaI* digestion, respectively. Wild-type amplicons of *OsEgl1* and *OsEgl2* submitted to the same digestion showed 168 bp/128 bp/98 bp/91 bp and 291 bp/174 bp, respectively. Then, potential undigested bands were sequenced. Concomitantly, the T7 endonuclease I (T7E1) assays (New England BioLabs Inc.) were carried out using *OsEgl1* and *OsEgl2* amplicons, which were denatured, and annealed in a thermocycler using the following program: 95 °C for 5 minutes ramping down to 85 °C at the rate of 2 °C/sec, 25 °C at the rate of 0.1 °C/sec. The mixture was then digested with 0.5 μL of the T7E1 enzyme (10 U/μL) at 37 °C for 60 minutes (Shan et al., 2014). Samples were electrophoresed on 1% agarose gel.

3.3.6. Heterologous Expression of *SBLIC1*

3.3.6.1. Cloning *Sblic1* into the bacterial expression vector pET30

Besides editing rice *endo-(1,3;1,4)-β-D-glucanases*, we wanted to characterize the SBLIC1 endo-(1,3;1,4)-β-D-glucanase. Thus, we tried to express this protein for an eventual viscosimetric assay. All results regarding this approach are found in Appendix B (Figure 27).

A partial DNA sequence of *Sblic1* CDS (368 bp) was cloned (Table 5 in Appendix A) into pGEM-T-Easy and used to transform the *E. coli Stbl3* cell. This partial construction was sequenced and considered our positive control. GenScript synthesized the full *Sblic1* coding sequence (1056 bp) and cloned it into the pUC57 vector. We cut out *Sblic1* CDS upon *NdeI*/*XhoI* digestion and electrophoresis. The insert was purified from agarose and cloned into pET30b/KanR (3:1 insert: vector molar ratio), previously digested by *NdeI*/*XhoI*. Ligation was confirmed upon *NdeI*/*XhoI* digestion and fragment release. The resulting construct and the

positive control were used to transform chemically competent cells [One Shot ® BL21(DE3) – Invitrogen], plated on solid SOC medium/KanR at 37 ºC overnight. A single colony was picked and grown in liquid LB medium/KanR at 37 ºC overnight and shaking at 225 rpm. Lastly, plasmids carrying the construct were extracted, subjected to digestion, and subjected to electrophoresis for confirmation.

3.3.6.2. *SBLIC1* expression and purification

An overnight culture of BL21DE3 cells containing the *Sblic1*/pET30b construct was grown under kanamycin selection. Half mL of the overnight culture was diluted into a fresh 25 mL (1/50) in pre-warmed liquid LB/Kan. As a negative control, the empty vector (BL21DE3/pET30b) was used. At OD ≅ 0.5, we induced SBLIC1 synthesis by adding IPTG at a final concentration of 0.5 mM. To maintain the samples' proportional cell number, we collected samples based on the initial volume (V_{TO}) and OD (OD_{TO}), using the following equation: $V_{TX} = (OD_{To} \times V_{To})/ OD_{TX.}$ Here, OD_{TX} means an OD at any given time (TX). The optimal point was four hours after IPTG induction. Pellets were centrifugated at 4,000 g at 4º C for 10 min, then stored at - 80 ºC.

Protein extraction and inclusion body solubilization were performed according to handbooks of CellLyticTM (Sigma) and CelLytic B (Sigma), respectively. According to Qiagen's protocols, His-Tag protein purification was carried out using an affinity chromatography matrix (Ni-NTA Agarose).

Precast Gels from Bio-rad (Mini-PROTEAN TGX) were used for protein electrophoresis, and subsequent procedures followed Laemmli 's work (1970). SBLIC1 has a mass of 37.12 kDa, and an appropriate protein marker was used to visualize bands around this mass.

All results regarding this particular experiment are found in Appendix B (Figure 27).

3.4. RESULTS

3.4.1. Expression profile of *OsEgl1* and *OsEgl2*

Figure 13 shows the expression level of *OsEgl1* and *OsEgl2* in different tissues. In rice roots, *OsEgl1* has a high expression level, while *OsEgl2* has a medium expression level. Therefore,

both genes were candidates for CRISPR-editing. The values were obtained from microarray data using Genevestigator Software (Hruz et al., 2008).

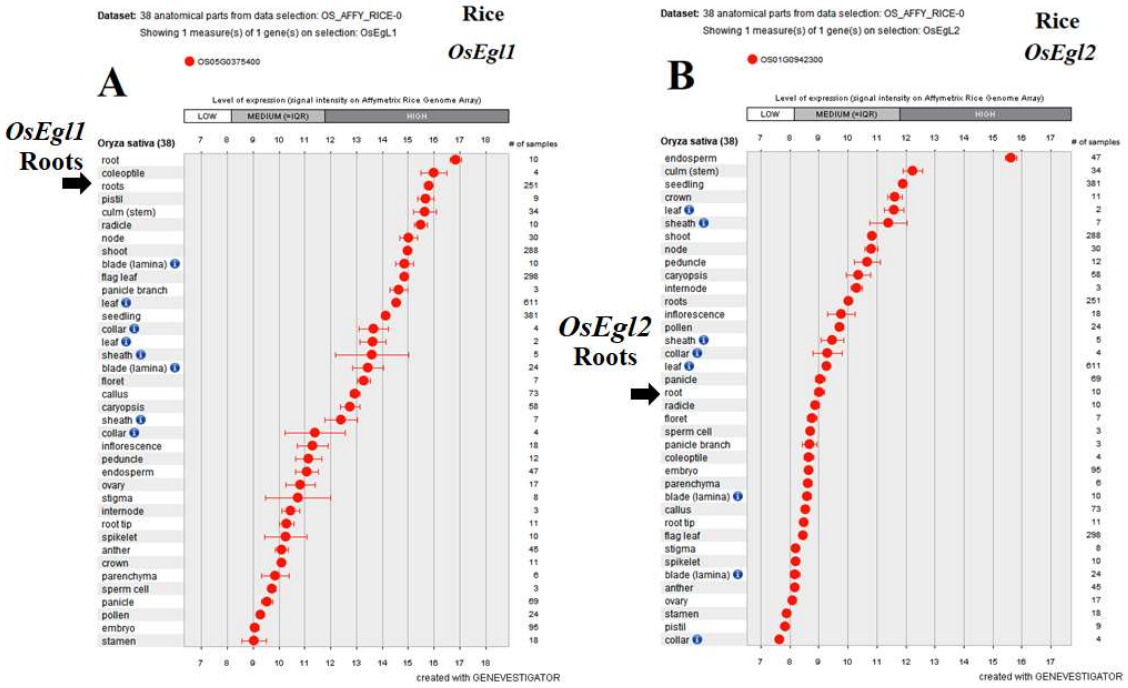

Figure 13. *OsEgl1* and *OsEgl2* expression level in roots. In (A), the black arrow indicates a high expression for *OsEgl1* in roots. In (B), the black arrow indicates medium expression for *OsEgl2* in roots. The figures were adapted and obtained using the Genevestigator tool (Hruz et al., 2008), whose analyses are based on public microarray data (Rice Genome Affymetrix).

3.4.2. Genotyping

3.4.2.1. Cas9 confirmation

The presence of the Cas9 complex (300 bp) was found in the genome of edited plants for *OsEgl1* (RD365) and *OsEgl2* (RD366). We found two lines containing Cas9 for *OsElg1,* RD365s (Figure 14A). In contrast, we detected the Cas9 in several lines (1-24) for *OsEgl2,* RD366s (Figure 14A and 14B). Despite the high number of potential transgenic plants for RD366s, all plants, including RD365s, did not survive. At this point, we still had some plants for further analysis.

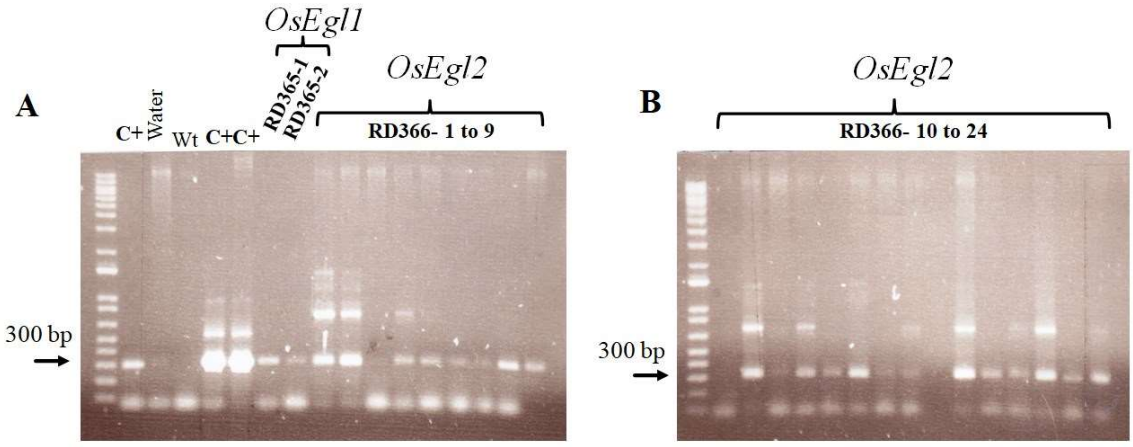

Figure 14. Cas9 confirmation. (A) and (B) show amplification of Cas9 (300 bp) in all samples. C+ are positive controls; Wt means wild type. RD365s are edited plants for *OsEgl1*, and RD366s are *OsEgl2*.

3.4.2.2. *OsEgl1* and *OsEgl2* amplifications using edited gDNA

Figure 15 shows amplicons of RD365 and RD366 using edited gDNA as templates. Bands were cut out and purified. Considering all plants did not survive, we analyzed only those plants that were still alive.

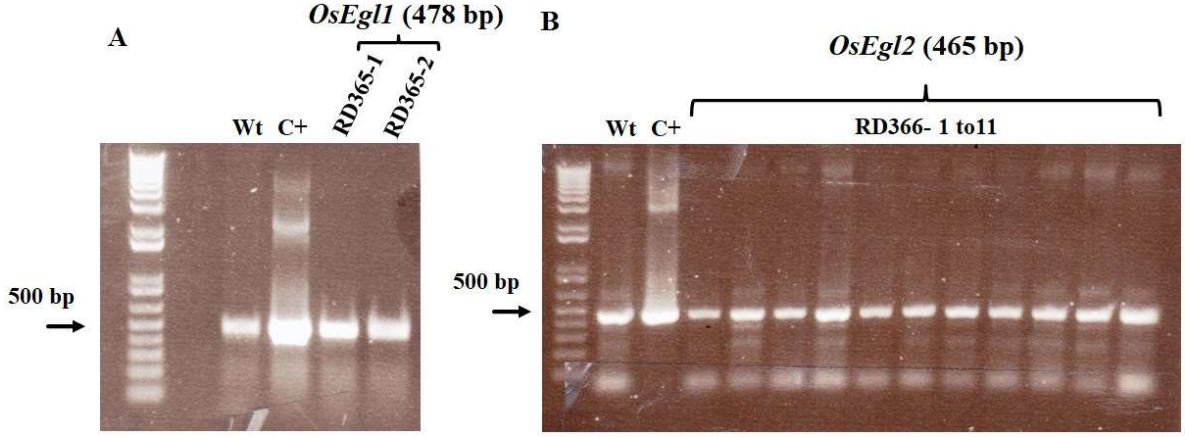

Figure 15. *OsEgl1* and *OsEgl2* amplifications using genome-edited plants as templates. (A) Partial *OsEgl1*amplifications (478 bp) are bands in RD365-1 and RD365-2. (B) Partial *OsEgl2* amplification (465 bp) are bands in RD366-1 to 11. RD365 are *OsEgl1* edited plants, and RD666 are *OsEgl2*. Positive controls (C+) are plasmids containing both partial sequences we previously cloned. Besides, we also amplified amplicons using wild type (Wt) gDNA.

3.4.2.3. *OsEgl1* and *OsEgl2* RFLP analysis

Figure 16 shows *OsEgl1* amplicons (RD365-1 and 2) upon *SacII* digestion, generating bands around 200 bp. The results indicated no on-target mutations because bands are similar to those that resulted upon wild-type digestion.

Figure 17 shows *OsEgl2* amplicons (RD365-1 and 2) digested by *XmaI*, resulting in four to five bands. Besides, are noticeable undigested 465 bp bands, which could be the outcome of incomplete digestion and on-target mutation at the *XmaI* restriction site. Either way, we cut the 465 bp bands out for sequencing and T7E1 assays.

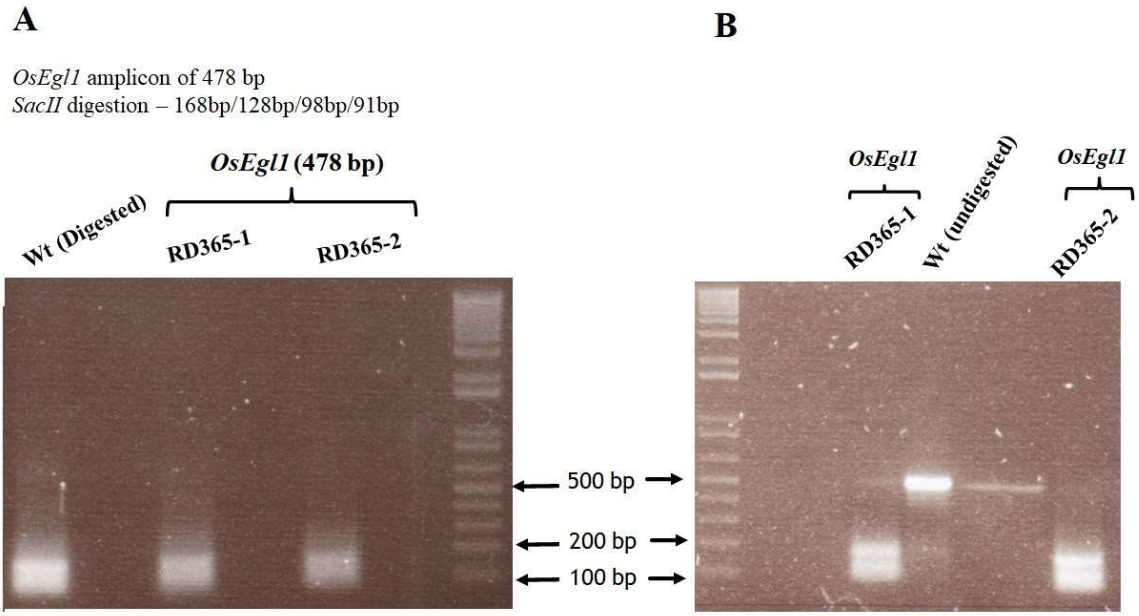

Figure 16. *OsEgl1* RFLP analysis. (A) The scheme above photos indicates the bands would be generated from wild-type (Wt) amplicon upon *SacII* digestion. Both, digested and undigested Wt are controls. RD365-1 and RD365-2 (A and B) upon *SacII* digestion generated bands like the digested Wt, indicating no on-target mutation.

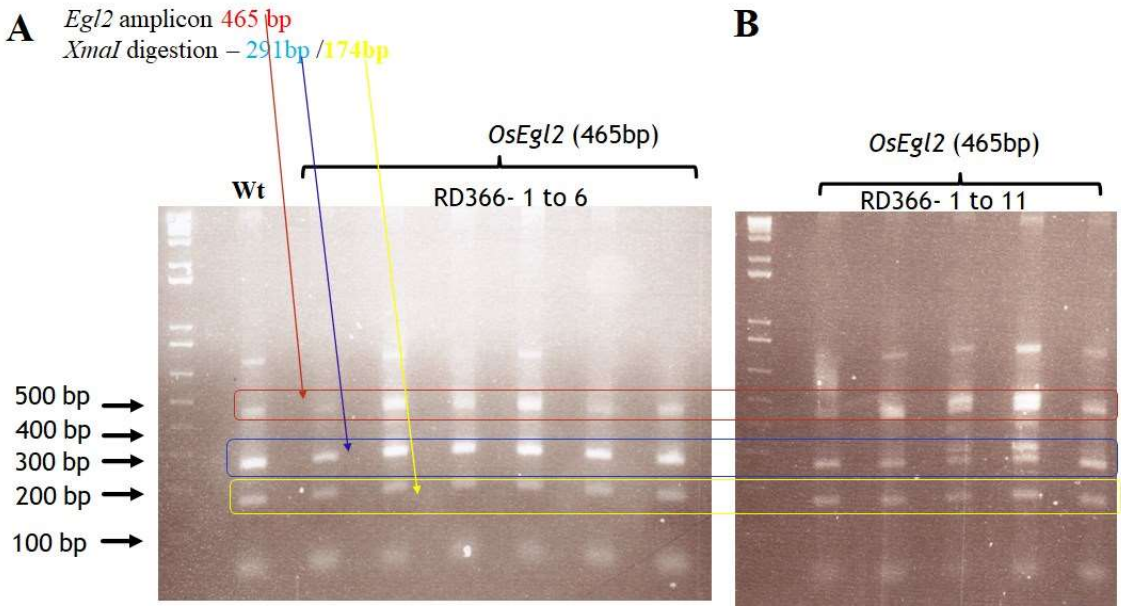

Figure 17. *OsEgl2* RFLP analysis. (A) and (B) have OsEgl2 amplicons (465 bp). Bands around 291/174 bp indicates eventual digestion by XmaI. Digested RD366s amplicons may contain undigested bands and incomplete digestion (465 bp).

3.4.2.4. T7E1 assay

Although *OsEgl1* RFLP suggested no on-target mutations, we used the *OsEgl1* amplicon for the T7E1 assays, which revealed single bands, thereby indicating no heteroduplex DNA sequences (Figure 18).

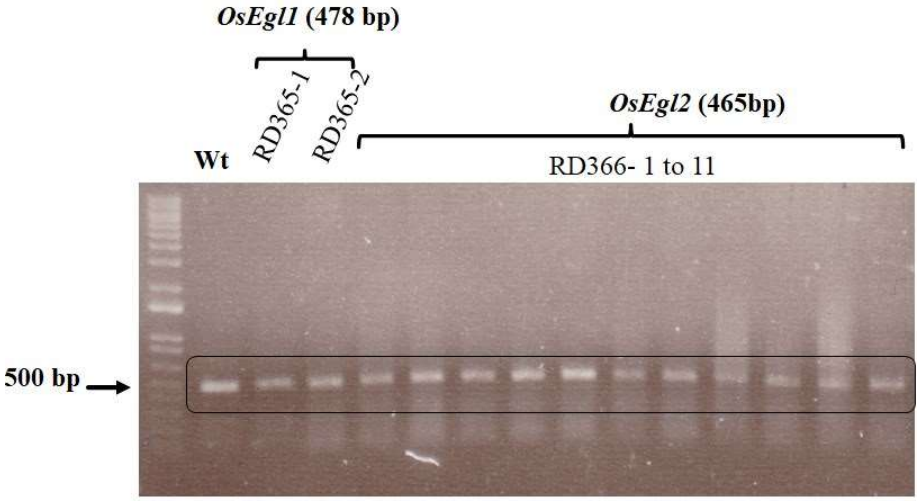

Figure 18. T7E1 assays. RD365s are *OsEgl1*amplicons (478 bp) and RD366s are *OsEgl2* (465 bp). The arrow indicates 500 bp. Single bands suggested no DNA heteroduplexes.

3.4.2.5. Sanger sequencing

The undigested bands (465 bp) from *OsEgl2* RFLP (Figure 17) were sequenced. One sample revealed two off-target point mutations in *OsEgl2* CDS. However, when the alleged mutated sequence was aligned with our previously cloned wild-type *OsEgl2* amplicon, the point mutations would result in amino acid sequence changes. Furthermore, the "mutated sequence" did not indicate point mutations compared to sequences at the Phytozome database.

3.4.3. Acquisition of *OsEgl2* T-DNA line

Public databases showed the existence of rice lines containing T-DNA insertion for *OsEgl1* and *OsEgl2*. However, only *OsEgl2* Taiwan Rice Insertional Mutants (TRIM) seeds were available at International Rice Functional Genomics Center. They are T2 seeds of M00089780 mutant. Besides, this mutant is a Tainung 67 rice variety. So, we also acquired a wild-type Tainung 67.

The wildtype and M00089780 mutant alignment revealed the T-DNA insertion in the CDS final region and 3'UTR (Figure 28 in Appendix B). Thus, the mutant might be a good line to investigate a possible *OsEgl2* loss of function.

3.5. DISCUSSION

Profile expression of *OsEgl1* and *OsEg2* indicated significant expression for both genes in roots. Genotyping verified the presence of Cas9 in the genome of several edited plants, thereby indicating potential transgenics. However, RFLPs revealed no mutation for *OsEgl1*, whereas *OsEgl2* contained undigested bands, meaning possible point mutations. Some bands were then cut off and sequenced. The data suggested no mutation or eventual changes in amino acid sequences for OsEGL2. We transformed more calli and obtained some plants that survived, although we did not genotype them.

Despite the fact we did not obtain an edited line using CRISPR/Cas9, the last surviving plants could be further investigated. Significantly, the T-DNA line acquisition is an excellent candidate for MLG studies vis-à-vis aerenchyma development.

3.6. CONCLUSION

We did not obtain on-target mutants for *OsEgl1* and *OsEgl2*. Therefore, we were unable to analyze the aerenchyma. However, there are still potential transgenic plants for further investigation. More importantly, the *OsEgl2* T-DNA line is a precious material that could indicate if MLG hydrolysis is associated with aerenchyma development.

REFERENCES

Akiyama, T., Jin, S., Yoshida, M., Hoshino, T., Opassiri, R., and Ketudat Cairns, J. R. (2009). Expression of an endo-(1,3;1,4)-β-glucanase in response to wounding, methyl jasmonate, abscisic acid and ethephon in rice seedlings. *J. Plant Physiol.* 166, 1814–1825. doi:10.1016/j.jplph.2009.06.002.

Akiyama, T., Kaku, H., and Shibuya, N. (1996). Purification and partial characterization of an endo-(1→3, 1→4)-β-glucanase from rice, Oryza sativa L. *Biosci. Biotechnol. Biochem.* 60, 2078–2080. doi:10.1271/bbb.60.2078.

Ansede, M. (2017). Francis Mojica, de las salinas a la quiniela del Nobel. *El País*. Available at: https://elpais.com/elpais/2017/05/18/eps/1495058731_149505.html.

Barrangou, R., Fremaux, C., Deveau, H., Richards, M., Boyaval, P., Moineau, S., et al. (2007). CRISPR provides acquired resistance against viruses in prokaryotes. *Science (80-.).* doi:10.1126/science.1138140.

Bolotin, A., Quinquis, B., Sorokin, A., and Dusko Ehrlich, S. (2005). Clustered regularly interspaced short palindrome repeats (CRISPRs) have spacers of extrachromosomal origin. *Microbiology*. doi:10.1099/mic.0.28048-0.

Buckeridge, M. S., Rayon, C., Urbanowicz, B., Tiné, M. A. S., and Carpita, N. C. (2004). Mixed Linkage (1→3),(1→4)-β- d -Glucans of Grasses. *Cereal Chem.* 81, 115–127. doi:10.1094/CCHEM.2004.81.1.115.

Čermák, T., Baltes, N. J., Čegan, R., Zhang, Y., and Voytas, D. F. (2015). High-frequency, precise modification of the tomato genome. *Genome Biol.* doi:10.1186/s13059-015-0796-9.

Chauhan, B. S., Jabran, K., and Mahajan, G. (2017). *Rice Production Worldwide*. doi:10.1007/978-3-319-47516-5.

Chen, L., Li, W., Katin-Grazzini, L., Ding, J., Gu, X., Li, Y., et al. (2018). A method for the production and expedient screening of CRISPR/Cas9-mediated non-transgenic mutant plants. *Hortic. Res.* doi:10.1038/s41438-018-0023-4.

Chu, C. C., Wang, C. C., Sun, C. S., Hsu, C., Yin, K. C., Chu, C. Y., et al. (1975). Establishment of an efficient medium for anther culture [in breeding] of rice through comparative experiments on the nitrogen sources. *Sci Sin*.

Dang, Y., Jia, G., Choi, J., Ma, H., Anaya, E., Ye, C., et al. (2015). Optimizing sgRNA structure to improve CRISPR-Cas9 knockout efficiency. *Genome Biol.* doi:10.1186/s13059-015-0846-3.

Deveau, H., Garneau, J. E., and Moineau, S. (2010). CRISPR/Cas System and Its Role in Phage-Bacteria Interactions. *Annu. Rev. Microbiol.* doi:10.1146/annurev.micro.112408.134123.

European Commission (2021). Ethics of Genome Editing. doi:10.2777/763.

Eva, N. (2020). The Nobel Prize in Chemistry 2020. *R. Swedish Acad. Sci.* Available at: https://www.nobelprize.org/uploads/2020/10/press-chemistryprize2020.pdf.

Feng, Z., Mao, Y., Xu, N., Zhang, B., Wei, P., Yang, D. L., et al. (2014). Multigeneration analysis reveals the inheritance, specificity, and patterns of CRISPR/Cas-induced gene modifications in Arabidopsis. *Proc. Natl. Acad. Sci. U. S. A.* doi:10.1073/pnas.1400822111.

Feng, Z., Zhang, B., Ding, W., Liu, X., Yang, D. L., Wei, P., et al. (2013). Efficient genome editing in plants using a CRISPR/Cas system. *Cell Res.* doi:10.1038/cr.2013.114.

Fernández, J. (2021). Francis Mojica, investido doctor honoris causa por la Complutense. *Trib. Complutense, Univ. Complut. Madrid.* Available at: https://www.euni.de/unidir_popup.php?content=showJob&jobid=137551&jobtyp=5&jtyp=1&university=Universidad+Complutense+de+Madrid&sid=5097&country=ES&title=Licenciatura+en+Geografía.

Garris, A. J., McCouch, S. R., and Kresovich, S. (2003). Population Structure and Its Effect on Haplotype Diversity and Linkage Disequilibrium Surrounding the xa5 Locus of Rice (Oryza sativa L.). *Genetics*.

Gasiunas, G., Barrangou, R., Horvath, P., and Siksnys, V. (2012). Cas9-crRNA ribonucleoprotein complex mediates specific DNA cleavage for adaptive immunity in bacteria. *Proc. Natl. Acad. Sci. U. S. A.* doi:10.1073/pnas.1208507109.

Gasperini, M., Findlay, G. M., McKenna, A., Milbank, J. H., Lee, C., Zhang, M. D., et al. (2016). Paired CRISPR/Cas9 guide-RNAs enable high-throughput deletion scanning (ScanDel) of a Mendelian disease locus for functionally critical non-coding elements. *bioRxiv*, 92445. doi:10.1101/092445.

Grandis, A., Leite, D. C. C., Tavares, E. Q. P., Arenque-Musa, B. C., Gaiarsa, J. W., Martins, M. C. M., et al. (2019). Cell wall hydrolases act in concert during aerenchyma development in sugarcane roots. *Ann. Bot.* doi:10.1093/aob/mcz099.

Hruz, T., Laule, O., Szabo, G., Wessendorp, F., Bleuler, S., Oertle, L., et al. (2008). Genevestigator V3: A Reference Expression Database for the Meta-Analysis of Transcriptomes. *Adv. Bioinformatics*. doi:10.1155/2008/420747.

Ishino, Y., Shinagawa, H., Makino, K., Amemura, M., and Nakatura, A. (1987). Nucleotide sequence of the iap gene, responsible for alkaline phosphatase isoenzyme conversion in Escherichia coli, and identification of the gene product. *J. Bacteriol.* doi:10.1128/jb.169.12.5429-5433.1987.

Jinek, M., Chylinski, K., Fonfara, I., Hauer, M., Doudna, J. A., and Charpentier, E. (2012). A programmable dual-RNA-guided DNA endonuclease in adaptive bacterial immunity. *Science (80-.).* doi:10.1126/science.1225829.

Kato, S., Kosaka, H., and Hara, S. (1928). ON THE AFFINITY OF RICE VARIETIES AS SHOWN BY THE FERTILITY OF HYBRID PLANTS. in.

Khush, G. S. (1997). Origin, dispersal, cultivation and variation of rice. *Plant Mol. Biol.* doi:10.1007/978-94-011-5794-0_3.

Kido, N., Yokoyama, R., Yamamoto, T., Furukawa, J., Iwai, H., Satoh, S., et al. (2015). The matrix polysaccharide (1;3,1;4)-β-D -glucan is involved in silicon-dependent strengthening of rice cell wall. *Plant Cell Physiol.* 56, 268–276. doi:10.1093/pcp/pcu162.

Laemmli, U. K. (1970). Cleavage of structural proteins during the assembly of the head of bacteriophage T4. *Nature*. doi:10.1038/227680a0.

Leite, D. C. C., Grandis, A., Tavares, E. Q. P., Piovezani, A. R., Pattathil, S., Avci, U., et al. (2017). Cell wall changes during the formation of aerenchyma in sugarcane roots. *Ann. Bot.* 120, 693–708. doi:10.1093/aob/mcx050.

Liu, X., Xie, C., Si, H., and Yang, J. (2017). CRISPR/Cas9-mediated genome editing in plants. *Methods*. doi:10.1016/j.ymeth.2017.03.009.

Luttenegger, D. G., and Nevins, D. J. (1985). Transient Nature of a (1 → 3), (1 → 4)-β-d-Glucan in Zea mays Coleoptile Cell Walls. *Plant Physiol.* 77, 175–178.

Ma, Y., Chen, W., Zhang, X., Yu, L., Dong, W., Pan, S., et al. (2016). Increasing the efficiency of CRISPR/Cas9-mediated precise genome editing in rats by inhibiting NHEJ and using Cas9 protein. *RNA Biol.* doi:10.1080/15476286.2016.1185591.

Makarova, K. S., Grishin, N. V., Shabalina, S. A., Wolf, Y. I., and Koonin, E. V. (2006). A putative RNA-interference-based immune system in prokaryotes: Computational analysis of the predicted enzymatic machinery, functional analogies with eukaryotic RNAi, and hypothetical mechanisms of action. *Biol. Direct.* doi:10.1186/1745-6150-1-7.

Mao, Y., Zhang, H., Xu, N., Zhang, B., Gou, F., and Zhu, J.-K. (2013). Application of the CRISPR–Cas System for Efficient Genome Engineering in Plants. *Mol. Plant* 6, 2008–2011. doi:10.1093/mp/sst121.

Marraffini, L. A., and Sontheimer, E. J. (2008). CRISPR interference limits horizontal gene transfer in staphylococci by targeting DNA. *Science (80-.).* doi:10.1126/science.1165771.

Mojica, F. J. M., Díez-Villaseñor, C., García-Martínez, J., and Soria, E. (2005). Intervening sequences of regularly spaced prokaryotic repeats derive from foreign genetic elements. *J. Mol. Evol.* doi:10.1007/s00239-004-0046-3.

Mojica, F. J. M., Díez-Villaseñor, C., Soria, E., and Juez, G. (2000). Biological significance of a family of regularly spaced repeats in the genomes of Archaea, Bacteria and mitochondria. *Mol. Microbiol.* doi:10.1046/j.1365-2958.2000.01838.x.

Mojica, F. J. M., Ferrer, C., Juez, G., and Rodríguez-Valera, F. (1995). Long stretches of short tandem repeats are present in the largest replicons of the Archaea *Haloferax mediterranei* and *Haloferax volcanii* and could be involved in replicon partitioning. *Mol. Microbiol.* doi:10.1111/j.1365-2958.1995.mmi_17010085.x.

Mojica, F. J. M., Juez, G., and Rodriguez-Valera, F. (1993). Transcription at different salinities of *Haloferax mediterranei* sequences adjacent to partially modified PstI sites. *Mol. Microbiol.* doi:10.1111/j.1365-2958.1993.tb01721.x.

Murashige and Skoog, 1962Chu, C. C., Wang, C. C., Sun, C. S., Hsu, C., Yin, K. C., Chu, C. Y., et al. (1975). Establishment of an efficient medium for anther culture [in breeding] of rice through comparative experiments on the nitrogen sources. *Sci Sin.*

Nishida, K., Arazoe, T., Yachie, N., Banno, S., Kakimoto, M., Tabata, M., et al. (2016). Targeted nucleotide editing using hybrid prokaryotic and vertebrate adaptive immune systems. *Science (80-.).* doi:10.1126/science.aaf8729.

Piatek, A., Ali, Z., Baazim, H., Li, L., Abulfaraj, A., Al-Shareef, S., et al. (2015). RNA-guided transcriptional regulation in planta via synthetic dCas9-based transcription factors. *Plant Biotechnol. J.* doi:10.1111/pbi.12284.

Pourcel, C., Salvignol, G., and Vergnaud, G. (2005). CRISPR elements in Yersinia pestis acquire new repeats by preferential uptake of bacteriophage DNA, and provide additional tools for evolutionary studies. *Microbiology.* doi:10.1099/mic.0.27437-0.

Qi, Y., Zhang, Y., Zhang, F., Baller, J. A., Cleland, S. C., Ryu, Y., et al. (2013). Increasing frequencies of site-specific mutagenesis and gene targeting in Arabidopsis by manipulating DNA repair pathways. *Genome Res.* doi:10.1101/gr.145557.112.

Roulin, S., Buchala, A. J., and Fincher, G. B. (2002). Induction of (1→3,1→4)-β-D-glucan hydrolases in leaves of dark-incubated barley seedlings. *Planta* 215, 51–59. doi:10.1007/s00425-001-0721-1.

Roulin, S., and Feller, U. (2001). Reversible accumulation of (1→3,1→4)-β-glucan endohydrolase in wheat leaves under sugar depletion. *J. Exp. Bot.* 52, 2323–2332.

Schulman, A. H., Oksman-Caldentey, K. M., and Teeri, T. H. (2020). European Court of Justice delivers no justice to Europe on genome-edited crops. *Plant Biotechnol. J.* doi:10.1111/pbi.13200.

Shan, Q., Wang, Y., Li, J., and Gao, C. (2014). Genome editing in rice and wheat using the CRISPR/Cas system. *Nat. Protoc.* 9, 2395–2410. doi:10.1038/nprot.2014.157.

Slakeski, N., Baulcombe, D. C., Devos, K. M., Ahluwalia, B., Doan, D. N. P., and Fincher, G. B. (1990). Structure and tissue-specific regulation of genes encoding barley (1→3, 1→4)-β-glucan endohydrolases. *MGG Mol. Gen. Genet.* 224, 437–449. doi:10.1007/BF00262439.

Sun, Y., Zhang, X., Wu, C., He, Y., Ma, Y., Hou, H., et al. (2016). Engineering Herbicide-Resistant Rice Plants through CRISPR/Cas9-Mediated Homologous Recombination of Acetolactate Synthase. *Mol. Plant.* doi:10.1016/j.molp.2016.01.001.

Veillet, F., Perrot, L., Chauvin, L., Kermarrec, M. P., Guyon-Debast, A., Chauvin, J. E., et al. (2019). Transgene-free genome editing in tomato and potato plants using Agrobacterium-mediated delivery of a CRISPR/Cas9 cytidine base editor. *Int. J. Mol. Sci.* doi:10.3390/ijms20020402.

Wälti, M., Roulin, S., and Feller, U. (2002). Effects of pH, light and temperature on (1→3,1→4)-β- glucanase stability in wheat leaves. *Plant Physiol. Biochem.* 40, 363–371. doi:10.1016/S0981-9428(02)01373-6.

Wang, Z. P., Xing, H. L., Dong, L., Zhang, H. Y., Han, C. Y., Wang, X. C., et al. (2015). Egg cell-specific promoter-controlled CRISPR/Cas9 efficiently generates homozygous mutants for multiple target genes in Arabidopsis in a single generation. *Genome Biol.* doi:10.1186/s13059-015-0715-0.

Woo, J. W., Kim, J., Kwon, S. Il, Corvalán, C., Cho, S. W., Kim, H., et al. (2015). DNA-free genome editing in plants with preassembled CRISPR-Cas9 ribonucleoproteins. *Nat. Biotechnol.* doi:10.1038/nbt.3389.

Xing, H. L., Dong, L., Wang, Z. P., Zhang, H. Y., Han, C. Y., Liu, B., et al. (2014). A CRISPR/Cas9 toolkit for multiplex genome editing in plants. *BMC Plant Biol.* doi:10.1186/s12870-014-0327-y.

Zhang, D., Zhang, H., Wang, M., Sun, J., Qi, Y., Wang, F., et al. (2009). Genetic structure and differentiation of Oryza sativa L. in China revealed by microsatellites. *Theor. Appl. Genet.* doi:10.1007/s00122-009-1112-4.

Zhang, Z., Mao, Y., Ha, S., Liu, W., Botella, J. R., and Zhu, J. K. (2016). A multiplex CRISPR/Cas9 platform for fast and efficient editing of multiple genes in Arabidopsis. *Plant Cell Rep.* doi:10.1007/s00299-015-1900-z.

Zong, Y., Chen, Z., Innes, J. B., Chen, C., Wang, Z., and Wang, H. (2007). Fire and flood management of coastal swamp enabled first rice paddy cultivation in east China. *Nature.* doi:10.1038/nature06135.

4. FINAL CONSIDERATIONS

Sorghum bicolor will get more attention due to its high flexibility in growing in a vast range of environments, especially in a future scenario where climatic events are expected to be more extreme. Data obtained from primary sorghum roots have strengthened our MLG hydrolysis's correlation with the constitutive aerenchyma development in this work. A seven-day-old non-branching root system, whose diameter is adequate for in vivo analysis, enabled the acquisition of high-resolution X-images in a couple of hours, contributing to the establishment of roots into segments and their ensuing anatomical characterization. The precise identification of gas spaces within segments facilitated obtaining more robust data regarding gene expression, enzymatic assays, and cell wall fractionation.

CRISPR-editing *endo-β-(1,3;1,4)-glucanases* were carried out using rice, though, considering its genetic transformation stability. Even editing rice *endo-β-(1,3;1,4)-glucanases* in a year were challenging, and it turned out to be more complicated than we expected. Nonetheless, the acquisition of an *OsEgl2* T-DNA might help to conclude whether MLG hydrolysis and aerenchyma development have a cause-and-effect relationship with one another. Also, researchers will eventually conclude if *Sblic1* is directly involved in aerenchyma development or not. Notably, *Sblic2* is roughly 900-fold more expressed in young leaves than roots and may fit better for biotechnology purposes. Indeed, researchers have explored Poaceae *endo-β-(1,3;1,4)-glucanases* genes and alleles to get more thermostable and efficient enzymes for MLG hydrolyses. Thus, our phylogeny will contribute to explore the MLG *endo-β-(1,3;1,4)-glucanases* in biotechnology.

In my opinion, the most trending topic of MLG is related to its evolution. MLG's presence throughout divergent living organisms. The lack of information regarding its synthases and hydrolysis are questions that remain to be elucidated. The recent findings of GH16 transglycosylases capably of grafting backbones of MLG into xyloglucan are intriguing. Similarly, eudicot does not have MLG, but a recent find showed an MLGase activity in *Vitis vinifera*. Exempting bacteria and monocots, we do not know which genes perform MLG biosynthesis in such organisms.

Interestingly, our inferences indicated *CslHs* genes in Magnoliids, a clade in which MLG has never been detected. Although many genes are related to MLG biosyntheses in monocots, like the monocot-specific *cellulose synthase-like F* and *H*, the *bacterial cellulose synthases A* has been emerged as MLG synthase, owing homology with *Csls*. Therefore, the polymer's multiple origins

theory could need to be attested again in the future because such homology, from bacteria to monocots, indicates evolutionary conservation.

It could be that some clades have genes to synthesize MLG but do not express them, and, therefore, we would not see MLG presence. For instance, the magnoliids clade could be under this hypothesis, in which our phylogeny indicated *CslHs* within magnoliids, although researchers have never detected MLG in this clade.

Either way, MLG evolution remains a trending topic with intriguing questions to be solved among those who have studied MLG intensively.

APPENDIXES

Appendix A

Table 5. List of primers.

CHAPTER I			
Reference genes for *Sorghum bicolor*			
Gene Target/ID (Phytozome)	**Primer Name**	**Sequences (5' to 3')**	**Description**
Sobic.004G147800/*CYP*	Sobic.004G147800_CYP_F	GTATCTGTGCTCGCCGTCTCT	qRT-PCR (Sudhakar Reddy et al. 2016)
Sobic.004G147800/*CYP*	Sobic.004G147800_CYP_R	TTCACCCAACTCCTCAACCCC	qRT-PCR (Sudhakar Reddy et al. 2016)
Sobic.004G039400/*EIF4a*	Sobic.004G039400_EIF4α_F	CAACTTTGTCACCCGCGATGA	qRT-PCR (Sudhakar Reddy et al. 2016)
Sobic.004G039400/*EIF4a*	Sobic.004G039400_EIF4α_R	TCCAGAAACCTTAGCAGCCCA	qRT-PCR (Sudhakar Reddy et al. 2016)
Sobic.004G092500/*PP2A*	Sobic.004G092500_PP2A_F	AACCCGCAAAACCCCAGACTA	qRT-PCR (Sudhakar Reddy et al. 2016)
Sobic.004G092500/*PP2A*	Sobic.004G092500_PP2A_R	TACAGGTCGGGCTCATGGAAC	qRT-PCR (Sudhakar Reddy et al. 2016)
GH 17 *endo-(1,3;1,4)-β-D-glucanases* of *S. bicolor*			
Gene Target/ID (Phytozome)	**Primer Name**	**Sequences (5' to 3')**	**Description**
Sobic.003G421900.1	Sb003G421900_Sblic1_F	GATCGGAGGGGTCGATACTT	*Sblic1* (qRT-PCR)
Sobic.003G421900.1	Sb003G421900_Sblic1_R	TACTGCTACGCTACGCATGG	*Sblic1* (qRT-PCR)
Sobic.009G119400.1	Sb009G119400_F_Sblic2_F	GACCACTGGGAGTGTCGAAT	*Sblic2* (qRT-PCR)
Sobic.009G119400.1	Sb009G119400_R_Sblic2_R	CTTCACACGTCGCTGATGAC	*Sblic2* (qRT-PCR)
Sobic.009G119200.1	Sb009G119200_Sblic3_F	CTGGGACGAGAGAGATCGAG	*Sblic3* (qRT-PCR)
Sobic.009G119200.1	Sb009G119200_Sblic3_R	CCCCACACACATACCGTACA	*Sblic3* (qRT-PCR)
Sobic.009G119200.1	Sb009G119200_2_Sblic3_F	TACAAGTCGAACGGCATCAC	*Sblic3* (qRT-PCR)
Sobic.009G119200.1	Sb009G119200_2_Sblic3_R	GAAGGAGACGGAAGGGTACG	*Sblic3* (qRT-PCR)

Continues

Table 6 (Continued)

Cellulose synthase-like F and *H* of *Sorghum bicolor*			
Gene Target/ID (Phytozome)	**Primer Name**	**Sequences (5' to 3')**	**Description**
Sobic.007G050600.1	SbCslF6_F	CCAGCATCTATCGTCAAGCATGC	*SbCslF6* (qRT-PCR) (Ermawar et al., 2015)
Sobic.007G050600.1	SbCslF6_R	CTGTGTGGGGTTGCTGTGTAGTC	*SbCslF6* (qRT-PCR) (Ermawar et al., 2015)
Sobic.002G334100.1	SbCslF3-1_F	CATTTGCTCGAACACCTGAA	*SbCslF3-1* (qRT-PCR) (Ermawar et al., 2015)
Sobic.002G334100.1	SbCslF3-1_R	CGCTGTCTTCCAATTCCATT	*SbCslF3-1* (qRT-PCR) (Ermawar et al., 2015)
Sobic.002G334200.1	SbCslF3-2_F	TCTTGCTGCCAGTTGTCCTTGT	*SbCslF3-2* (qRT-PCR) (Ermawar et al., 2015)
Sobic.002G334200.1	SbCslF3-2_R	TTACATTGCCTTCTATATCGCCTAG	*SbCslF3-2* (qRT-PCR) (Ermawar et al., 2015)
Sobic.002G333900.1	SbCslF4_F	TTGCAGCTGGGTCATCAGGGTAG	*SbCslF4* (qRT-PCR) (Ermawar et al., 2015)
Sobic.002G333900.1	SbCslF4_R	CACCGCCAGGGTCTTGTTT	*SbCslF4* (qRT-PCR) (Ermawar et al., 2015)
Sobic.001G242000.1	SbCslF7_F	GCCTGCTATTTGACTGATGACTAG	*SbCslF7* (qRT-PCR) (Ermawar et al., 2015)
Sobic.001G242000.1	SbCslF7_R	GCCACATGCATTGTCGTAGACATG	*SbCslF7* (qRT-PCR) (Ermawar et al., 2015)
Sobic.002G171200.3	SbCsFl10-1_F	TGACAGGTACGCCGACATAT	*SbCslF10-1* (qRT-PCR) (Ermawar et al., 2015)
Sobic.002G171200.3	SbCslF10-1_R	TCGCAGACCACACTCCATTGTC	*SbCslF10-1* (qRT-PCR) (Ermawar et al., 2015)
Sobic.002G334400.1	SbCslF10-2_F	CCAAGCAATTTGTAAAAGGGTGAT	*SbCslF10-2* (qRT-PCR) (Ermawar et al., 2015)
Sobic.002G334400.1	SbCslF10-2_R	CCTGAGCTACTTTGAGACATTCGTGAC	*SbCslF10-2* (qRT-PCR) (Ermawar et al., 2015)
Sobic.002G334500.1	SbCslF10-3_F	TTTGTGCAGCGGCTACTGTG	*SbCslF10-3* (qRT-PCR) (Ermawar et al., 2015)
Sobic.002G334500.1	SbCslF10-3_R	AGGTAAAACGCATGACACTCGGC	*SbCslF10-3* (qRT-PCR) (Ermawar et al., 2015)
Sobic.006G080600.2	SbCSlH-1_F	CCGACGCCAGAATATCATCTAGG	*SbCslH-1* (qRT-PCR) (Ermawar et al., 2015)
Sobic.006G080600.2	SbCSlH-1_R	CCTGGCCTTTTACGTGCTCAT	*SbCslH-1* (qRT-PCR) (Ermawar et al., 2015)
Sobic.006G080700.2	SbCslH-2_F	TGTGACGACGGGAATCAATCA	*SbCslH-2* (qRT-PCR) (Ermawar et al., 2015)
Sobic.006G080700.2	SbCslH-2_R	AGTAGGATCACAGACTCATAGAC	*SbCslH-2* (qRT-PCR) (Ermawar et al., 2015)
Sobic.006G080800.1	SbCslH-3_F	GACACAGTGTTAGTCAATGAAAGC	*SbCslH-3* (qRT-PCR (Ermawar et al., 2015)
Sobic.006G080800.1	SbCslH-3_R	GTTGAATTGGTCTGTACGTCTGC	*SbCslH-3* (qRT-PCR) (Ermawar et al., 2015)

Continues

Table 7 (Continued)

CHAPTER II			
GH 17 *endo-(1,3;1,4)-β-D-glucanase* of *S. bicolor*			
Gene Target/ID (Phytozome)	**Primer Name**	**Sequences (5' to 3')**	**Description**
Sobic.003G421900.1	D975_F	CCGGAGACGGTGGTGCAGG	
Sobic.003G421900.1	D974_R	GGGAGCTCTCAGGCTCCGAAGGTGATGG	Partial *Sblic1* (368 bp) as C+ for protein expression
GH 17 *endo-(1,3;1,4)-β-D-glucanases* of *Oryza sativa*			
Gene Target/ID (Phytozome)	**Primer Name**	**Sequences (5' to 3')**	**Description**
LOC_Os05g31140	*OsEgl1* SacII-24sense	TGGCACCTCGCCGCCAGCCCCGCCGCGG	to change to the *OsEgl1* SacII sequence in psg9-Cas9-Os
LOC_Os05g31140	*OsEgl1* SacII-24antisense	AAACCCGCGGCGGGGCTGGCGGCGAGGT	to change to the *OsEgl1* SacII sequence in psg9-Cas9-Os
LOC_Os01g71474	*OsEgl2* XmaI-20sense	TGGCATCTACTCATACAACCCGGG	to change to the *OsEgl2* XmaI sequence in psg9-Cas9-Os
LOC_Os01g71474	*OsEgl2*XmaI-20antisense	AAACCCCGGGTTGTATGAGTAGAT	to change to the *OsEgl2* XmaI sequence in psg9-Cas9-Os
LOC_Os05g31140	*OsEgl1* 3272F	GCCGCCGGCGAGCTCGGTG	to PCR partial sequence of *OsEgl1* (478 bp)
LOC_Os05g31140	*OsEgl1* 3749R	GGGGTAGATGTTGGCGAGC	to PCR partial sequence of *OsEgl1* (478 bp)
LOC_Os01g71474	*OsEgl2* 2878F	GGTGACGACGTCGATCTCCC	to PCR partial sequence of *OsEgl2* (465 bp)
LOC_Os01g71474	*OsEgl2* 3342R	GGCGAACACGTACGTCTCCG	to PCR partial sequence of *OsEgl2* (465 bp)
	D426	GGGCCATGAAGCCTTTCAGG	to amplify Cas9 (300 bp) (Feng et al., 2013)
	D847	TGGCGCACGCGCTACGGAC	to amplify Cas9 (300 bp) (Feng et al., 2013)

Table 5 (Concluded)

Table 6. Rice tissue culture media.

Medium name	2N6 medium	N6CO medium	MSRE medium	MSRT medium
Inorganic Salts	N6	N6	MS	MS
Organic Compounds	N6 vitamins (3.99g/L) 1.0 mg/mL casamino acids	N6 vitamins (3.99g/L)	MS vitamins (4.33 g/L)	MS vitamins (4.33 g/L)
Saccharides	30.0 mg/mL sucrose	30.0 mg/mL sucrose 10.0 mg/mL dextrose	30.0 mg/mL sucrose 30.0 mg/mL sorbitol	
Plant Hormones	2 μg/mL 2,4-D	2 μg/mL 2,4-D	2 μg/mL 2,4-D	1 μg/mL NAA 2 μg/mL BAP
pH	pH 5.8	pH 5.2	pH 5.8	pH 5.8
Gelzan	2.5 g/L	2.5 g/L	2.5 g/L	2.5 g/L
Antibiotics			30 μg/mL hygromycin (Add after autoclave)	30 μg/mL hygromycin (Add after autoclave)
Containers	Plates (diameter 100 mm)	Plates (diameter 100 mm)	Plates (diameter 100 mm)	Plant growth pots

N6 (Phytotech Lab) (Chu et al., 1975); MS (Phytotech Lab) (Murashige and Skoog, 1962); NAA (1-Naphthaleneacetic acid); BAP (6-Benzylaminopurine

Appendix B

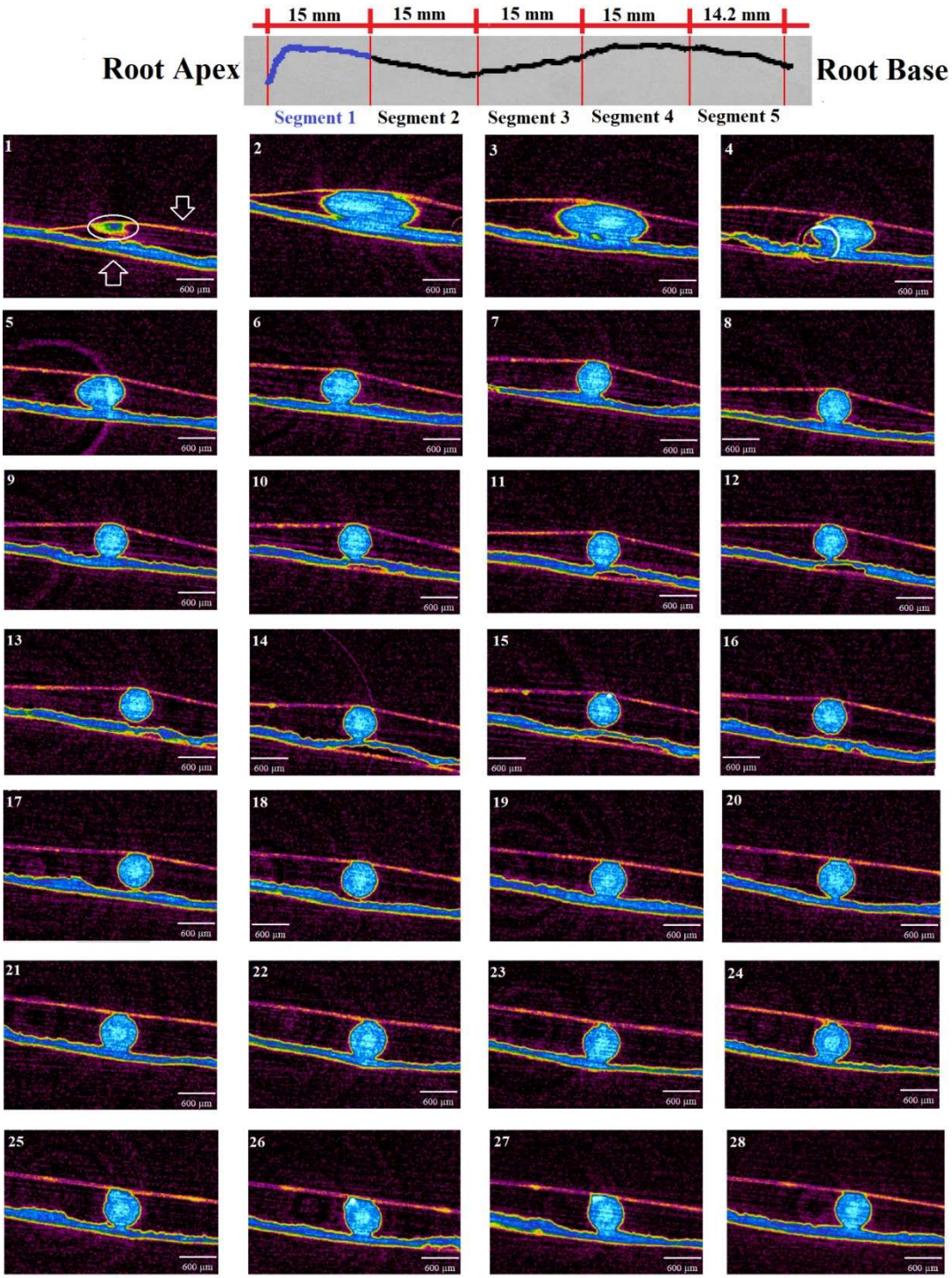

Figure 19. Micrograph of the first segment. The first segment starts at the root apex and has no aerenchyma. The diagram above comprises the whole primary root of this microtomography, divided into 5 segments, and the first one is in blue. All images are equidistantly displayed from each other (from root apex towards the base). In (1), the ellipse shows the beginning of the apex. The up arrow constitutes the foam material on which the roots were placed for analysis and the down arrow the plastic that involves the root. The root's diameter is slightly larger in (2) and (4) due to the plastic's compression. Images were subjected to color density range using software CT-Analyser.

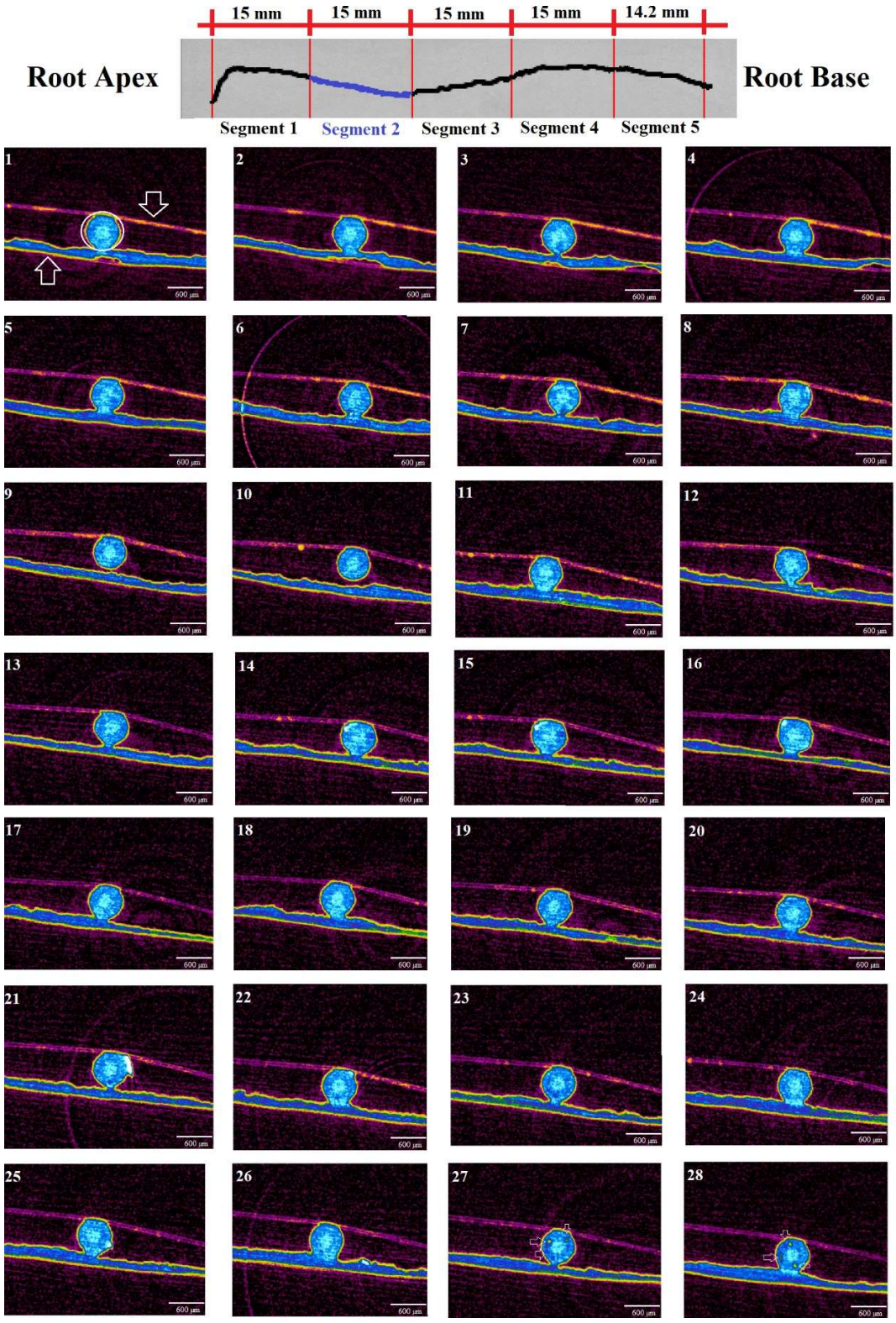

Figure 20. Micrograph of the second segment. The second segment is the initiation of aerenchyma development. The diagram above comprises the whole primary root of this microtomography, divided into 5 segments, and the second one is in blue. All images are equidistantly displayed from each other (from root apex towards the base). In (1), the circle shows the root. The up arrow constitutes the foam material on which the root was placed for analysis and the down arrow the plastic that involves the root. The first gas spaces start to develop and are noticeable in (27) and (28), indicated by arrows. Images were subjected to color density range using software CT-Analyser.

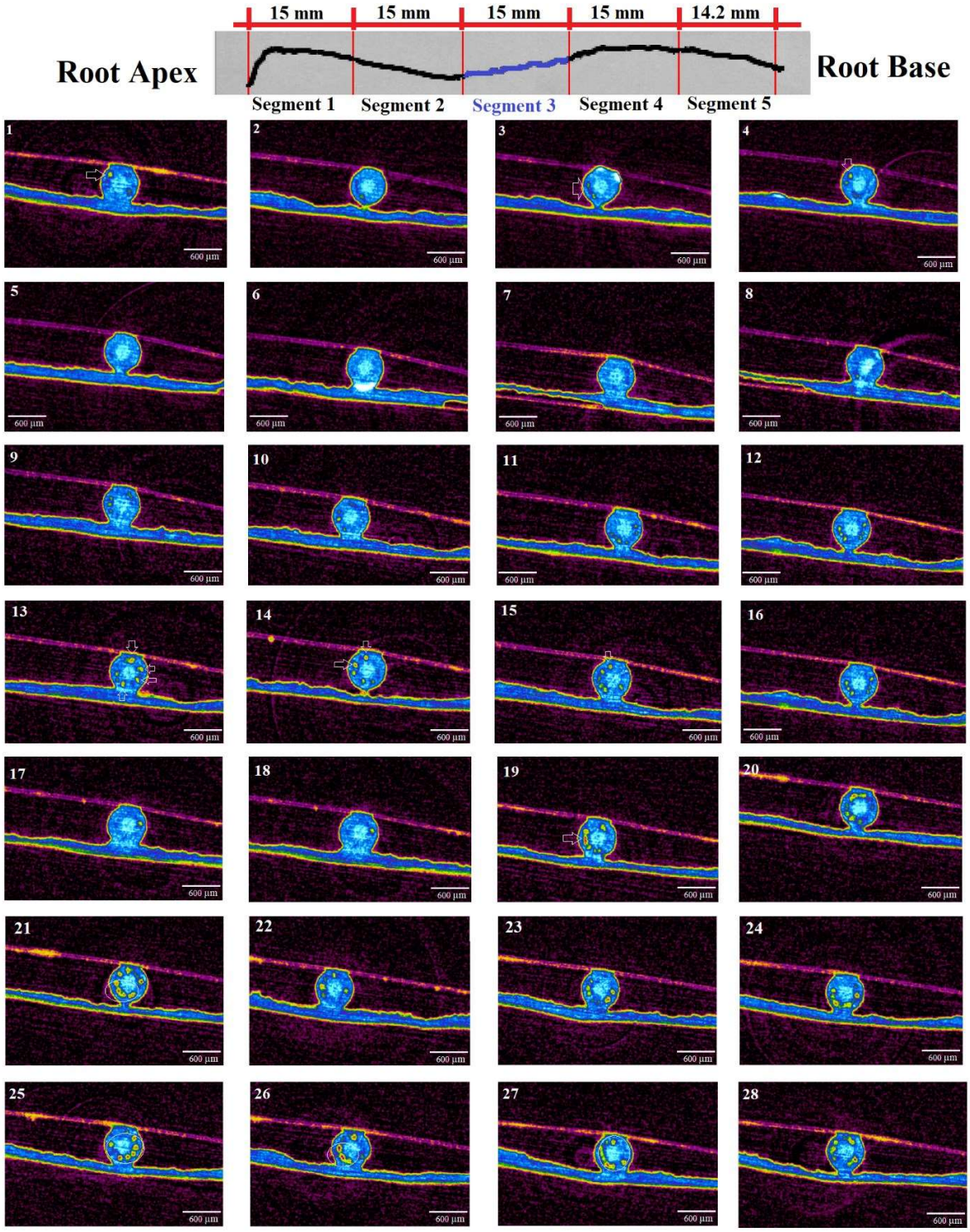

Figure 21. Micrograph of the third segment. The third segment is the aerenchyma under development. This pattern has been found in the fourth and fifth segments as well. The diagram above comprises the whole primary root of this microtomography, divided into 5 segments, and the third one is in blue. All images are equidistantly displayed from each other (from root apex towards the base). White arrows indicate some gas spaces in (1), (3), (4), (13), (14), (15), and (19). The ellipses represent a set of merged gas spaces in (21) and (26). Images were subjected to color density range using software CT-Analyser.

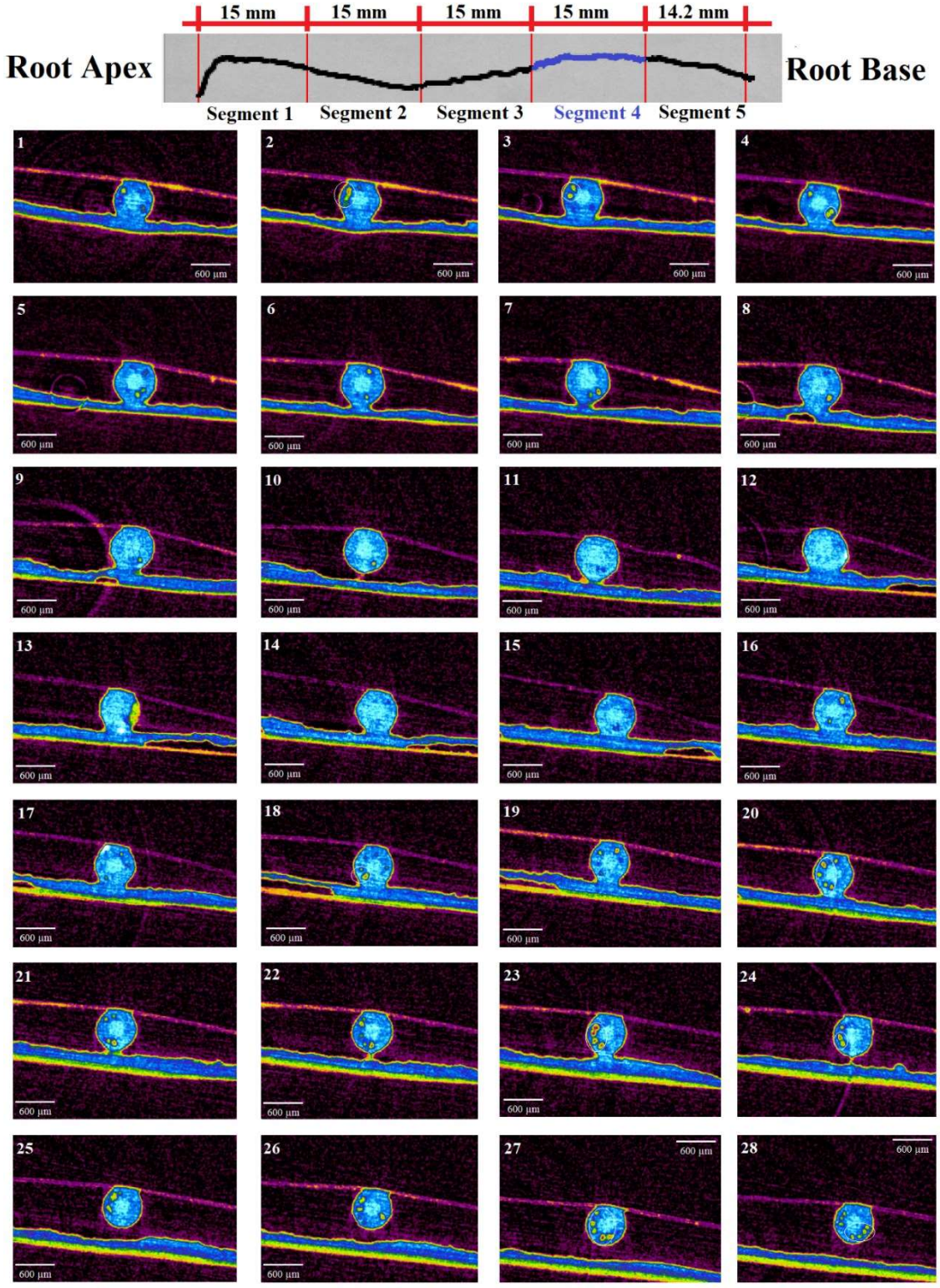

Figure 22. Micrograph of the fourth segment. The fourth segment is the aerenchyma under development. This pattern has been found in the third and fifth segments. The diagram above comprises the whole primary root of this microtomography, divided into 5 segments, and the fourth one is in blue. All images are equidistantly displayed from each other (from root apex towards the base). The ellipses represent a set of merged gas spaces in (2), (3), (4), (18), (20), (23), (24), (27), (28). Images were subjected to color density range using software CT-Analyser.

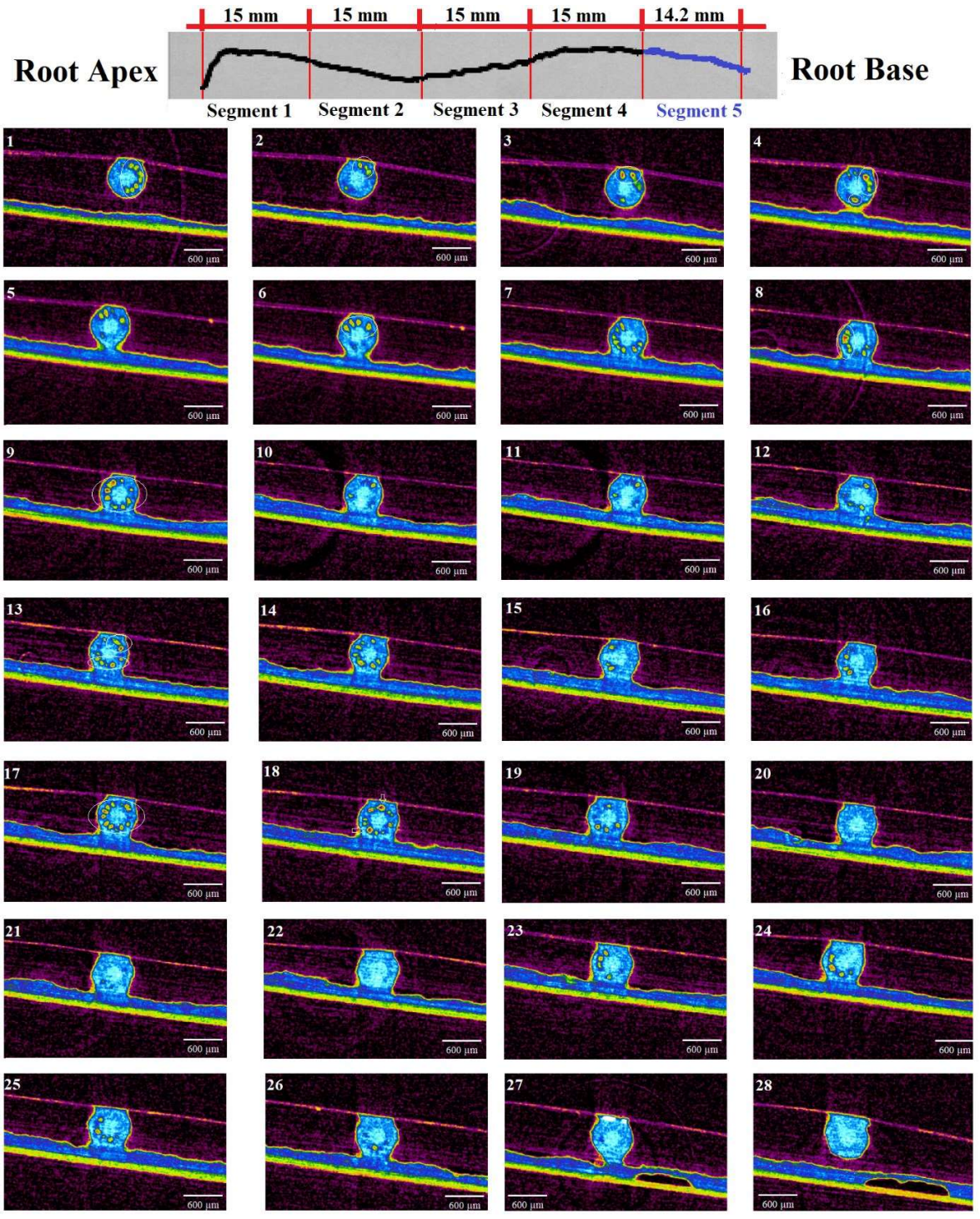

Figure 23. Micrograph of the fifth segment. The fifth segment is the aerenchyma under development. This pattern has been found in the third and fourth segments as well. The diagram above comprises the whole primary root of this microtomography, divided into 5 segments, and the fifth one is in blue. All images are equidistantly displayed from each other (from root apex towards the base). The ellipses represent a set of merged gas spaces in (1), (2), (3), (4), (6), (8), (9), (13), and (17). White arrows indicate some gas spaces in (18). Images were subjected to color density range using software CT-Analyser.

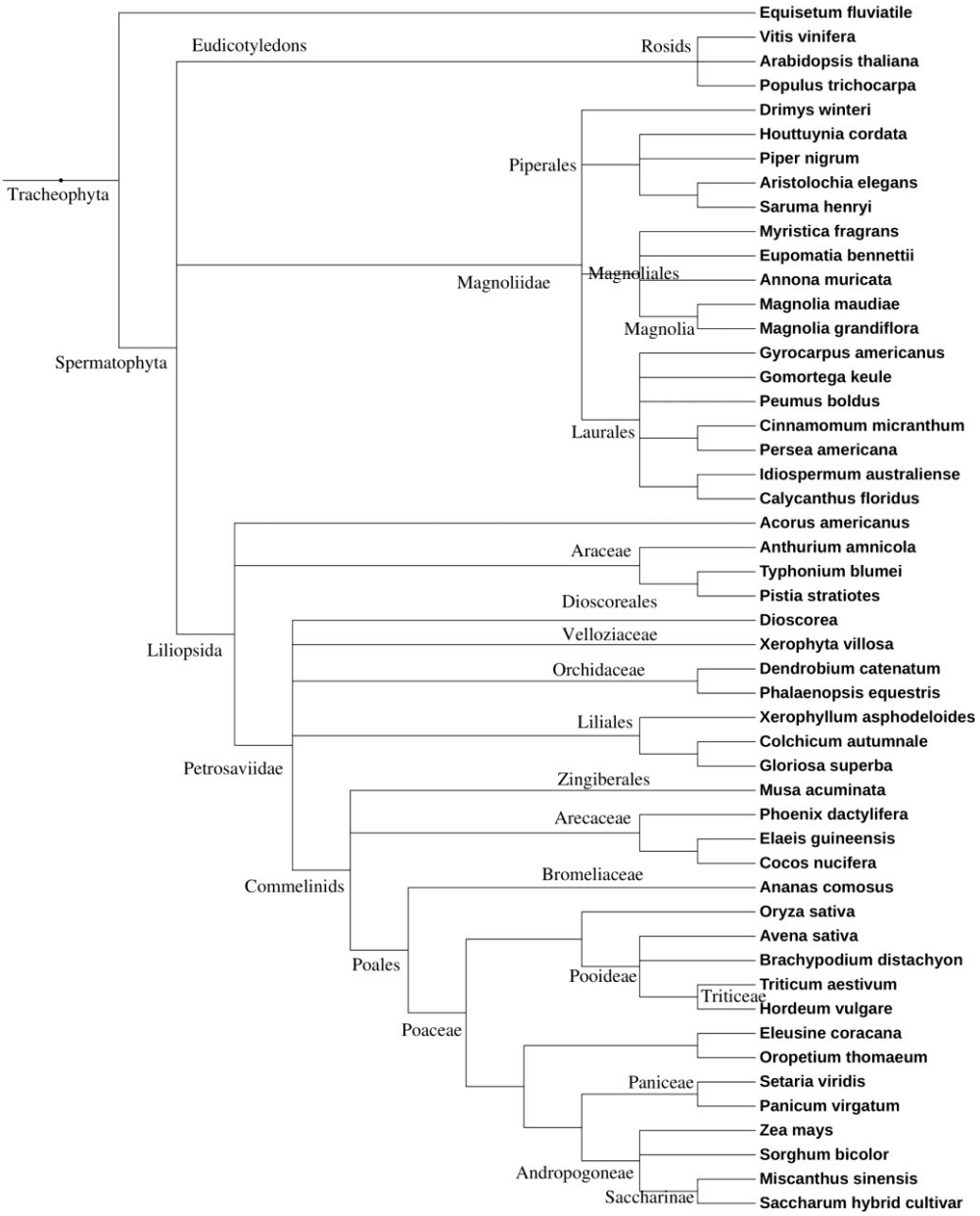

Figure 24. Species tree of tracheophytes. The cladogram shows the clustering pattern of some species used in our work. The cladograms were generated in PhyloT (Letunic and Bork, 2007) with NCBI taxonomic data. There are groups with polytomy that are unranked.

Figure 25. Evolutionary tree of GH17 *endo-(1,3;1,4)-β-glucanases* in Poaceae. Each node's values are related to each branch's length and may represent the extent of divergence. The arrows indicate the sorghum genes. The estimated change average of *Sblic1* is higher than *Sblic2* and *Sblic3*. The two merged red triangles are *endo-(1,3)-β-glucanases* related to callose used as root point.

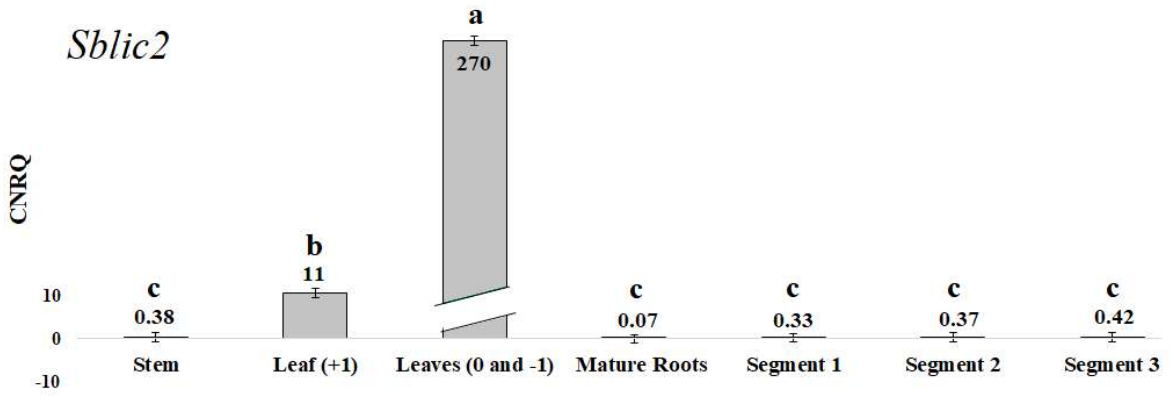

Figure 26. *Sblic2* expression profile. *Sblic2* stands out for its elevated expression in young leaves (0 and -1). Stem, leaves, and mature roots were obtained from sixty-day-old sorghum, while segments were acquired from seven-day-old seedlings. Values are means (n=3) ± standard errors, and letters represent the statistical significance among samples according to Tukey's test ($p < 0.05$).

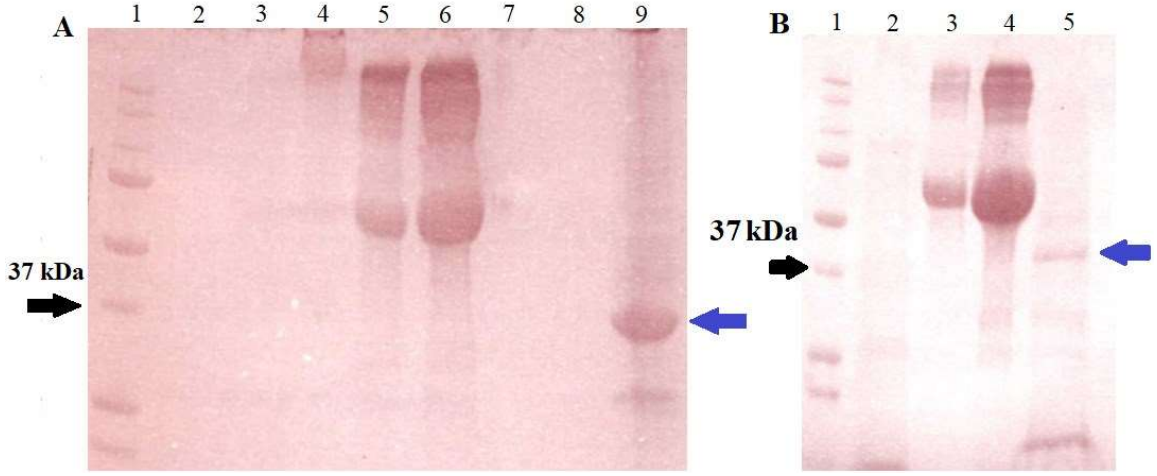

Figure 27. Heterologous expression of SBLIC1 and its solubilization from inclusion bodies. In (A), (1) Molecular eight; (2) pET30b (empty vector); (3) Purified soluble fraction; (4) 1 μg of BSA; (5) 5 μg of BSA; (6) 10 μg of BSA; (9) Cell debris (inclusion bodies). SBLIC1 was found in inclusion bodies (ninth column indicated by blue arrow) but not in the soluble fraction (third column) after protein extraction. In (B), (1) molecular weight; (2) inclusion bodies submitted to affinity purification; (3) 2 μg of BSA; (4) 5 μg of BSA; (5) inclusion bodies not submitted to purification. Eventually, SBLIC1 did not bind to collum upon purification. Bovine serum albumin (BSA), black arrows are 37 kDa, and blue arrows indicate SBLIC1 (37.12 kDa).

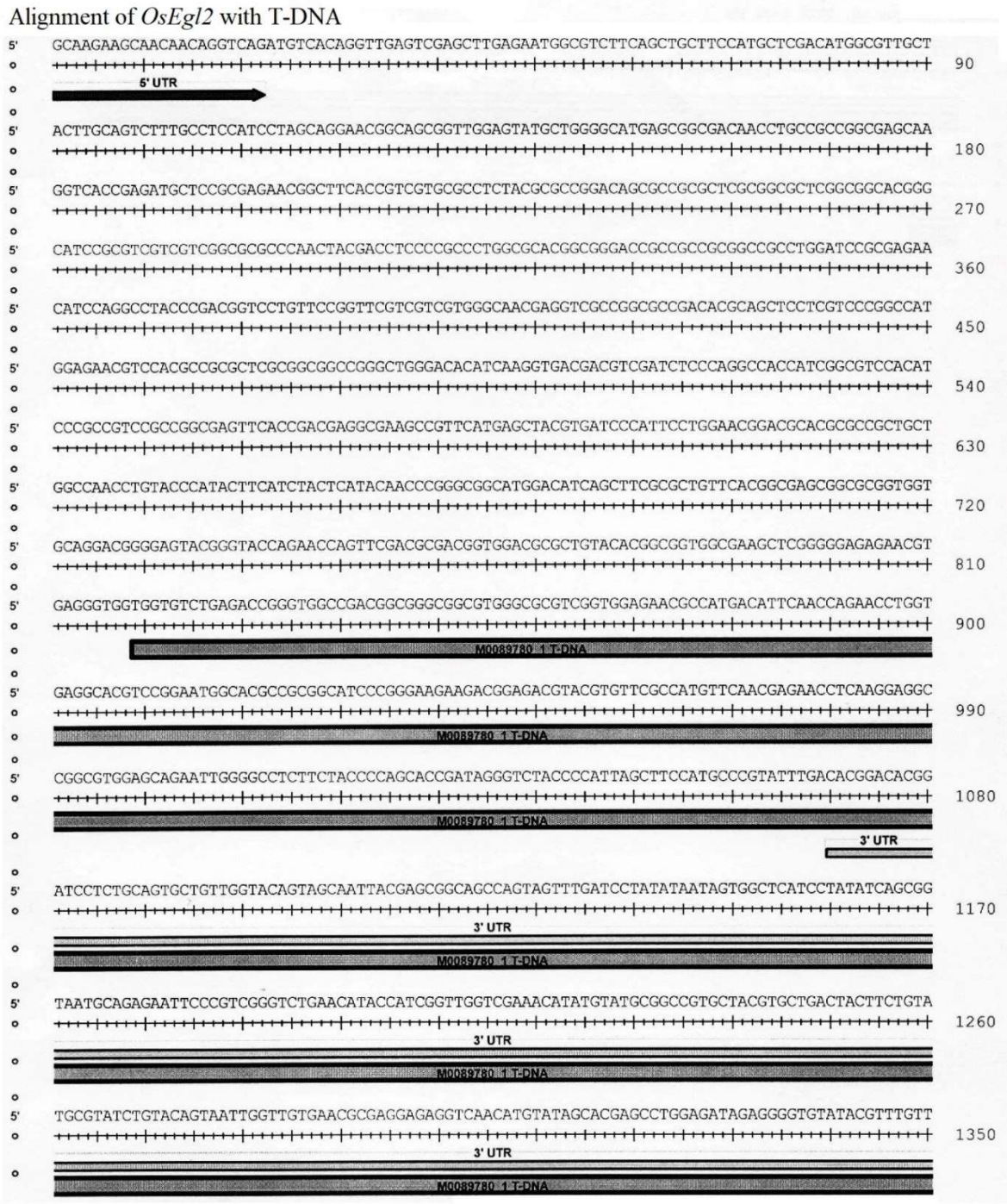

Figure 28. Sequence of *OsEgl2* T-DNA line aligned with wild type. The alignment of wild type with-DNA line revealed the T-DNA insertion within *OsEgl2* CDS and in the 3'UTR. The mutant ID is M00089780 and was acquired from Taiwan.